Identification of dexamethasone-induced metabolic vulnerabilities in glioblastoma

Maria Francesca Allega BSc., MSc.

Thesis submitted to the University of Glasgow in fulfilment of the requirements for the Doctor of Philosophy

Institute of Cancer Sciences
College of Medical, Veterinary and Life Sciences
University of Glasgow
May 2022

CRUK Beatson Institute
Garscube Estate
Switchback Road
Glasgow G61 1BD

Abstract

Glioblastoma represents the most aggressive and common high-grade (IV) malignant brain tumour in adults. Despite many efforts have been done in order to ameliorate the clinical outcome of this disease, the standard of care has not substantially changed in the last 20 years, and is based on surgical resection followed by radiotherapy and chemotherapy with the alkylating agent temozolomide. Nonetheless, the aggressiveness and recurrence of this tumour make the prognosis still very poor and the median survival for glioblastoma patients is 12-18 months from the time of diagnosis. Since 1960's, patients presenting with clinical symptoms associated with glioblastoma are invariably treated with dexamethasone, a potent anti-inflammatory drug that reduces the peritumoral oedema, and alleviates the neurological symptoms caused by the increased intracranial pressure. Given the clinical relevance of dexamethasone for the management of glioblastoma patients, several studies have been performed to understand the effects of dexamethasone on patients' survival. A retrospective clinical analysis of three independent glioma patient cohorts found that steroids treatment associates with shorter survival. As indicated by the name, glucocorticoids regulate glucose metabolism. Dexamethasone increases glycaemia, and this has been linked to a shorter survival of glioblastoma patients. Nevertheless, because of its effectiveness, affordability and accessibility, dexamethasone will remain a mainstay of glioblastoma patients' therapy. On these bases, we employed naïve patient-derived cell lines that have been demonstrated to retain the pathophysiological features of the tumour in the patients to identify the metabolic effects of dexamethasone on glioblastoma cells and characterize specific drug-induced vulnerabilities. In particular, we studied the metabolic reactions altered by dexamethasone treatment with the aim to exploit them as therapeutic targets. Therefore, we cultured the cells in serum-free physiological media (Plasmax) to retain the stem cells subpopulation and expose them to the same metabolites concentrations found in human plasma. We found that the glucocorticoid receptor, the dexamethasone main target, was expressed in all cell lines, and translocated to the nucleus upon dexamethasone treatment. While the effects of dexamethasone on proliferation were cell line-dependent, we profiled a dexamethasone-dependent transcriptional signature common to all cell lines. Orthogonal transcriptomic and metabolomics analyses

identified nicotinamide *N*-methyltransferase, NNMT, to be transcriptionally and functionally upregulated by dexamethasone. NNMT transfers methyl groups from *S*-adenosyl-methionine (SAM) to nicotinamide, producing *N*1-methylnicotinamide. Dexamethasone-mediated NNMT over-activation caused a shortage in SAM and an increase in *N*1-methylnicotinamide levels in all cell lines. Unexpectedly, dexamethasone treatment did not sensitize glioblastoma cells to sub-physiological and growth-limiting concentrations of methionine. We validated these findings in 10 naïve human glioblastoma cell lines and in glioblastoma tumours orthotopically implanted in immunocompromised mice. *In vivo*, dexamethasone decreased the methionine levels in tumour and contralateral brain tissue without altering its circulating levels. Dexamethasone administration significantly decreased tumour volume assessed by MRI and proliferation index. Notably, the levels of NNMT and *N*1-methylnicotinamide were markedly higher in tumour tissue compared to contralateral normal brain, and these differences were amplified by dexamethasone treatment. Moreover, we demonstrated that the activity of NNMT is increased in tumour tissues derived from glioblastoma patients, compared to adjacent oedematous brain tissue. These results suggest that NNMT activity could be targeted for the development of a novel PET tracer for the visualization of invasive tumours, aiding the diagnosis and the response to therapy of glioblastoma patients. Moreover, these tumour-specific dexamethasone-induced metabolic alterations may lead to a rationally designed therapeutic plan for glioblastomas with heterogeneous mutational status.

Table of Contents

List of Figures

List of Tables

List of Abbreviations

2-HG	2-hydroxyglutarate
ATP	Adenosine 5'-triphosphate
BSA	Bovine serum albumin
CSF	Cerebrospinal fluid
DEX	Dexamethasone
DMEM	Dulbecco's Modified Eagle Medium
ECM	Extracellular matrix
EGFR	Epidermal growth factor receptor
FDG	^{18}F-2-Fluoro-2-deoxy-D-glucose
FKBP5	FKBP prolyl isomerase 5
FLT	^{18}F-fluorotymidine
GBM	Glioblastoma
G-CIMP	Glioma CpG island methylator phenotype
GR	Glucocorticoid receptor
GRE	Glucocorticoid responsive element
GS	Glutamine synthetase
GSC	Glioblastoma stem cells
hBFGF	Human basic fibroblast growth factor
hCRF	Human corticotropin-releasing factor
hEGF	Human epidermal growth factor
hESCs	Human embryonic stem cells
H&E	Hematoxylin and Eosin
IDH	Isocytrate Dehydrogenase
KLF9	Krüppel like factor 9
LC-MS	Liquid chromatography-mass spectrometry
MEM	Eagle's Minimal essential medium
MGMT	O^6-methylguanine–DNA methyltransferase
MPP+	1-methyl-4-phenylpyridinium ion
MRI	Magnetic resonance imaging
MRS	Magnetic resonance spectroscopy
MTA	5'-methylthioadenosine
MTAP	5'-Methylthioadenosine Phosphorylase
NAA	*N*-acetylaspartate
N1-MNA	*N*1-methylnicotinamide
NAD+	Nicotinamide Adenine Dinucleotide
NAM	Nicotinamide
NAMPT	Nicotinamide phosphoribosyltransferase
NNMT	Nicotinamide-*N*-methyltransferase
OCR	Oxygen consumption rate
PARP1	Poly(ADP-ribose) polymerase 1
PDOX	Patient-derived orthotopic xenografts

PET	Positron emission tomography
RT	Retention time
SAH	S-adenosyl-L-homocysteine
SAM	S-adenosyl-L-methionine
SVZ	Subventricular zone
UGDH	UDP-glucose-6-dehydrogenase
VEGF	Vascular endothelial growth factor

Acknowledgements

Dear Saverio, thank you. Firstly, for trusting me and giving me the chance to work on this project. But mostly thank you for being there when I most needed it, inside and outside of the lab. Thank you for not getting upset every time I sent you drafts to correct the day before the deadline. Thank you for all the inputs and feedbacks, and for teaching me how to be the first reviewer of my own work.

Thanks to my R16 pals Ruhi, Tobias and Victor. Working with you has been an absolute pleasure. Your guidance and assistance (both mental and practical) in the lab were crucial during these past four years. Thanks to everyone (past and present) in Y75 group David, Rachel, Engy, Gillian and Giovanny for the help over the years.

Thanks to the patients, and to the volunteers and the people donating their time and resources to Cancer Research UK, that made the funding for this project available. To all the fantastic people I met at the Beatson Institute during these years. If I started naming them, I am sure I would forget someone. For the small or big part you had in this project and in my life, thank you. To the mice, without them this project would not have been possible. Working with animals made me experience feelings and responsibilities that I had not anticipated, but it gave me awareness of what animal research means.

Thanks to my family. To my dear mum and dad, the most loving parents a daughter could desire, and to my brother and rock Babbo. Without your constant practical and emotional support, I would not have been able to enjoy the many opportunities that led me to this special place that is Glasgow. Thanks for complaining about the distance not more than a wee bit and for accepting what I became over the years. To my Uncle Enzo, for checking up on me and trying to stress me about this thesis months before I had actually started writing it (I should have listened to you). To my Aunt Elena and Uncle Francesco for the sweet calls, and the reminder of what familial love means. To my sister-in-law Francesca and wee Tommaso we are all waiting for, thanks for entering our life and family with your brightness and tenderness. To my dear, strong, and annoying cousin Michela, with whom we shared an amazing and memorable tour of Scotland. To Marianna,

thanks to your woollen socks and jumpers the Scottish winter was sweeter, and to my inspiring cousin Flavia.

Thanks to my friends here. To Christoph, for being you and for the gigs, the hikes, the exhibitions, the camping trips, the dinners. To Marti, for all the hours-long discussions and to my pals Martha and Marco, for being the sweetest friends I could have desired to meet. Wherever we will all go next, I will not easily forget what we shared. To Sergi, for being there, for our prosecco-birthdays and getting me into bouldering (we will see how long I will last). To Lucas, Maria, Christos, Declan, Michalis, Laura, Dominika, Nadja and Aimee. You all had special places in my Glaswegian experience.
Thanks to my friends there. To Rebecca, living in the UK at the same time as you and knowing that I could visit and bother you anytime I wanted was fantastic. To Alessandra, the longest-distance friendship I have ever been. Canada with you always seemed behind the corner. Rebi, Ale e Giulio, I am glad I met you in Bologna. To Elisa (and to your sweetheart Andrea), witnessing your achievements from a distance was a challenge but you are family to me and no distance will ever change this. To Chiara, for continuously checking up on me during the writing and for opening up when we both needed it the most. “Having you” down in London for a little bit was amazing. Thanks to Francesca and Gioia, for being there every time I unexpectedly (:)) came back to Rome. To Claudio, Andrea, Bianco and Lorenzo, years pass by and every time I see you it is as if I have never really left. I will not easily forget you promised to come to Glasgow a hundred times and eventually never came. To Costanza, and all the great people I met in Copenhagen. Some of you are the reason I landed up here and I am extremely grateful for this. Peppe and Salva, I am talking about you two.

Living in Glasgow has changed myself and my perception of the world on many levels. I lived through the pandemic from an extremely privileged position but I am grateful for the friends, books and yoga (Maggie and Ashia, thank you) that kept me sane in the last two years. All the people I met in the past four Glaswegian years had a role in what this thesis represents. I believed in this project since the day I started working on it and hope that reading the fruit of the work we collected in this thesis will be as exciting as describing and discussing them has been.

Glasgow, 2nd May 2022

Author's declaration

I hereby declare that the work presented in this thesis is the result of my own independent investigation unless otherwise stated. The Introduction of this thesis contains a figure from a review published by our group in the journal *Trends in Molecular Medicine* (Deshmukh R, Allega MF, Tardito S. A map of the altered glioma metabolism. *Trends Mol Med*. 2021 Nov; 27(11):1045-1059.)

I confirm that this work has not been previously submitted for consideration of any other degree.

Maria Francesca Allega

Chapter 1. Introduction

1.1 Glioblastoma

Glioblastoma (GBM) or high-grade (IV) glioma is the most aggressive and common malignant brain tumour in adults. Glioblastomas are divided in *primary* if arising *de novo*, or *secondary* if developing from previously diagnosed low-grade gliomas [1]. Malignant gliomas represent approximately 70% of new cases of malignant primary brain tumours, and the median survival for glioblastoma patients is only 12 to 15 months [2]. The incidence rates shown in Figure 1-1 are expected to rise by 6% in the United Kingdom between 2014 and 2035 [3]. Moreover, in comparison with other cancer types, the risk factors leading to development of brain tumours are largely unknown, challenging their early detection.

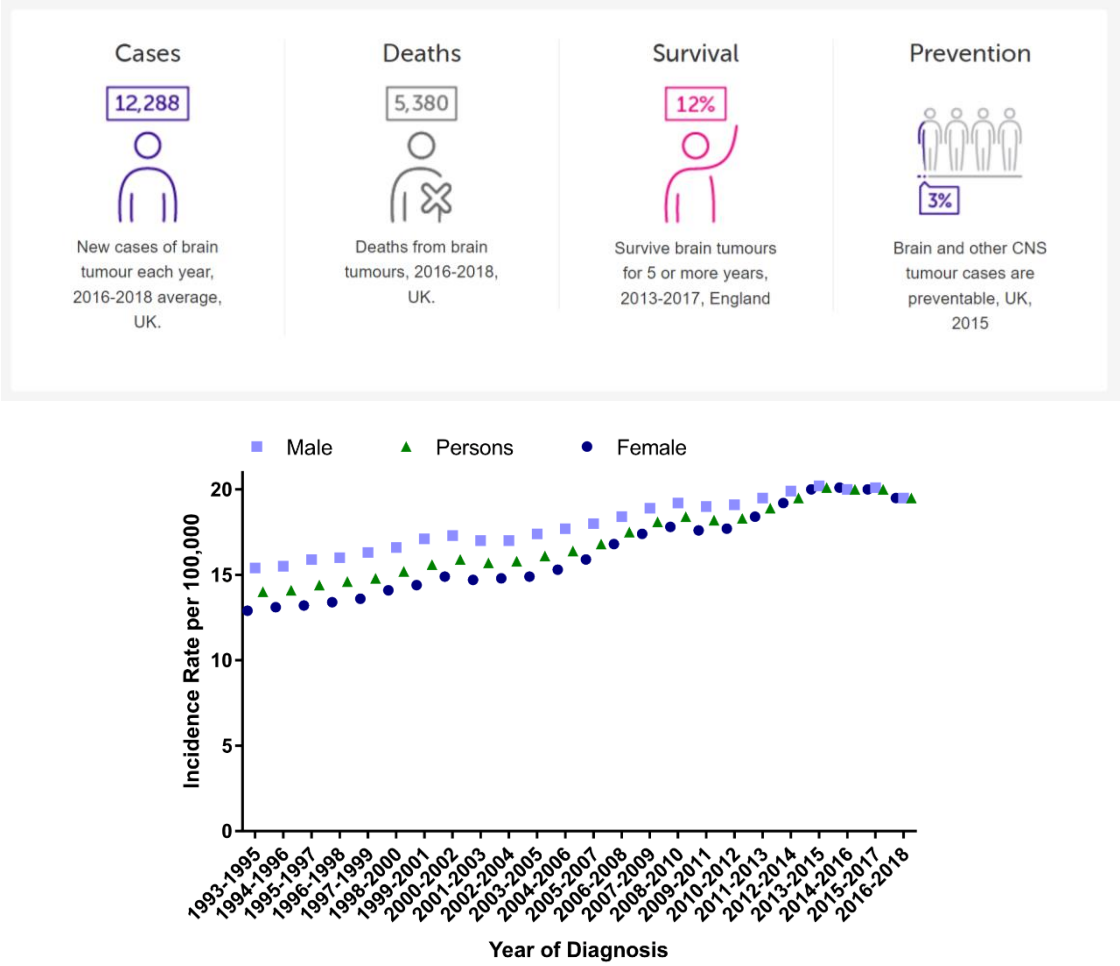

Figure 1-1 Average per Year European Age-Standardised Incidence Rates per 100,000 Population (UK) of Brain, Other CNS and Intracranial Tumours: 1993-2018

Source: Cancer Research UK, cruk.org/cancerstats, accessed April 2022.

1.1.1 Glioblastoma cells of origin, an unsolved dilemma

Differently from other cancer types, the exact identity of the cells responsible for glioblastoma initiation is still uncertain. The first classification of gliomas can be traced back to 1926 when Percival Bailey and Harvey Cushing proposed "A Classification of the Tumors of the Glioma Group on a Histogenetic Basis with a Correlated Study of Prognosis" and coined the term 'glioblastoma multiforme' [4]. This name – not in use anymore - was originally referring to the highly heterogeneous cellular composition and appearance of glioblastoma [5]. As also the name recalls, gliomas were believed to derive from the transformation of a glial, oligodendroglial or precursor cell, until it was proposed that they were instead originating from the population of neural stem cells found in specific areas of the brain [6]. In 2004 Galli et al. isolated from post-surgery human tissues of glioblastomas a population of tumour neural stem cells, as defined by their 'ex vivo multipotency' and 'ability to establish and expand glioblastoma-like tumours' by serial transplantation [7]. A contemporary study from Singh et al. showed that the expression of the cell surface antigen CD133, a marker of the neural stem cells, was associated with tumour initiation in xenografted immunocompromised mice [8]. These studies proposed a hierarchical model where transplanted CD133-positive cells give rise to the majority of CD133-negative cells found in the xenograft tumours. It remained to be defined if these glioblastoma stem cells derived from the transformation of neural stem cells or from a process of dedifferentiation of a more mature brain. More recently, Lee at al. supported the hypothesis that these tumour neural stem cells were located in the subventricular zone (SVZ), a neurogenic niche of the human brain containing resident neural stem cells [9]. Sequencing tumour tissue and normal SVZ tissue from glioblastoma patients highlighted that the normal tissue in the subventricular zone (geographically away from the tumour) contained low-level of glioblastoma driver mutations that were highly frequent in the matching tumours. These mutated SVZ cells were able to migrate to distant brain regions and drive glioblastoma development [10]. Additionally, several studies indicate that oligodendrocyte precursor cells (OPCs) would be the high proliferative subtype of stem cells responsible of glioblastoma initiation [11].

1.1.2 Genomic profiling

The genomic characterization of glioblastoma biopsies has highlighted some of the most frequently deregulated pathways in this tumour type: in particular, the over-activation of the epidermal growth factor receptor (EGFR) signalling leads to the increased signalling of the Ras and PI3K/PTEN/Akt pathways. In addition, the methylation of the retinoblastoma (Rb) promoter and consequent silencing of its expression as well altered TP53 are frequently found in glioblastoma [12, 13]. Based also on the genetic information collected from a cohort of glioblastoma patients by the Cancer Genome Atlas (TCGA) Research Network, Verhaak et al. proposed in 2010 a categorization of glioblastoma in four primary subtypes: classical, mesenchymal, proneural and neural, with each subtype defined by a specific transcriptional profile [14]. Despite this classification has managed to correlate each glioblastoma subtype with a certain degree of aggressivity and led to the identification of genetic glioma biomarkers [15], it has failed to implement the stratification of glioblastoma patients for treatment.

1.1.3 Available prognostic factors in glioblastoma

One of the main challenges presented by glioblastoma is the absence of known risk factors predictive of tumour occurrence. Few prognostic factors are routinely used in the clinics to stratify patients' to the few available therapy options. The first prognostic factor identified in glioblastoma was the methylation of O^6-methylguanine–DNA methyltransferase (*MGMT*) promoter. MGMT is a DNA repair enzyme responsible for the repair of the DNA lesions O^6-methylguanine and the less frequent O^4-methylthymine, either spontaneously occurring or caused by treatment with alkylating agents. These compounds are widely used in cancer therapy due to their cytotoxicity targeting actively replicating cells. The lack of a functional MGMT increases the sensitivity to alkylating agents [16]. The finding that around 40% of gliomas lack *MGMT* expression suggested that these tumours were more sensitive to alkylating drugs, such as temozolomide, a standard-of-care for glioblastoma patients [17]. In fact, in response to temozolomide treatment, the patients with a methylated *MGMT* promoter displayed a significantly improved survival compared to those with an unmethylated *MGMT* promoter [18].

Mutations in the genes encoding for the metabolic enzymes Isocytrate Dehydrogenase 1 (*IDH1*) and 2 (*IDH2*) have been found to have prognostic value. The aforementioned genomic analysis by Verhaak et al. grouped IDH1-mutant glioblastoma cases in the *proneural* subtype. *IDH1* mutations are found in 70% of low-grade gliomas and about 10% of glioblastomas. Patients with *IDH1* and *IDH2* mutated glioblastomas have been found to have a median survival of 31 months *versus* the 15 months median survival of patients with *IDH* wild-type tumours [19]. The profound epigenetic changes caused by IDH1 mutations have been shown to cause a hypermethylated phenotype in glioma tumours [20]. In fact, the glioma CpG island methylator phenotype (G-CIMP) has been found in younger glioblastoma patients with improved survival and a relatively better prognosis. This suggested that the genes that are hypermethylated and therefore silenced in these patients are the ones responsible for the more aggressive mesenchymal subtype [21].

In a retrospective analysis on glioblastoma patients, Shinojima et al. showed that simultaneous EGFR amplification and overexpression of the mutated form EGFRvIII represent a poor prognostic factor for patients [22]. This conclusion was opposed by a study from Heimberger et al. which found that overexpression of EGFRvIII was an independent negative prognostic factor only in patients surviving less than a year. They argued that the study from Shinojima et al. had the limitation of including a heterogeneous group of patients who had been subjected to a variety of treatments including 'gross-total resection, partial resection, and biopsy' [23]. Despite this controversial and frenzied research for glioblastoma prognostic markers, glioblastoma remains a lethal cancer and better or worse prognosis does not prospect a disease-free survival for any patient affected.

1.1.4 *In vitro* and *in vivo* models to study glioblastoma

As for other cancer types, heterogeneity is one of the main challenges to study glioblastoma. Heterogeneity is especially problematic to recapitulate *in vitro*, but over the years several factors have been identified to improve the reliability of *in vitro* models to study glioblastoma biology and metabolism. As compared with the more expensive and ethically challenging animal models, the availability and affordability of established cell lines made them a widely employed model in cancer research. Nevertheless, the genomic characterization of established cell lines widely used in glioblastoma research has highlighted the genetic derangement that prolonged *in vitro* culturing causes [24]. Even before this discovery, glioblastoma researchers had started employing patient-derived cells [25]. It had also been observed that the widely used U87MG glioblastoma cell line failed to recapitulate the typical migratory and invasive behaviour of glioblastomas when implanted in mice [7]. Glioblastoma patient-derived cells come from the mechanical disruption of tissues collected upon surgery of glioblastoma patients and, when intracranially implanted in immunocompromised mice, they successfully recapitulate the histopathological features of the parental tumours [26].

Another factor that has been found to be responsible for the inconsistency between established glioma cells and the *in vivo* tumours is the serum added to most culture media. In fact, starting from the observation that neural stem cells were cultured in serum-free media to avoid their differentiation [27], Lee et al. found that in glioblastoma the stem cells population was being lost upon culturing in serum-containing media [28]. Since this discovery, the glioblastoma research field has seen an important shift towards the use of cells cultured in the absence of serum, replaced instead by selected growth factors.

Relatively to the study of glioblastoma and more generally cancer metabolism, a recent important advancement in the field has been offered by the formulation of physiological culture media. Dulbecco's Modified Eagle Medium (DMEM) [29], one of the most common media used for culturing cancer cells, was formulated through the addition of supra-physiological concentrations of nutrients to the previously developed Eagle's minimal essential medium (MEM) [30]. These culture media date back to the ‘60s, but they have been and still are extensively used in

cancer research [31]. Given the far-from-physiological concentrations of most of the nutrients present in DMEM and similar media, it did not come as a surprise that *in vitro* cultured cancer cells were exhibiting a metabolism different from the *in vivo* reality [32]. Understanding the cellular behaviour and metabolism in an environment closer to the physiological context has been found to be crucial also for predicting cancer cells response to therapy [33]. Therefore, the last decade has seen the development of different physiological culture media that are now considered a mainstay for studying cellular metabolism [34, 35]. Further to refining the culture media, also the culturing system has recently been in the spotlight. It has been found that, when grown as three-dimensional spheroids, glioblastoma cells possess a genomic profile closer to the original tumour, whereas adherent cell cultures are more susceptible to genomic changes [36]. Moreover, the population of glioblastoma stem cells – identified as responsible of chemo- and radio-resistance – is better preserved in the spheroids than in the monolayers [37]. On the basis of their increased affinity with the original tumours, it has been suggested that glioblastoma patients-derived spheroids used to generate patients-derived xenografts in immunocompromised mice could represent patient avatars to be used for personalized medicine approaches [38].

In 1959, Russell and Burch published "The Principles of Humane Experimental Technique" to propose a framework for the ethical use and the scientific justification of animal experimentation [39, 40]. Since then, a lot of discussion has been dedicated to the Replacement-Reduction-Refinement (3Rs) of animal research in the scientific field. Despite a reductionist approach in medical research is needed for economical and practical reasons, the complexity of cancer as a multi-organ disease requires a systemic approach to its study [41]. This also applies to glioblastoma research, as highlighted by recently discovered concepts such as 'the gut-brain axis', pointing at the role of gut microbiota in brain tumour progression [42] and the capacity of glioblastoma cells to form synaptic connections with normal neurons [43, 44]. It is similarly hard to recapitulate *in vitro* the interaction between the blood-brain barrier and glioblastoma cells, and how this affects glioblastoma response to treatment [45]. Therefore, the huge effort in developing reliable animal models to study glioblastoma has produced so far three main systems: human-derived tumours xenografts in immunocompromised mice, chemically-induced brain tumours, and genetically

engineered mouse models in immunocompetent mice. Each of these systems carries certain pitfalls that need to be considered when employing them, although the collective knowledge obtained through these models can recapitulate human glioblastomas [46].

1.2 Glioblastoma metabolism and its relevance for therapy

In 2011 the 'reprogramming of cancer metabolism' was acknowledged as a cancer hallmark [47].This marked a turning point in the study of cancer metabolism, not anymore to be considered a passive consequence of damaged mitochondria (as postulated by Otto Warburg) but an oncogenic-directed and –directing process, highlighted by the discovery of *oncometabolites* [48]. Glioblastoma cells also display this metabolic reprogramming that over the years has been exploited for glioma classification and therapy.

1.2.1 IDH mutation-centric classification of gliomas

In 2016 the World Health Organization compiled a new classification of CNS tumours based on the integration of histopathological (phenotypic) and molecular (genetic) features [49]. In 2021 a revised classification was released and among the genetic alterations used to classify gliomas, IDH1 and IDH2 mutations had a central role [50]. Despite the centrality of the mutation status of a metabolic enzyme for gliomas classification, exploiting therapeutically metabolic vulnerabilities has marginally improved the prognosis for glioma patients, especially for patients affected by IDH wild-type glioblastoma. Nevertheless, characterizing the metabolism of glioblastoma has led to the development of new diagnostic tools and driven the recent advancements in the strategies to therapeutically target this type of tumour.

1.2.2 Mapping the altered glioma metabolism

Last year, our group published a review highlighting the metabolic reactions that are dysregulated in glioblastoma [51]. All these reactions have been mapped in Figure 1-2 and highlighted in red if overactive, or blue if downregulated in gliomas. This metabolic map is an attempt to visualize the current understanding of the network of reactions in central carbon and nitrogen metabolism found to be altered in gliomas. Finally, we reviewed and highlighted the pathways for which a therapeutic approach has been proposed.

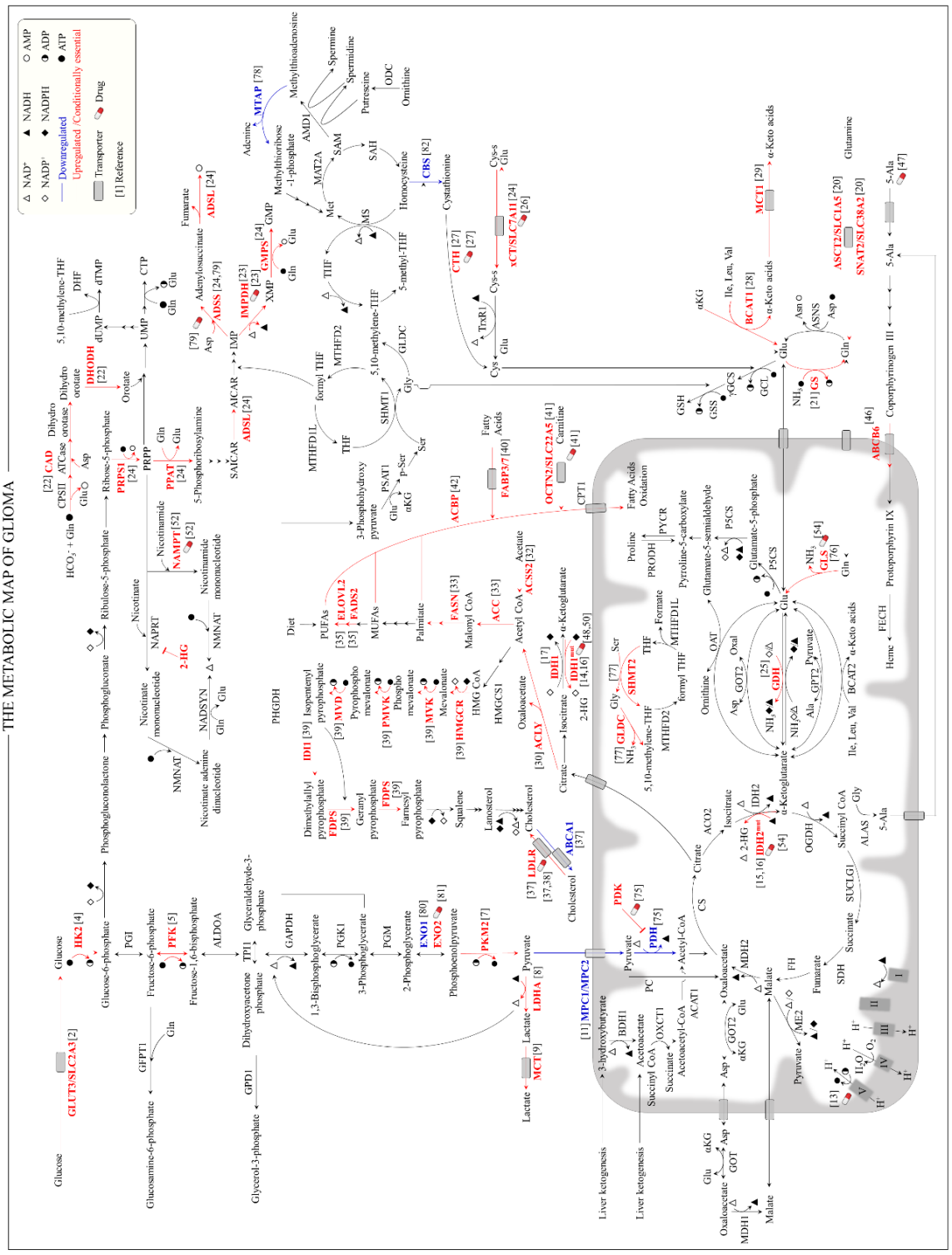

Figure 1-2 A map of the altered glioma metabolism

1.2.3 Metabolic imaging

In order to diagnose and guide the treatment of glioblastoma patients, non-invasive imaging techniques such as magnetic resonance imaging (MRI) and computed tomography (CT) are routinely used in the clinics. In addition to informing about tumour burden and disease stage, these techniques help distinguishing glioblastoma progression from pseudoprogression [52]. Pseudoprogression can occur after radio- and chemo-therapy and it appears as a contrast enhancement of the region where the tumour has been surgically de-bulked. This confounding effect is caused by the inflammatory reaction triggered by therapy-induced necrosis [53]. Recognizing pseudoprogression is critical to avoid unnecessary surgical resection or treatment, and advanced metabolic and physiologic MRI techniques provide more information than conventional MRI about the tumour microenvironment and metabolism [54]. The glucose analogue ^{18}F-2-Fluoro-2-deoxy-D-glucose (FDG) represents the most commonly used tracer for positron emission tomography (PET)-based imaging of non-brain tumours, but the elevated glucose uptake from normal brain cells weakens the accuracy of FDG-based PET imaging [55]. This has led to the development of amino acids PET tracers, in particular radiolabelled analogues of tyrosine, methionine and phenylalanine targeting the known overexpression of L-type amino acid transporters (LAT) in brain tumours cells [56]. ^{18}F-fluorothymidine (FLT) has proven useful in PET imaging due to the high uptake from highly proliferating cancer cells [57]. In fact, as compared to FDG, FLT produced a lower background and therefore a better contrast in grade III or IV brain tumours and was found to be a better predictor of tumour progression [58].

Magnetic Resonance Spectroscopy (MRS) represents another non-invasive imaging technique used to evaluate the metabolic activity of glioblastomas. One of the possible MRS applications exploits ^{13}C-labelled glucose and its conversion into ^{13}C-lactate or -pyruvate by cancer cells [59]. MRS has also been optimized to measure the tumour accumulation of 2-hydroglutarate (2-HG), the oncometabolite produced by mutant IDH1/2 gliomas [60]. Conversely, *N*-acetylaspartate (NAA) is an amino acid derivative almost exclusively produced by normal brain cells, and its levels decrease in pathological conditions [61], therefore the decrease of NAA during gliomas progression can be evaluated through MRS and used for glioma grading [62].

After a diagnosis of glioblastoma, whenever possible, the surgical resection of the tumour mass is carried out. Glioma cells have a truncated heme biosynthesis pathway and therefore accumulate the fluorescent precursor protoporphyrin IX [63]. This discovery has led to the development of fluorescence-guided surgery, where glioblastoma patients are given the protoporphyrin IX metabolic precursor, 5-aminolevulinic acid, to cause an accumulation of the fluorescent compound and guide the surgical resection of the tumour mass [64].

1.2.4 Targeting glioblastoma through the diet

Recognizing the role of cell metabolism in cancer progression and response to therapy has paved the way for developing therapeutic strategies based on dietary restrictions, with the aim of limiting the access to nutrients essential for cancer cell proliferation [65]. For instance, the ketogenic diet has been evaluated in preclinical models of glioblastoma based on the rationale that glioma cells do not efficiently use ketone bodies as a source of energy [66]. Originally introduced in 1920 as an anticonvulsant therapy for epileptic patients [67], this high-fat and low-carbohydrate diet induces a state of systemic *ketosis*, generating high circulating levels of ketone bodies and simultaneously decreasing glucose levels in the blood [68]. A ketogenic diet combined with a standard radiation therapy was able to slow the growth of brain tumours and improve the survival of mice implanted with intracranial tumours [69]. Despite the effects of a ketogenic diet on the metabolism on glioma cells have not been fully characterized yet, it has been shown that the diet reduced the production of reactive oxidative species and altered gene expression in both non-tumour and tumour tissues [70]. Hyperglycaemia has been demonstrated to significantly shorten the survival of glioblastoma patients [71], therefore the anti-tumour impact of the ketogenic diet could result from the lowered circulating glucose levels. Several clinical trials on glioblastoma patients highlighted the safety and general tolerability of a ketogenic diet [72, 73]. However, a consensus on the clinical benefits of the ketogenic diet, even when combined with standard radiotherapy and caloric restriction, has not been reached [74].

1.3 Dexamethasone in glioblastoma standard-of-care

1.3.1 Glioblastoma standard-of-care

One of the reasons behind the high rate of morbidity and mortality of glioblastoma is that the clinical symptoms that lead to glioblastoma diagnosis start arising in patients when the tumour is already advanced.

The most common neuropsychiatric symptoms include [75]:

- neuropsychological disorders, such as aphasia, apraxia, and cognitive deficits;
- intracranial pressure causing headache, singultus, nausea and vomiting;
- epileptic seizures, paresis.

Compared to other cancer types, the advancements in the genomic characterization of glioblastoma have not produced noteworthy changes in glioblastoma patients' standard of care that has stayed fundamentally unaltered for the last 30 years.

1.3.1.1 Surgery

Upon diagnosis of glioblastoma, surgical resection with the aim of "debulking" the tumour mass represents the first line of treatment for glioblastoma clinical management. Despite glioblastoma remains a lethal tumour, several factors have been identified as significantly correlating with patients' survival: age at time of diagnosis; partial or total resection (if compared with biopsy only); Karnofsky Performance status; location of the tumour (with frontal tumours correlating with longer survival) [76]. The tumour size at the time of diagnosis does not seem to predict survival and in a multicentre cohort of 1033 glioblastoma patients, the time between diagnosis and surgery was not found to be associated with patient outcome and one month was the maximally acceptable for diagnosis-to-surgery time [77].

1.3.1.2 Radiotherapy

Upon surgical removal of the tumour mass, glioblastoma patients are administered radiotherapy based on ionizing radiation with the aim of causing DNA damage, and therefore targeting the highly proliferating and replicating cancer cells [78]. Radiation doses closer to 60 Gy have been found to be more effective than lower doses [79], therefore the current standard-of-therapy consists in radiotherapy

with 60 Gy delivered in 30 fractions and combined with temozolomide [80]. Whole-brain irradiation represents an older radiotherapy approach, whereas over recent years both dose and fractionation schedule of radiotherapy have been refined in order to maximize the efficacy and minimize the long-term side effects of irradiating normal brain cells [81]. On this basis, the use of adaptive radiotherapy has been proposed in order to adapt the radiotherapy treatment plan to changes in tumour and normal brain tissue during the treatment, assessed through repeated MRIs [82]. Moreover, recent advancements in MRI techniques could improve the definition of the tumour area to be targeted with radiotherapy, reducing the radiation-induced toxicity [83]. Onset of radioresistance represents one of the issues related to the clinical management of glioblastoma. Carruthers et al. showed that high levels of replication stress drive constitutive DNA-damage response and radiation resistance, that can be targeted through a dual inhibition of ataxia telangiectasia and Rad3-related protein (ATR) and Poly (ADP-ribose) polymerase (PARP) proteins [84]. The characterization of other radioresistance mechanisms mediated by factors such as tumour microenvironment, hypoxia, and altered metabolism have led to the identification of potential radiosensitizers, although a lack of promising preclinical data halted their progress to clinical trials [85].

1.3.1.3 Chemotherapy

In 2005, Stupp et al. showed in a cohort of 573 patients from 85 centres the statistically significant improvement in survival coming from the addition of temozolomide to the glioblastoma standard-of-care based on maximal surgical resection followed by radiotherapy [80]. Temozolomide is an alkylating agent whose antitumor activity as a single agent had been already observed in the treatment of recurrent glioma [86]. Before the introduction of temozolomide, glioblastoma chemotherapy was based on the nitrosoureas introduced in the 1970s, even though the survival advantage of radiotherapy and carmustine (a nitrosourea drug) combination had not been proven by a Phase III clinical trial [87]. A more recent study investigating a chemotherapeutic regimen based on another nitrosourea, i.e. nimustine, in glioblastoma patients pretreated with temozolomide showed that the drug was not effectively improving patients' progression-free survival [88]. The discovery of the major role played by the vascular endothelial growth factor (VEGF) in regulating the highly angiogenic

properties of glioblastoma [89] led to the hypothesis that the VEGF inhibitor, bevacizumab, could be an effective treatment for glioblastoma. In 2009, the United States Food and Drug Administration granted accelerated approval for bevacizumab, a humanized monoclonal antibody, as a single agent treatment for recurrent GBM. On the other hand, the European Medicines Agency did not approve it due to the lack of enough clinical evidence supporting its benefit for glioblastoma patients [90]. MRI-based studies had showed that bevacizumab treatment was effective at reducing tumour microvessels and therefore vascularization [91], although favouring the invasiveness of glioblastoma cells in the normal brain [92]. The molecular analysis of tumour samples of a deceased glioblastoma patient who had undergone bevacizumab treatment upon tumour recurrence showed that VEGF inhibition was accompanied by increased expression of matrix metalloproteinases, known to have a role in sustaining tumour invasion [93]. In fact, upon anti-VEGF therapy, the expression of other proangiogenic and proinvasive factors render glioblastoma cells resistant to this type of treatment [94]. In the clinical settings, the addition of bevacizumab to the combination of radiotherapy and temozolomide has not proven effective at improving glioblastoma patients overall survival [95]. Moreover, a more recent clinical trial showed that the combination of the nitrosourea drug, lomustine, and bevacizumab failed at prolonging survival over lomustine single treatment [96]. Overall, the benefit deriving from the clinical use of bevacizumab as a single agent is questionable and has been recommended as a last-line treatment upon failure of radiotherapy, temozolomide and lomustine [97].

1.3.1.4 Corticotherapy for the management of tumour-associated oedema

Even before proceeding with the surgical and radio-chemotherapy treatments, glioblastoma patients are usually subjected to corticotherapy, i.e. administration of synthetic corticosteroids, to decrease the tumour-associated oedema therefore reducing the intracranial pressure and transiently ameliorate patients' symptoms [98]. The glioblastoma-induced oedema is both 'cytotoxic', due to the extreme cellular swelling and consequent cell death, and 'vasogenic' because of the disruption of the blood-brain barrier [99]. In peritumoural oedema, whole plasma leaks even at distance from the tumour due to the increase in the microvascular permeability of the blood-brain barrier [100]. The introduction of corticotherapy in the clinical management of glioblastoma dates back to 1961, when Galicich,

French and Melby described the effects of dexamethasone on dramatically reducing brain oedema and consequently the mortality and morbidity of brain tumour patients [101]. Since then, corticosteroids have been considered a ‘revolution in neurosurgical and neurological care’, even though concerns have been raised about the side effects of prolonged treatments, given the broad range of targets for glucocorticoids in normal tissues and organs [102]. Controlled clinical trials to directly address glucocorticoids impact on glioblastoma patients are missing, and for this reason the choice and dose of glucocorticoids for the treatment of brain tumour-associated oedema are still empirical. Compared to other glucocorticoids such as hydrocortisone, cortisone and prednisolone, dexamethasone represents the glucocorticoid of choice for glioblastoma patients because of a long half-life and limited mineralocorticoid activity [103], and is administered in the range of daily 4-16 mg for most of the patients and 24-100 mg for patients with severe symptoms [104].

1.3.2 Glucocorticoids mechanisms of action

Natural corticosteroids are hormones derived from cholesterol and whose synthesis and secretion by the adrenal glands (*zona fasciculata*) is regulated through the hypothalamic-pituitary-adrenal axis following circadian and ultradian rhythms [105]. Synthetic glucocorticoids are more potent and have a higher bioavailability than their natural counterparts, but both physiological and synthetic glucocorticoids exert most of their functions through their main target, the glucocorticoid receptor (GR), a nuclear receptor encoded by the *NR3C1* gene [106]. The responses mediated through the GR can be divided in 'genomic', dependent on the regulation of gene expression, and 'non-genomic', more rapid and not requiring nuclear GR-mediated gene regulation. The 'genomic' actions represent the most characterized effects of glucocorticoids signalling and are mediated by their direct binding to the GR. When ligand-bound, GR homodimerizes and translocates to the nucleus, where it acts as a transcription factor binding to the glucocorticoids regulated elements in the promoters of target genes [107]. The 'non-genomic' mechanisms are still poorly understood but several reports point at the existence of membrane-associated glucocorticoid receptors, able to activate downstream signalling cascades [108, 109]. As shown in Figure 1-3, among the genes whose transcription is increased by glucocorticoids, we found genes encoding glucocorticoid-induced leucine zipper (GILZ), tristetraproline (TTP) and annexin 1 (ANXA1). Despite some effects exerted by glucocorticoids can be highly organ-specific, the systemic consequences of the glucocorticoid receptor are the increased expression of anti-inflammatory genes and the repression of pro-inflammatory cytokines [107]. Differently from the glucocorticoids genomic actions, non-genomic actions of glucocorticoids do not involve transcriptional changes, causing more rapid and acute cellular effects. Glucocorticoids can affect basal calcium homeostasis, increasing or reducing CA^{2+} levels depending on the cell type considered, but they have also been shown to impact on the production of reactive oxygen and nitrogen species [110]. There are still many open questions about the non-genomic side of glucocorticoids-mediated signalling, and answering these questions is particularly relevant in the quest for therapeutic alternatives to glucocorticoids.

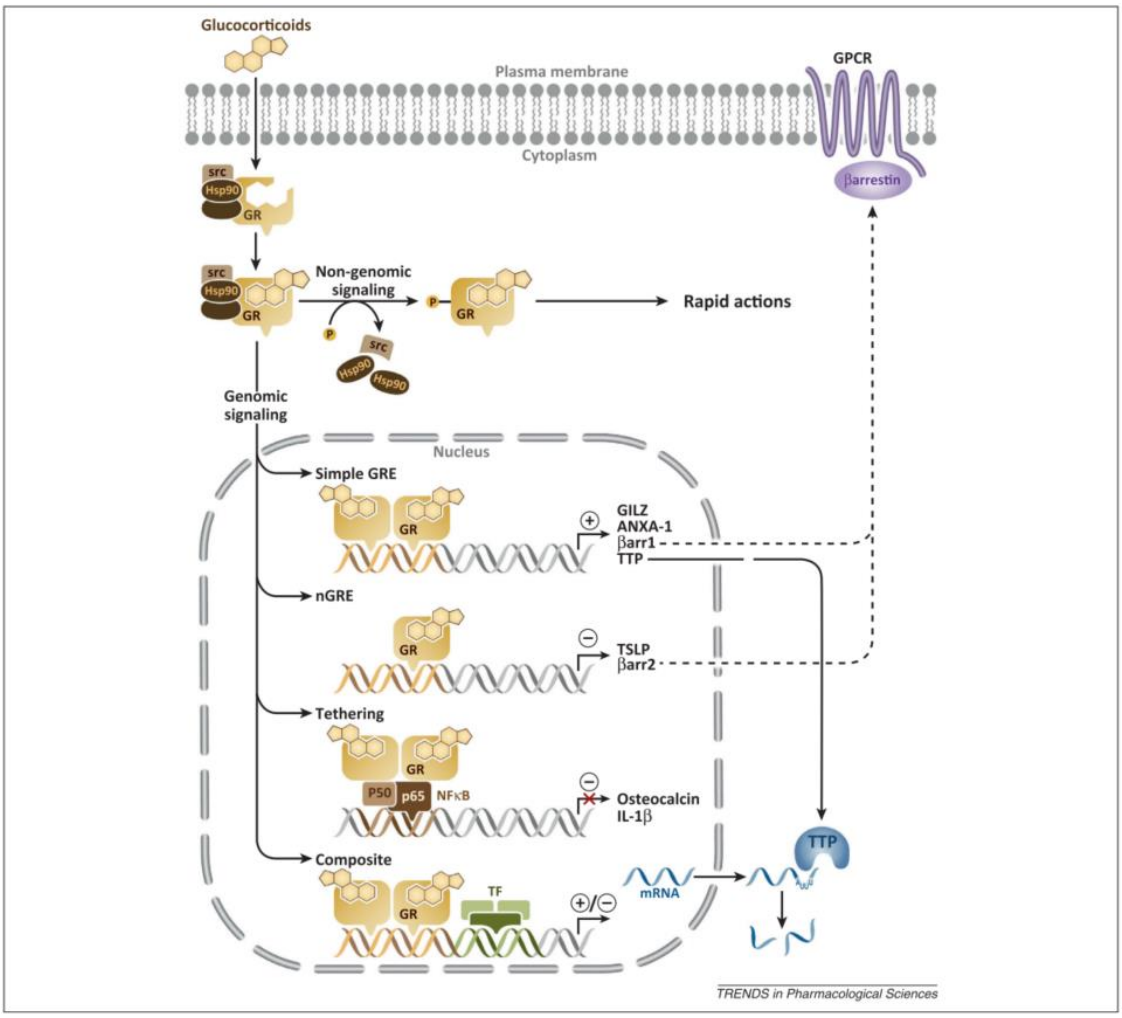

Figure 1-3 Glucocorticoids mechanism of action

The figure has been adapted from Kadmiel, M. & Cidlowski, J. A. Glucocorticoid receptor signaling in health and disease. Trends in Pharmacological Sciences 34, 518-530, doi:10.1016/j.tips.2013.07.003 (2013) [107]. The figure shows glucocorticoids mechanism of action, as summarized in the text.

1.3.3 Glucocorticoids effects on glioblastoma models and patients' survival

Synthetic glucocorticoids – such as prednisolone, dexamethasone and methylprednisolone – represent key drugs in the treatment of acute lymphoblastic leukaemia because of their ability to induce apoptosis in immature lymphoid cells [111]. Differently, glucocorticoids have been reported to increase or inhibit glioblastoma cells proliferation depending on cell types and culture conditions. Notably, most of the observations in support of a cytotoxic effect of glucocorticoids in glioblastoma have been obtained using concentrations exceeding those achievable in patients [112]. The dual effects of dexamethasone on glioblastoma cells proliferation have been demonstrated to be dependent on GR activity, since they were counteracted by the glucocorticoids antagonist RU486 [113]. As already discussed, one of the pathologic effects of glioblastoma is the disruption of the blood-brain barrier, causing vasogenic oedema. Few *in vivo* studies have shown that dexamethasone reduces the permeability of the disrupted barrier through a GR-dependent response [114]. The cells forming the blood-brain barrier are bound through tight junctions that are made up of two kinds of integral membrane proteins, such as occludins and members of claudin family. Thanks to the presence of a glucocorticoid-responsive element in the promoter of the occludin (*OCLN)* gene, glucocorticoids are able to induce its expression, explaining at least in part the GR-mediated effects on the barrier integrity [115]. Moreover, glucocorticoids can change glioma cells morphology and migratory capacity [116]. In rat C6 glioma cells hydrocortisone has been shown to induce an alteration of the cell surface through the deposition of fibronectin and rearrangement of the microtubules [117].

Corticotherapy is usually associated with radio- and chemo-therapy, and several studies have investigated the effects of chemotherapeutic drugs and glucocorticoids combination *in vitro* and *in vivo*. However, these studies have produced conflicting results, showing that dexamethasone can either protect glioma cells from the cytotoxic and antiproliferative effects of chemotherapy [118, 119] or synergize against glioma cells proliferation [120]. For example, a pre-treatment of U87MG xenografts with dexamethasone increased the efficacy of carboplatin and gemcitabine [121]. It is clear that brain tumour patients benefit from corticotherapy to control tumour-associated oedema and consequent

neurological symptoms, but these contradictory results on glioma cell biology primed the investigation of dexamethasone effects on glioblastoma patients' survival. In 2002, a retrospective analysis on 138 patients with either brain metastases or glioblastomas showed that upon combination of long-term dexamethasone treatment with radiotherapy, there was a pronounced decrease in clinical improvement and an increase in dexamethasone-induced side effects after radiotherapy [122]. In a retrospective analysis from 2015 looking at glioblastoma patients undergoing radiotherapy and temozolomide treatment, dexamethasone proved to be an indicator of poor prognosis and reduced progression-free survival, unless the patients had been concurrently treated with bevacizumab [123]. In fact, several groups investigating bevacizumab as an anti-angiogenic therapy had highlighted its anti-oedema properties, suggesting that this drug could represent a valid alternative to corticotherapy [93, 124]. Corticosteroids impact on patients' survival and the effectiveness of VEGF inhibition as an anti-oedema therapy have been investigated in a retrospective analysis on glioblastoma patients. In 2016, Pitter et al. observed that in three independent patients' cohorts corticotherapy at the start of radiotherapy was associated with poor prognosis, independently from temozolomide treatment [125]. The study also highlighted that bevacizumab was effective at reducing oedema-related neurological signs in murine glioma models and, despite not being able to prolong the overall survival of newly diagnosed glioblastoma patients, it prolonged the progression-free survival. In [126] a dexamethasone induced gene signature was identified as predictive of poor survival in glioblastoma patients. Another clinical study suggested that the dexamethasone-related global immunosuppression reduced the efficacy of temozolomide-based chemotherapy when combined with the electric-field based therapy (TTFields) [127]. The latter is a treatment currently approved for recurrent glioblastomas and based on the emission of alternating electric fields targeting cells undergoing mitosis. The lack of clear cut results about the benefit of anti-VEGF therapy in glioblastoma patients [90, 128] has led the search for further alternatives to corticotherapy.

Human corticotropin-releasing factor (hCRF) has been shown to be effective at reducing tumour-associated oedema through a direct effect on endothelial cells [129] and phase I/II clinical trials demonstrated its tolerability [130]. However, the limited efficacy of hCRF found in clinical trials prevented its approval for the

treatment of tumour-associated oedema. Vascular normalization through anti-VEGF therapy seems the most promising alternative to corticotherapy, and has led to development of a second generation of drugs whose effectiveness remains to be proven in clinical settings [131].

1.3.4 Metabolic alterations induced by glucocorticoids

Glucocorticoids modulate several metabolic pathways, particularly glucose and lipid metabolism. The high tissue-specificity of glucocorticoids-mediated effects explains part of the complexity of their consequences on cellular metabolism. In fact, in the liver they promote gluconeogenesis [132], whereas in skeletal muscle and white adipose tissue they cause a decrease in glucose uptake and usage, antagonizing the insulin signalling [133]. The glucocorticoids-mediated induction of gluconeogenesis is responsible for generating glucose from non-carbohydrate substrates in the liver, a process mediated by the transcriptional activation of genes such as Phosphoenolpyruvate carboxykinase (*PEPCK*), Phosphoenolpyruvate carboxykinase 1 (*PCK1*) and Glucose-6-phosphatase (*G6PC*) [134]. These glucocorticoids-mediated metabolic effects are critical during exposure to stress such as fasting or starvation, when plasma glucose levels have to be preserved to maintain the correct functioning of the brain [135]. The brain represents the most glucose-avid organ of the human body: although it accounts for ~ 2% of the body weight, it consumes ~20% of glucose intake [136]. Chronic exposure to dexamethasone has been demonstrated to significantly increase the glycaemia of brain tumour patients [137], possibly due to an impairment of the glucose transport system [138]. Glioblastoma cells are highly glycolytic, and enhanced levels of glycolysis are known to correlate with resistance to radiotherapy [139]. Therefore, lowering the hyperglycaemia of glucocorticoids-treated patients could be obtained by the ketogenic diet. Another metabolic gene containing a glucocorticoid responsive element in its promoter is *GLUL*, encoding for glutamine synthetase (GS) [140]. It has been reported that GS expression and activity are increased upon corticosteroids treatment in normal as well as in glioblastoma cells [141, 142]. Physiologically, mature astrocytes express high levels of GS, where it converts the potentially neurotoxic stimulatory neurotransmitter glutamate into glutamine. Therefore, the antiepileptic effects of corticosteroids could be explained by the combination of anti-inflammatory properties and their stimulatory effects on GS expression in the brain.

Finally, glucocorticoids are also known to orchestrate lipid metabolism. In fact, dexamethasone administration induces dysregulation of the expression of lipogenic genes in liver and adipose tissue, increasing *de novo* lipogenesis and inducing lipid accumulation (i.e. hyperlipidemia) [143]. The metabolomics

profiling of plasma samples withdrawn from of a cohort of healthy human males upon administration of 4 mg (single dose) dexamethasone highlighted the significant alteration of 150 metabolites, emphasizing the impact of glucocorticoids on systemic metabolism [144]. Moreover, early this year, in the context of acute kidney injury von Mässenhausen et al. showed that dexamethasone sensitizes to ferroptosis-mediated cell death through induction of Dipeptidase 1 (DPEP1) and decrease of GSH levels [145]. Unravelling if dexamethasone is able to exert analogous effects in the cancer context requires further investigation.

1.4 Aim of the project

The centrality of glucocorticoids in the treatment of the brain tumour-associated oedema has been unquestionable thus far, and dexamethasone effectiveness, affordability and accessibility are paramount for the clinical management of glioblastoma patients worldwide. However the knowledge of a plethora of side effects related to glucocorticoids administration moves the continuous search for alternatives. The aim of this project is to characterize the effects of clinically relevant doses of dexamethasone in naïve glioblastoma cells, in particular on their metabolism. This approach led to the identification of metabolic reactions that are selectively regulated by dexamethasone in glioblastoma cells and tumours, and that could ultimately be exploited for novel therapeutics and diagnostic approaches.

Chapter 2. Materials and Methods

2.1 Materials

2.1.1 Reagents

Reagent	Supplier	Catalogue #
Acetonitrile (HPLC grade)	VWR	75-08-5
Acrylamide solution-30% w/v	Severn Biotech	20-2100-05
Accutase (StemPro)	Gibco	A11105-01
AlbuMAX™ II Lipid-Rich BSA	Gibco	11021-037
Ammonium persulfate (APS)	Sigma-Aldrich	A3678
Antimycin A	Sigma Aldrich	A8674
Bovine Serum Albumin (BSA)	Millipore	12659
Cell Fractionation Kit	Cell Signaling Technology	9038S
CHS828	Tocris	6753
Core Histone Isolation Kit	Sigma-Aldrich	EPI024
Dexamethasone	Sigma-Aldrich	D1756
Dexamethasone-21-phosphate disodium salt	Sigma-Aldrich	D1159
Dimethyl Sulfoxide (DMSO)	Sigma-Aldrich	D8418
DNeasy Blood & Tissue Kit	Qiagen	69504
Earle's Balanced Salt Solution (EBSS)	ThermoFisher Scientific	24010-043
Ethanol	VWR	64-17-5
FCCP	Sigma-Aldrich	C2920
FK866 hydrochloride	Tocris	4808
Folin & Ciocalteu's phenol reagent	Sigma-Aldrich	F9252
Formic acid Optima LC-MS	ThermoFisher Scientific	A117-50
hBFGF	PeproTech	AF-100-18B
hEGF	PeproTech	AF-100-15
Heparin sodium salt from porcine intestinal mucosa	Sigma-Aldrich	H3393
Insulin, Transferrin, Sodium Selenite (ITS)	Gibco	41400

Laemmli Sample Buffer (4X)	Biorad	1610747
L-Glutamine	Gibco	25030-024
L-Methionine	Sigma-Aldrich	M5308
LGK974	Selleck	S7143
Matrigel® Matrix	Corning	356231
MEM Non-essential amino acids (100X)	Gibco	11140-035
Methanol (HPLC grade)	VWR	67-56-1
Minimum Essential Medium (MEM)	Gibco	21090-022
5-amino-1-methylquinolinium iodide (NNMTi)	Tocris	6900
*N*1-methylnicotinamide chloride	Sigma-Aldrich	SML0704
Nicotinamide	Sigma-Aldrich	N0636
Oligomycin A	Sigma-Aldrich	75351
PageRuler Prestained Protein Ladder	ThermoFisher Scientific	26616
Pierce Bicinchonic Acid (BCA) Assay Reagent A	ThermoFisher Scientific	23228
Pierce Assay Reagent B	ThermoFisher Scientific	1859078
Pierce™ protease and phosphatase inhibitor mini tablets	ThermoFisher Scientific	A32961
Protran Supported Western Blotting membranes, nitrocellulose 0.2 µm	Amersham	10600001
RIPA Lysis Buffer (10X)	Millipore	20-188
RNase-Free DNase Set (50)	Qiagen	79254
RNeasy Mini Kit	Qiagen	
Rotenone	Sigma-Aldrich	R8875
Seahorse XF Calibrant	Agilent	100840-000
Sodium Carbonate (Na_2CO_3)	Sigma-Aldrich	497-19-8
Sodium Chloride (NaCl)	ThermoFisher Scientific	7647-14-5
Sodium Copper EDTA	Fluka	03668
Sodium Deoxycholate (DOC)	Sigma-Aldrich	302-95-4
Sodium Hydroxide (NaOH)	Sigma-Aldrich	795429
Sodium Pyruvate	Sigma-Aldrich	S8636

Temozolomide	Merck	T2577
Tetramethylethylenediamine (TEMED)	Sigma-Aldrich	T9281
Trypsin 2.5% (10X)	Gibco	15090-046
Vitamin B12	Sigma-Aldrich	V6629
4-phenylpyridine	Sigma-Aldrich	P33429

2.1.2 General solutions

- LC-MS extraction solution: methanol 50%, acetonitrile 30%, water 20%
- Modified Lowry method:
    - Solution A: 5% Sodium Deoxycholate in water 10%, NaOH 5N 20%, Water 70%
    - Solution B: for a 2 L solution, Sodium Copper EDTA (0.5 g), Sodium Carbonate (40 g), NaOH (8 g)
    - Solution C: Folin Ciocalteu's Phenol

2.1.3 Antibodies

2.1.3.1 Antibodies for Western blotting

Antibody	**Supplier**	**Catalogue #**
B-catenin	Abcam	ab16051
BCL-xL	Cell Signaling Technology	2762
CD133	Abcam	ab226355
Glucocorticoid Receptor (D6H2L)	Cell Signaling Technology	12041S
Glutamine Synthetase	BD Biosciences	610517
Histone 3	Abcam	ab18521
H3K4me3	Abcam	ab8580
H3K9me3	Abcam	ab8898
H3K27me3	Abcam	ab272165
Nestin	Abcam	ab134017
NNMT	Abcam	ab119758
Sox2	Abcam	ab97959
UGDH	Abcam	ab246999
Vinculin	Cell Signaling Technology	13901

2.1.3.2 Antibodies for confocal microscopy

Antibody	Supplier	Catalogue #
Glucocorticoid Receptor	Cell Signaling Technology	12041S
Nestin	Abcam	ab134017

2.1.3.3 Antibodies for IHC

Antibody	Clone	Supplier	Catalogue #
Glucocorticoid Receptor	D6H2L	Cell Signaling Technology	12401
Ki67	D3B5	Cell Signaling Technology	12202
Nestin		Abcam	ab6320

2.2 Methods

2.2.1 Cell culture and media preparation

The patient-derived glioblastoma cell lines used for this project have been obtained from: Prof. Simone Niclou, Luxemburg Institute of Health (P3, P13, T16), Prof. Hrvoje Miletic, University of Bergen (BG7), Prof. Steve Pollard, University of Edinburgh (E1, E15, E22, E25, E27, E30, E34, E55, E56). For routine culturing, a supplemented version of MEM medium has been used (details can be found in Chapter 3 of this thesis), while Plasmax medium has been used for the experiments. Details of Plasmax composition and preparation can be found in [35]. GBM cells were routinely cultured as adherent monolayers for a limited number of passages (<15) on Petri dishes coated with a layer of Corning Matrigel® (diluted 2% in EBSS medium). Plates were coated with the Matrigel® solution and kept at 25˚C for 1 hour before plating the cells. Therefore, Matrigel® solution in excess was removed and the cells seeded. Short Tandem Repeat (STR) DNA analysis of BG7, P3, P13 and T16 cells was performed at the beginning of this project and all cell lines were routinely tested for absence of mycoplasma infection using the MycoAlert Mycoplasma Detection Kit (Lonza).

2.2.2 Cell proliferation assays

2.2.2.1 Cell Counting

2-6 x 10^4 cells/well were seeded on 24-well plates coated with Matrigel®. At the end of the experiment, the cells were quickly washed three times with PBS and 400 µL of Trypsin was added to each well. The content of each well was resuspended in cell counting solution, and counted with a CASY cell counter (Roche Applied Science).

2.2.2.2 Incucyte Live-Cell imaging

2-6 x 10^4 cells/well were seeded in 24-well plates coated with Matrigel®. After 24 hours the medium was replaced with Plasmax (2.5mL/well) and the index of cell confluence was recorded every hour with the IncuCyte Zoom imaging system (Essen Bioscience) for 4 days (maintained at 37˚C and 5% CO_2).

2.2.2.3 Spheroids growth

5×10^2-2×10^3 cells/well were seeded in round bottom ultra-low attachment 96-well plates (Corning®, #7007) in Plasmax medium. 24 h after seeding the medium was supplemented with vehicle or 0.1 µM dexamethasone. Every 7 days, pictures of the spheroids were taken and the medium was changed to avoid nutrient exhaustion. ImageJ was used to quantify the spheroids area.

2.2.3 Protein Quantification

2.2.3.1 BCA method

The Bicinchoninic Acid (BCA) assay was one of the methods employed for protein quantification [146]. A standard curve was prepared with BSA (0, 100, 250, 500, 750, 1250, 1250, 2000 µg/mL). The samples for the standard curve and the cellular extracts (2.5 or 5 µL) were placed in duplicates or triplicates in a 96-well plate, 200 µL of the BCA solution was added to each well and the plate was incubated for 30 min at 37˚C. The BCA solution was composed of Pierce Solution B and Pierce Solution A in a proportion 1:50. The solution reacted with the proteins contained in the extracts and developed a blue/purple colour, whose absorbance was read using a SpectraMax Plus (Molecular Devices).

2.2.3.2 Modified Lowry Assay

A modified version of the Lowry assay [147] was used to quantify the protein concentration upon metabolic extraction of both adherent monolayers and the three-dimensional spheroids.

<u>Adherent monolayers</u>

Briefly, after metabolites extraction the 6-well plates were air dried and kept at 4˚C. A standard curve was prepared with BSA in 6-well plates (0-800 µg BSA). Solution A (400 µL/well) was added and the plates were shaken vigorously at room temperature for 40 min. Solution B (4 mL/well) was added and the plates were shaken at room temperature for 10 min. Solution C (400 µL) was added and the plates were shaken slowly for 40 min at RT. 200 µL/well were transferred to a 96-well plate and the absorbance was read at 680 nm with a plate spectrophotometer.

Three-dimensional spheroids

A standard curve was prepared with BSA (0-4 mg) in 50 mL falcon tubes. Solution A (750 µL) was added to the frozen pellets obtained upon metabolic extraction of the spheroids. The pellets were vortexed and sonicated with 2-3 cycles of sonication. The solution was transferred to 50 mL falcon tubes and shaken for 30 min. 10 volumes (7.5 mL) of Solution B were added to each sample and the tubes were shaken for 10 min. Solution C (750 µL) was added and the tubes shaken slowly for 30 min. 200 µL/sample were transferred to a 96-well plate and the absorbance was read at 680 nm in a plate spectrophotometer.

2.2.4 Western blotting

2.2.4.1 Whole cell lysates preparation

3.5-5 x 10^5 cells/well were seeded in Plasmax medium in 6-well plates coated with Matrigel®. At the end of the experiment, cells were quickly washed with ice-cold PBS and 50-100 µL of RIPA buffer added to each well. The cells were lifted with a cell scraper, collected in an Eppendorf tube and stored at -20˚C. For protein quantification, the pellets were thawed on ice and centrifuged at 12000 g for 15 min. The supernatant was collected and quantified using the BCA method described above.

2.2.4.2 Samples preparation

After protein quantification, samples were prepared for loading at equal amounts (20-40 µg). 4X Laemmli Buffer was added to the samples that were mixed and boiled at 95˚C for 5 min.

2.2.4.3 SDS-Page and Western blotting

9.5% or 11.5% SDS-Page gels were prepared and poured in a Biorad tank and a layer of water was added to maintain a level surface. After the gels had solidified, the water was removed and the stacking gels were added. The wells were formed by inserting 10- or 15-wells gel combs. The comb was removed and the gel was transferred in a tank containing 1X SDS-PAGE running buffer. A pre-stained protein ladder (3-5 µL) was loaded and used as a reference for the proteins molecular

weights. Protein separation was obtained applying a constant voltage current at 80 V for 20 min followed by 1-2 h at 100 V.

Upon SDS-PAGE, proteins were transferred to a nitrocellulose membrane using a BioRad apparatus. The gel and membrane were placed between blotting paper and sponges. The tank was filled with 1X Blotting buffer and an ice pack was placed within the tank to keep the system cold during the transfer. The transfer was performed with constant current at 0.4 A for 1 h.

After the transfer, the nitrocellulose membranes were stained with Ponceau Red solution to control the levels of total proteins. The membranes were then washed in TBST solution to remove the Ponceau Red solution and incubated for 1 h in blocking solution, TBST containing 5% BSA or 5% milk powder. The membranes were then incubated at gentle shaking overnight at 4˚C with primary antibodies dissolved in the blocking solution. The membranes were washed three times in TBST for 10 min, and incubated for 1 h at room temperature with LI-COR secondary antibodies dissolved in 5% milk TBST solution. The membranes were then washed three times in TBST for 10 min and the proteins were visualized using the Odyssey DLx Imaging system.

2.2.5 RNA sequencing

3-5 x 10^5 cells/well were seeded in 6-well plates previously coated with Matrigel® and cultured in Plasmax medium for three days. After three days, Plasmax medium was refreshed and 24 h later the cells were counted using a Casy counter. The cells were harvested and RNA was extracted using the QIAshredder/RNeasy Mini Kit (Quiagen). On-column deoxynuclease-ribonuclease digestion was performed and 1.5 µg of RNA was diluted in 50 µL of water to check the quality of the purified RNA on an Agilent 2200 TapeStation using RNA screentape. Agilent 2200 TapeStation (D1000 screentape) and Qubit (Thermo Fisher Scientific) were used to assess quality and quantity of the DNA libraries, respectively. The libraries were run on the Illumina Next Seq 500 using the High Output 75 cycles kit (2 ×36 cycles, paired-end reads, single index). A PolyA selection was performed to enrich for messenger RNAs. Quality control of the raw RNA-seq data files was performed by FastQC (www.bioinformatics.babraham.ac. uk/projects/fastqc/) and fastq_screen (www.bioinformatics.babraham.ac. uk/projects/fastq_screen/).

Then, RNA-seq reads were aligned to the human genome (GRCh38.75) and resulting bam files were processed with htseq_count (https://htseq.readthedocs.io/en/ release_0.10.0/). The RNA sequencing was performed by William Clarke and data analysis performed by Robin Shaw at the Cancer Research UK Beatson Institute.

2.2.6 Liquid Chromatography-Mass Spectrometry

2.2.6.1 Metabolic extraction

Adherent monolayers

GBM cells were seeded in 6-well plates coated with Matrigel®, and cultured in Plasmax medium supplemented with vehicle (ethanol 100%) or 0.1 µM dexamethasone. After 3 days, Plasmax medium was refreshed and 24 h later the cells were extracted. The cells were quickly washed three times with ice-cold PBS and the intracellular metabolites were extracted with 400 µL ice-cold extraction solution (20% water, 30% acetonitrile and 50% methanol) for 5 min at 4˚C. The extracted samples were then centrifuged 10 min at 12,000 g, 4˚C to remove cellular debris. The clear supernatant was transferred to LC-MS vials and stored at -74˚C until analysed. The 6-well plates were air dried and stored at 4˚C until the proteins were quantified with a modified Lowry protein assay.

Three-dimensional spheroids

This protocol was adapted from [35]. GBM cells were transferred to Ultra-low attachment surface 75 cm^2 flask (Corning®, #3814) to favour the aggregation of suspension of spheroids. Cells were incubated in Plasmax medium supplemented with vehicle (ethanol 100%) or 0.1 µM dexamethasone for 3 days. After three days, in order to refresh Plasmax medium, spheroids were transferred to a 50 mL falcon tube, centrifuged 5 min at 300 g and the resuspended in the flask in 50 mL freshly prepared Plasmax. After 24 h, the spheres were collected for metabolic extraction. 30 mL of medium were removed from each flask, being careful not to disrupt the spheroids. The spheres were then collected in a 50 mL falcon tube, quickly spin (1 min at 600 g), and the supernatant was removed. The pellet was transferred to an Eppendorf tube, where it was washed with 1 mL Ice-cold PBS and spun for 10 s. The PBS was carefully removed and the spheres were extracted in 1 mL extraction solution, vortexed and incubated for 5 min at 4˚C. The

extracted samples were then centrifuged (10 min at 13,000 g, 4˚C), and the supernatants were transferred to LC-MS vials, whereas the cellular pellets were stored at -20˚C for protein quantification with a modified Lowry protein assay.

Mice tissues

Frozen tissue fragments (10-30 mg) were weighted and extracted in 25 µL of extraction solution/mg of tissue. The tissues samples were homogenized by using the Precellys® beads (CK14 Lysing Kit, Bertin). For the serum samples, 5 µL were diluted in 245 µL LC-MS extraction solution. The extracted tissues were centrifuged for 10 min at 12000 g, 4˚C and the supernatant was stored at -80˚C until LC-MS analysis.

2.2.6.2 Targeted and untargeted metabolic analysis

The LC-MS was performed as described in [35]. A Q Exactive Plus Orbitrap Mass Spectrometer (Thermo Fisher Scientific) was employed coupled with a Ultimate 3000 high-performance liquid chromatography (HPLC) system (Thermo Fisher Scientific). The monolayers, spheroids or tissues extracted samples were injected (5 µL) and separated on a ZIC-pHILIC column (SeQuant; 150 mm by 2.1 mm, 5 µm; Merck KGaA, Darmstadt, Germany) coupled with a ZIC-pHILIC guard column (SeQuant; 20 mm by 2.1 mm) held at 45˚C. The chromatographic separation was performed with a resolution of 35,000 (at 200 m/z) with electrospray ionization and polarity switching, to detect both positive and negative ions over a mass range of 75-1000 m/z. The metabolites were separated with a 15 min mobile phase gradient, which started at 80% acetonitrile / 20% ammonium carbonate (20 mM, pH 9.2), and decreased to 20% acetonitrile / 80% ammonium carbonate with a flow rate of 200 µL/min (total run time of 24.5 min).

Compound Discoverer software (version 2.1.0.401, Thermo Fisher Scientific) was employed to perform the untargeted metabolomics analysis. The retention times were aligned across all samples (maximum shift, 2min; mass tolerance, 5 ppm). The unknown compounds were detected and grouped using a minimum peak intensity of 1 x 10^5, a mass tolerance of 5 ppm, and a maximum peak width of 0.5 min (RT tolerance, 0.2 min). Compound Discoverer “Fill Gap” feature was used to fill the missing values (mass tolerance, 5 ppm; signal/noise tolerance, 1.5). The compounds were identified by comparing the mass and retention time of experimental peaks to an in-house library generated using commercial standards. Data dependent fragmentation was also employed to aid metabolite identification by matching the MS2 fragmentation spectra to mzCloud (https://www.mzcloud.org/). LC-MS analysis was carried out as described above

using a representative sample and the Q Exactive was operated in positive and negative polarity mode separately, with the addition of a data dependent fragmentation experiment (MS2, top 10, min AGC target 1e3, max IT = 100 ms, NCE: 25,60,95).

TraceFinder software (Version 4.1, Thermo Fisher Scientific) was used to perform the targeted metabolomics analysis. The metabolites peak areas were determined by using the exact mass of the singly charged ions (5 ppm, mass accuracy) and the RT from an in-house library generated using commercial standards (5 ppm, mass accuracy) analysed through the same LC-MS apparatus.

For both the untargeted and targeted metabolomics analyses, the peak areas were normalized for the total extracted µL of serum/mg of tissue or µg of protein as measured through a modified Lowry protein assay.

2.2.6.3 Extracellular media and exchange rates quantification

The metabolites exchange rates were calculated as described in [148]. Briefly, the extracellular media was diluted 1:50 in extraction solution. The medium extracted from cell-free plates was used as reference. Both intracellular and media extracts were analysed by LC-MS as described above. Moreover, aliquots of freshly prepared Plasmax medium with nutrients diluted at different concentrations (0.25X, 0.5X, 1X, 2X, 4X) and spiked with higher concentrations of lactate were processed and used for metabolite quantification. For each metabolite (x) the secretion/consumption rate was quantified using the equation x=(2x(Δmetabolite)/AVG µg of protein)), where Δmetabolite=((x)nmol in cell-free medium – (x)nmol in spent medium).

2.2.6.4 DNA methylation analysis through LC-MS

The cellular DNA was isolated using the DNeasy kit (Qiagen) and measured using a Nanodrop Instrument. The DNA was extracted for metabolomics analysis following a method adapted from [149]. For each sample a volume containing 500 ng of DNA was transferred into an Eppendorf tube. The samples were desiccated with a heat block with blow-down nitrogen dryer at 40˚C. Formic acid (100 µL) was added to the samples and, after careful mixing, the tubes were incubated in a heat block at 130˚C for 3 h. The samples were cooled at room temperature and transferred

to a heat block with blown-down nitrogen dryer at 40˚C for 1h. 25 µL of LC-MS grade water was added to the dried samples, centrifuged and left at room temperature for 15 min. 100 µL of ice-cold extraction solution (methanol 50%, acetonitrile 30%, and water 20%) were added to each sample. The samples were centrifuged at 4˚C and transferred to LC-MS vials. The samples were analysed with a Q Exactive Plus Orbitrap Mass Spectrometer operated in positive polarity, selective ion monitoring mode (75-300 m/z) with a resolution of 70,000, employing the same chromatographic conditions as described above and a 19 min total runtime.

2.2.7 Metabolic assays

2.2.7.1 Oxygen Consumption Rate

5-6 x 103 cells/well were seeded in 96-well plates coated with Matrigel® and cultured in Plasmax medium for three days. Plasmax was then refreshed and the Seahorse cartridge was loaded with Oligomycin, CCCP, Rotenone and Antimycin A (final concentrations in the well: 1, 2, 0.5, 0.5 µM, respectively). Cells were incubated in 5% CO_2 and transferred to the Seahorse XF96 Analyzer. Because of the bicarbonate presence in Plasmax medium, only OCR was acquired while ECAR values were disregarded. After the assay, the plate was washed twice with PBS, dried and RIPA buffer (20 µL) was added to each well. The plate was kept overnight at -74˚C and the day after the protein content was quantified with a BCA quantification method.

2.2.7.2 Biochemistry analyzer-based exchange rates of main nutrients

6-12 x 10^5 cells/well were seeded in triplicates in 24-well plates coated with Matrigel® and cultured in Plasmax medium for three days. After three days, Plasmax medium (400 µL/well) was refreshed and after 0, 1, 3, 6, 12, 24 h media samples (200 µL) were collected and transferred to Eppendorf tubes. The tubes were then centrifuged for 5 min (300 g, 4˚C) and the supernatant transferred to new tubes. The samples were kept at -80˚C until three independent experiments had been performed. Reference wells containing medium but not cells were sampled in parallel. After sample collection, the plates were washed with PBS, air dried and kept at -20˚C for protein quantification using a modified Lowry protein assay. On the day of the analysis media samples were thawed, vortexed and

transferred to a 96-well plate. The plate was sealed and loaded onto the YSI 2900 Biochemistry Analyzer as per manufacturer instructions. Glucose, lactate, glutamine and glutamate concentrations were measured.

2.2.8 Animal work

2.2.8.1 Ethical approval for experiments with mice

The brain tumour xenografts experiments to assess tumour growth performed at the Luxemburg Institute of Health (Group head, Prof Simone Niclou) were approved by the animal welfare committee of the Luxembourg Institute of Health. The *in vivo* experiments performed at the CRUK Beatson Institute were performed under guidelines approved by the University of Glasgow Animal Welfare and Ethical Review Body and the UK Home Office under Saverio Tardito's Project Licence (P38F4A67E).

In order to assess the pharmacokinetics of dexamethasone *in vivo*, 10 female and 10 male NOD Scid Gamma mice were treated with dexamethasone-21-phosphate disodium salt (2 mg/kg). After 1, 3, 6, 12, 24 h from treatment, the mice were euthanized and serum, liver, brain tissues samples collected for LC-MS analysis. As a control, 2 female and 2 male mice were euthanized without being treated with dexamethasone and their serum, liver, brain tissues samples were collected for LC-MS analysis (time 0).

2.2.8.2 Primary orthotopic human GBM xenografts

P3, P13 and T16 cells have been derived from human glioblastoma biopsies, whose details (i.e. patients' age and sex, chromosomal aberrations, tumour subtype) are described in [26]. Relevant details for these lines have been recapitulated in Table 2-1.

Patient biopsy	Age	Sex	Chromosomal aberrations	Tumour subtype
P3	64	M	+ [Chr 7, Chr19, 20q], -[1q42-q43, Chr9, Chr10, 20p] –[PIK3R , CDKN2A/B]	Mesenchymal
P13	Unknown	F	+(Chr7, Chr19, Chr20), -(6q16.2-16.3, Chr10, 17q12), --CDKN2A/B	Neural
T16	52	F	++[EGFR , MDM2], +7q, - [Chr6q, Chr10, Chr11, 13q12-q32.2], -CDKN2A/B	Neural

Table 2-1 Clinical patient data and chromosomal aberrations of corresponding human GBM biopsies as obtained from [26]

Patient-derived GBM xenografts were generated as described in [91]. In order to assess the effects of dexamethasone on T16 GBM tumours, GBM patients-derived T16 spheroids were stereotactically implanted in the right hemisphere of 16 female Swiss Nu/Nu mice (Charles River) following the surgical procedures detailed in [150]. The tumour development was followed using T2 MRI imaging. After 3 weeks from tumours implantation, when the tumour became quantifiable through MRI, mice were randomly assigned to dexamethasone treatment or control group. 8 mice were treated with vehicle (Nacl 0.9%) and 8 mice were treated with dexamethasone-21-phosphate disodium salt (2 mg/kg) 5 days/week. The mice were euthanized upon experimental endpoint (tumour volume ≥ 80 mm^3) 4 h after the last dexamethasone treatment and samples of serum, liver, tumour and contralateral normal brain were collected for immunohistochemistry and LC-MS analyses.

In order to investigate the effects of nicotinamide supplementation on the metabolism of T16 GBM tumours, GBM-patients-derived T16 spheroids were stereotactically implanted in the right hemisphere of 9 female NOD Scid Gamma mice (Charles River) following the surgical procedures detailed in [150]. The tumour development was followed using T2 MRI imaging. After 5-6 weeks from tumours implantation, when the tumour became quantifiable through MRI, mice were randomly assigned to dexamethasone treatment or control group. 4 mice were treated with vehicle (Nacl 0.9%) and 5 mice were treated with dexamethasone-21-phosphate disodium salt (2 mg/kg) 7 days/week. Upon appearance of clinical endpoints (weight loss ≥ 20% compared to pre-operative weight, seizures, or persistent hunched back and limited motility), 4 hours after the last dexamethasone treatment, the mice were treated with nicotinamide (500 mg/kg) and 2 h later they were euthanized. Samples of serum, liver, tumour and contralateral normal brain were collected for LC-MS analyses.

2.2.8.3 Magnetic Resonance Imaging

Tumour growth was monitored by MRI as described in [38]. Briefly, 2.5 isoflurane was used to keep the mice under anesthesia during the image acquisition, with breathing and temperature under constant monitoring. For routine follow up, a MRI (FSE-T2 sequence, 3T MRI system, MR Solutions) was used and a Fast Spin Echo T2-weighted MRI sequence was applied (field of view=25 mm, matrix size= 256 ×

256, TE=68 ms, TR=3000 ms, and slice thickness=1 mm). MRI data was analyzed by ImageJ and tumour volume was calculated by tumour delineation in each slide, multiplyed by slice thickness.

2.2.8.4 Tissue collection

Upon either experimental or clinical endpoint, the mice were humanely euthanized and samples of serum, tumour, contralateral normal brain and liver were snap-frozen for metabolomics analyses (described above) or fixed in paraformaldehyde (4%) solution for immunohistochemistry analyses.

2.2.8.5 Immunohistochemistry

All Haematoxylin & Eosin (H&E) and Immunohistochemistry (IHC) staining was performed on 4 µm formalin fixed paraffin embedded sections (FFPE) previously kept at 60ºC for 2 hours. The following antibodies were stained on an Agilent Autostainer: Glucocorticoid Receptor (GR) (12401, Cell Signaling) and Nestin (ab6320, Abcam). FFPE sections were loaded into an Agilent pre-treatment module to be dewaxed and undergo heat-induced epitope retrieval (HIER) using either low or high pH target retrieval solution (TRS) (K8005, K8004, Agilent). Sections for Nestin staining underwent antigen retrieval using low pH TRS and sections for GR staining underwent antigen retrieval using high pH TRS. All sections were heated to 97ºC for 20 min in the appropriate TRS. After HIER, all sections were rinsed in flex wash buffer (K8007, Agilent) prior to being loaded onto the autostainer. The sections underwent peroxidase blocking (S2023, Agilent) for 5 min, then were washed with flex wash buffer. Sections for Nestin and GR were blocked using mouse-on-mouse kit (MKB2213-1, Vector Lab) before primary antibody application for 35 min at a previously optimised dilution (GR, 1/2000; Nestin, 1/750). The sections were then washed with flex wash buffer before application of appropriate secondary antibody for 30 minutes. Sections for Nestin had mouse envision applied (K4001, Agilent) and sections for GR staining had rabbit envision (K4003, Agilent) applied for 30 min. Sections were rinsed with flex wash buffer before applying Liquid DAB (K3468, Agilent) for 10 minutes. The sections were then washed in water and counterstained with haematoxylin z (RBA-4201-001 CellPath).

The sections for Ki67 (12202, Cell Signaling) staining were performed on a Leica Bond Rx autostainer. The FFPE sections underwent on-board dewaxing (AR9222, Leica) and antigen retrieval using ER2 solution (AR9640, Leica) for 20 min at 100°C. Sections were rinsed with Leica wash buffer (AR9590, Leica) before peroxidase block was performed using an Intense R kit (DS9263, Leica) for 5 min. Sections were rinsed with wash buffer before application of Ki67 antibody at 1/1000 dilution for 30 min. The sections were rinsed with wash buffer and had rabbit envision secondary antibody applied for 30 min. The sections were rinsed with wash buffer, visualised using DAB and then counterstained with haematoxylin in the Intense R kit. H&E staining was performed on a Leica autostainer (ST5020). Sections were dewaxed, taken through graded alcohols and then stained with Haem Z (RBA-4201-00A, CellPath) for 13 min. Sections were washed in water, differentiated in 1% acid alcohol, washed and the nuclei blu'd in scotts tap water substitute (in-house). After washing sections were placed in Putt's Eosin (in-house) for 3 min. To complete H&E and IHC staining, sections were rinsed in tap water, dehydrated through graded ethanol and placed in xylene. The stained sections were cover-slipped in xylene using DPX mountant (SEA-1300-00A, CellPath).

2.2.9 Human studies and analysis of publicly available datasets

The human glioblastoma samples were acquired at the Department of Neurosurgery, Haukeland University Hospital, Bergen N-5021, Norway as described in [148] and re-analysed with TraceFinder software to assess the levels of selected metabolites.

GTEx (https://www.gtexportal.org/home/) portal was used to investigate NNMT expression levels in normal tissue samples. GEPIA2 (http://gepia2.cancer-pku.cn/#index) platform was used to compare NNMT expression levels as found in GTEx normal tissue samples and TCGA-GBM dataset. Moreover, GEPIA2 was used to analyse the prognostic value of NNMT on GBM patients' disease-free survival.

2.2.10 Histones methylation analysis

Core histones were extracted from contralateral normal brain and tumour tissues using the Core Histone Isolation Kit (Sigma-Aldrich, EPI024). Briefly, the tissue samples were cut and washed twice in ice-cold PBS. Upon centrifugation, the

supernatant was discarded and the pellets resuspended in ice-cold Lysis Buffer and homogenized with a Dounce homogenizer (15 strokes). The lysates were further processed with Extraction reagent and Neutralization buffer. Isolated histones were quantified with BCA protein quantification assay and loaded on SDS-PAGE for Western blotting (described above).

2.3 Statistical analysis

GraphPad Prism 7 software was employed to plot the data and perform the statistical analyses shown in all figures. Statistical significance was assessed by two-tailed unpaired or paired t-tests as specified in the figure captions. The number of independent experiments (n) and technical replicates is specified in each figure caption. Statistical significance was not tested on multiple technical replicates (e.g. wells) when the experiments were performed only once.

Chapter 3. Characterization of the effects of dexamethasone on glioblastoma cells proliferation

The intra- and inter-heterogeneity of glioblastoma makes this malignant brain tumour difficult to model *in vitro*. In addition, several reports have shown that cell culture can cause novel aberrations to arise in established glioblastoma cell lines, leading to results that are poorly representative of the primary tumour biology [24]. Therefore, choosing a relevant model for the human disease represented a critical step at the start of this project.

3.1 Developing a relevant cellular model for glioblastoma

For this project, four different patient-derived cell lines have been employed. Three of them (P3, P13 and T16) have been established and characterized in the NORLUX Laboratory of Prof Simone Niclou [38], while the fourth one (BG7) has been established at the University of Bergen, Norway by the Group of Prof Hrvoje Miletic. The general procedure used to produce these cell lines is illustrated in Figure 3-1.

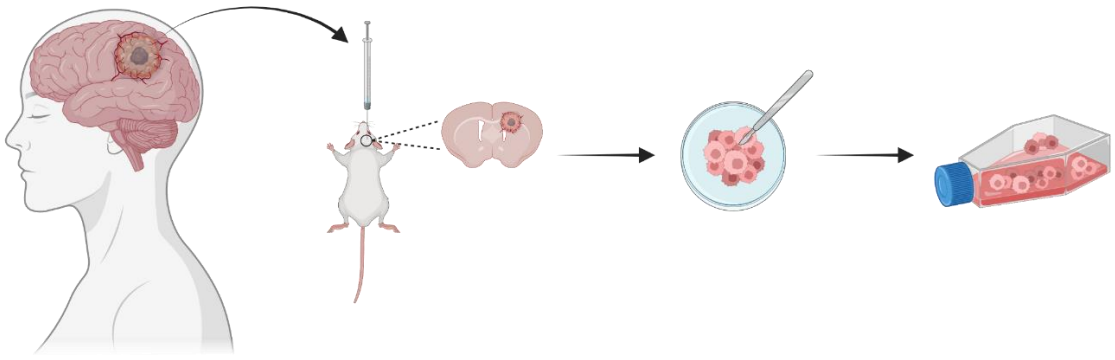

Figure 3-1 Protocol to establish glioblastoma patient-derived xenograft cell lines

The tumour tissue is obtained during surgery for tumour removal from glioblastoma patients. Once primary organoids are produced in culture, they are implanted into the brain of NSG mice to establish primary xenografts. These brain tumours are then processed to establish *in vitro* cell cultures [150]. The figure has been created with BioRender.com.

3.1.1 Selection of the culture media

The cell culture media represents another key factor for obtaining more relevant *in vitro* results. For the reasons discussed in the introduction, we were interested in culturing the cells in two main conditions: serum-free and with metabolites concentrations comparable to the physiological levels. For all the experiments, cells were incubated in a modified Plasmax, a medium based on levels of nutrients found in human plasma [35], while for the routine culture we employed Minimum Essential Medium (MEM), supplemented as illustrated in Table 3-1.

MEM	Final Concentration	Plasmax™
Albumax™ II Lipid-Rich BSA	400 mg/L	Albumax™ II Lipid-Rich BSA
hBFGF	20 ng/mL	hBFGF
hEGF	20 ng/mL	hEGF
Heparin	2 µg/mL	Heparin
ITS: Insulin Transferrin Sodium Selenite	 1 g/L 0.55 g/L 0.00067 g/L	ITS: Insulin Transferrin Selenite
L-Glutamine	0.65 mM	
Non-essential amino acids	0.1 mM	
Sodium Pyruvate	0.1 mM	
Vitamin B12	0.0068 mg/L	

Table 3-1 Components added to MEM (Gibco) or Plasmax to obtain cell culture media

3.2 Dexamethasone effects on the proliferation of glioblastoma cells are line– and culture condition–specific

3.2.1 Results from adherent monolayers

As discussed in the introductory section, since the introduction of glucocorticoids in glioblastoma standard-of-care, many studies have investigated the effect of these drugs on glioblastoma cells proliferation. Dexamethasone has shown both stimulatory and inhibitory effects on glioma cells proliferation *in vitro* and *in vivo*. The lack of consistency can be explained at least in part by the following factors: presence or absence of serum in the culture medium, level of glucocorticoid receptor (GR) expression in specific cell lines, cell density and concentration of glucocorticoids used [98]. Based on the concentrations of dexamethasone detected in patients-derived plasma samples [151-154], we defined 0.1-1 μM as a range of clinically relevant concentrations. To investigate the effect of dexamethasone on proliferation, we tested this range of concentrations and counted the GBM cells at different time-points. As shown in Figure 3-2 and Figure 3-3, the minimal concentrations of drug used (0.1 μM) was sufficient to elicit the minimal response observed. Cell proliferation was differentially affected by dexamethasone treatment: it was slightly inhibited in BG7, not altered in P3 and P13, and significantly increased in T16. Measuring cell confluence with the IncuCyte® instrument and using it as a readout for cellular proliferation partially recapitulated these results. BG7 and P3 cells confluence was not significantly altered by dexamethasone. In P13 dexamethasone had a slightly inhibitory effect, and in line with the results obtained through cell counting, dexamethasone boosted the proliferation of T16 cells (Figure 3-3). In these assays we did not detect a concentration-dependent response, thus we proceeded on using the lowest effective concentration of dexamethasone. Next, we tested if cell culture density could modulate dexamethasone effects on cell proliferation. Three different seeding densities were tested and cells counted at different time points (Figure 3-4). For two of the cell lines (BG7, P13) the seeding density did not alter the dexamethasone-dependent effects on cell proliferation. P3 cells exhibited a density-dependent proliferation defect upon exposure to dexamethasone. Surprisingly, a higher seeding cell number attenuated the proliferative advantage conferred by dexamethasone to T16 cells.

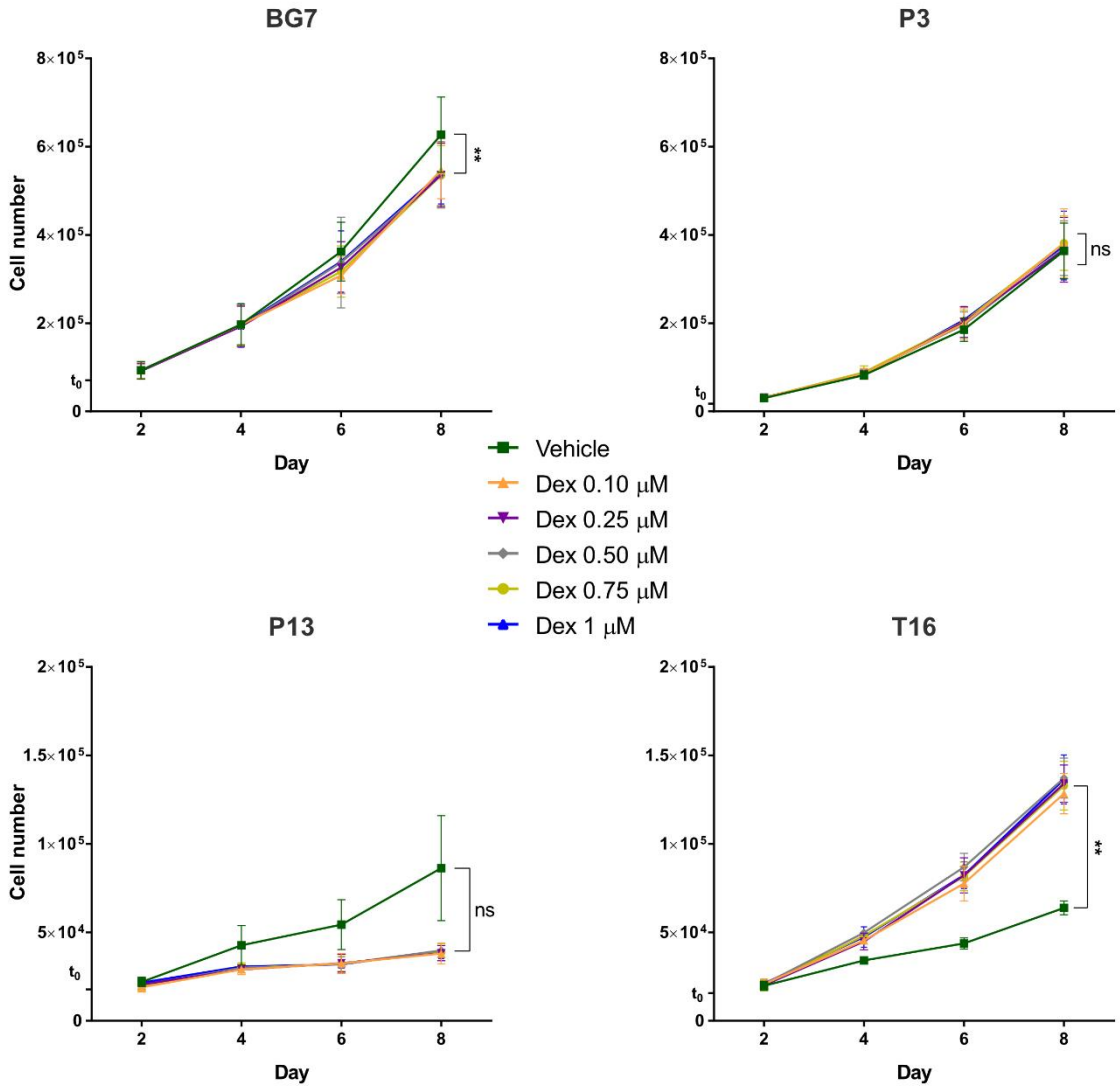

Figure 3-2 Dose-response experiments with clinically relevant concentrations of dexamethasone

The four PDX-derived cell lines have been cultured as adherent monolayers in Plasmax medium containing vehicle (ethanol) or the indicated concentrations of dexamethasone up to 8 days. The cells were counted every 2 days to assess cell growth. After 4 days, the culture medium was replaced to avoid nutrient exhaustion (n=4 independent experiments for BG7, P3 and T16; n=3 independent experiments for P13; 4 wells were counted for each condition). Data are mean +/- SD and were analysed by Paired t-test.

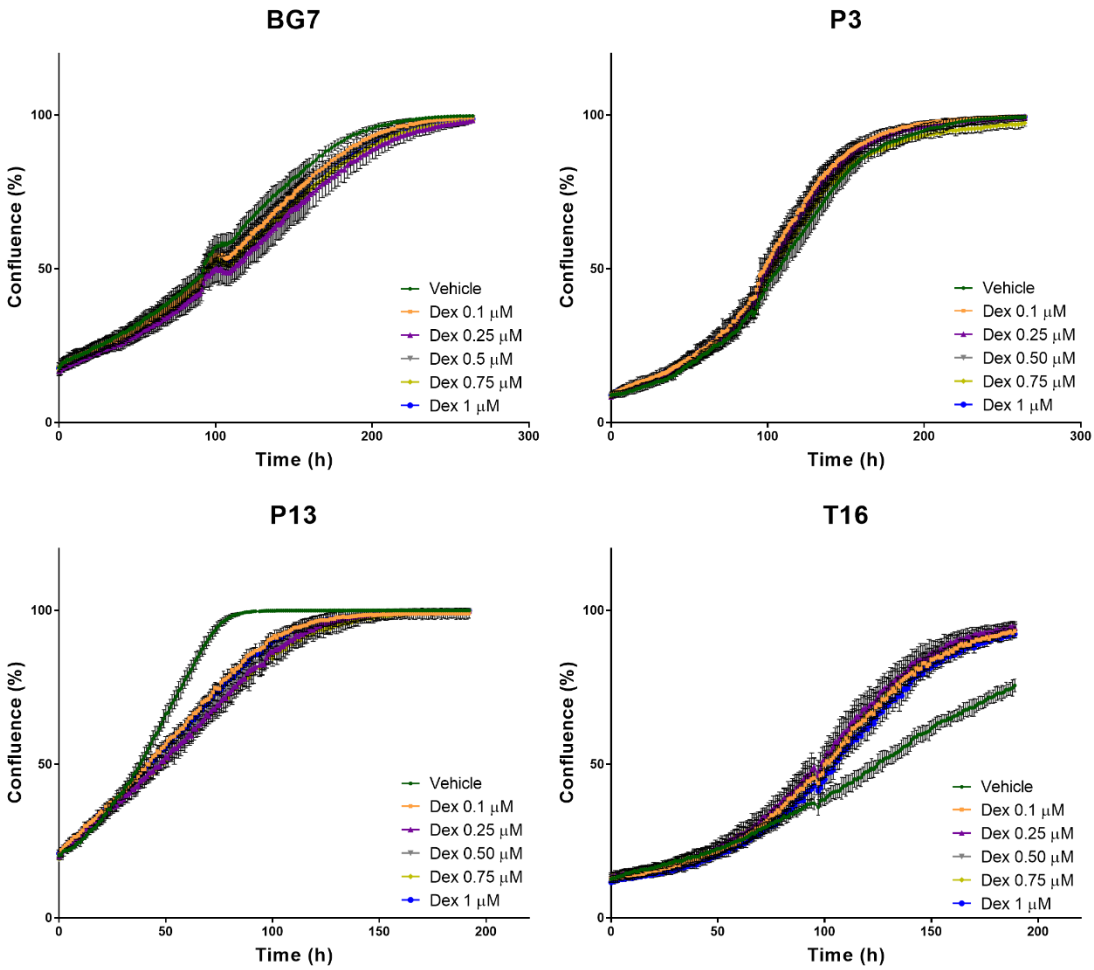

Figure 3-3 Proliferation experiments measuring cell confluence by IncuCyte® live-cell analysis

The four PDX-derived cell lines have been cultured as adherent monolayers in Plasmax medium containing vehicle (ethanol) or the indicated concentrations of dexamethasone up to 11 (BG and P3) or 8 (P13 and T16) days. Every 4 days, the culture medium was replaced to avoid nutrient exhaustion (n=4 independent experiments, 4 wells have been measured for each condition).

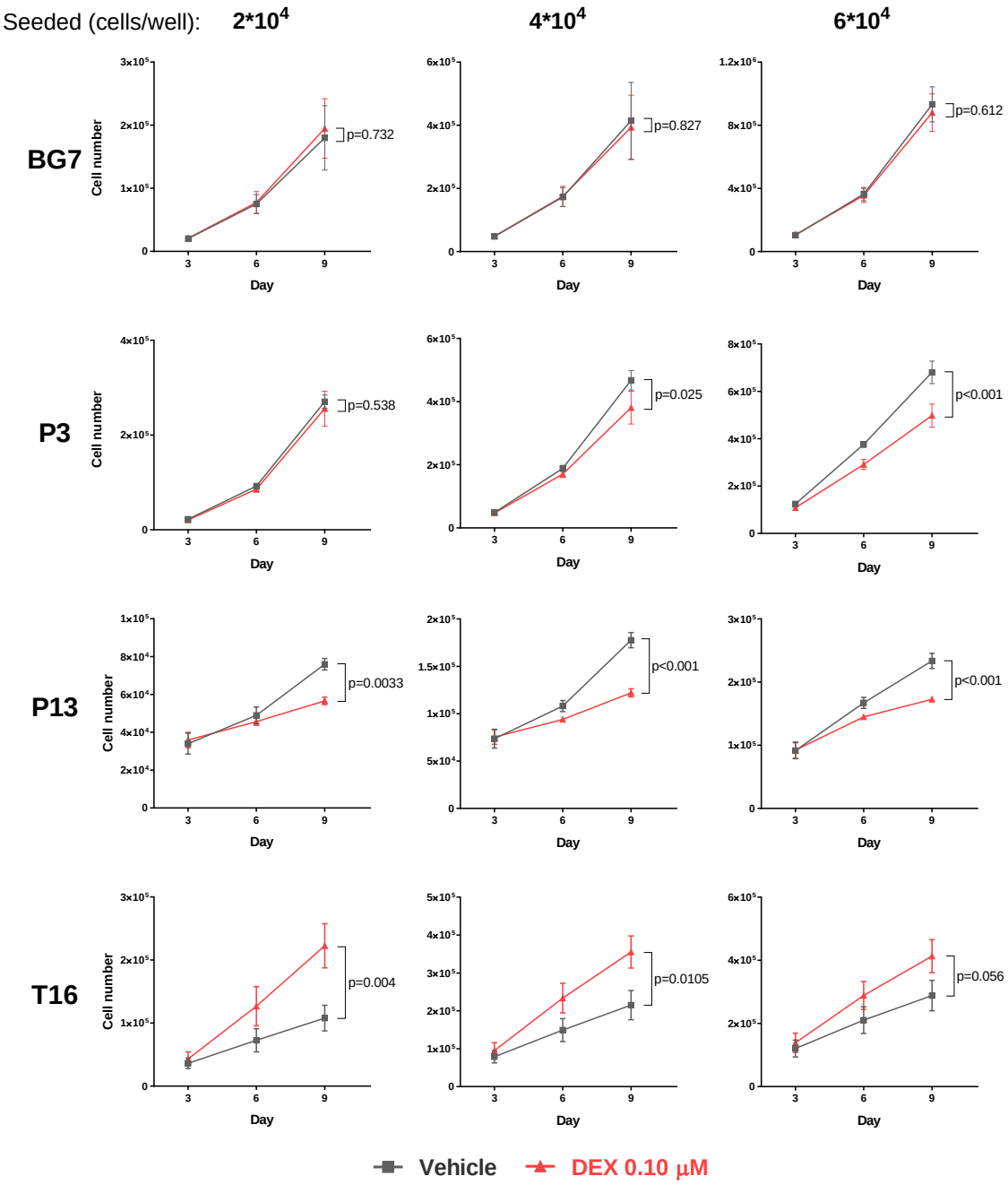

Figure 3-4 Seeding density effects on cell proliferation under dexamethasone treatment

The four PDX-derived cell lines have been cultured as adherent monolayers in Plasmax medium containing vehicle (ethanol) or 0.1 µM dexamethasone up to 9 days. The cells were counted every three days to assess cell growth and every 3 days, the culture medium was replaced to avoid nutrient exhaustion (n=3 independent experiments for BG7, P13 and T16; n=5 independent experiments for P3; 4 wells were counted for each condition). Data are mean +/- SEM and were analysed by multiple t-test.

3.2.2 Dexamethasone effects on GBM spheroids growth

Traditionally, cancer cells have been cultured as adherent monolayers but a growing body of literature has highlighted that two-dimensional cell cultures fail to reliably predict *in vivo* results, especially when it comes to drug discovery and preclinical testing [155]. Many laboratories are now using spheroids as preclinical cancer models thanks to their ability to better recapitulate a three-dimensional microenvironment. This could be due to their multi-layered-structures, recreating the uneven access to nutrients characterizing tumours [156]. As already mentioned, glioblastoma research suffers the lack of appropriate preclinical model systems, and patient-derived organoids are considered a valuable alternative to expensive and difficult-to-establish animal models [38, 157]. In order to test dexamethasone effect in a three-dimensional context, we cultured the GBM naïve cells as spheroids by plating 500 cells/well in low-adherence 96-well plates (Figure 3-5). By measuring the size of each individual spheroid over time, we observed that BG7, P3 and T16 efficiently formed spheres that grew over time. For all 3 cell lines the size of the spheres was smaller when they were treated with dexamethasone. This result was particularly striking with regard to the T16 for which a significant and consistent increase in proliferation had been observed in two-dimensional adherent monolayers. Vehicle-treated P13 cells did not form spheroids but only loose amorphous aggregates, while upon dexamethasone treatment P13 seemed to form more structured spheres.

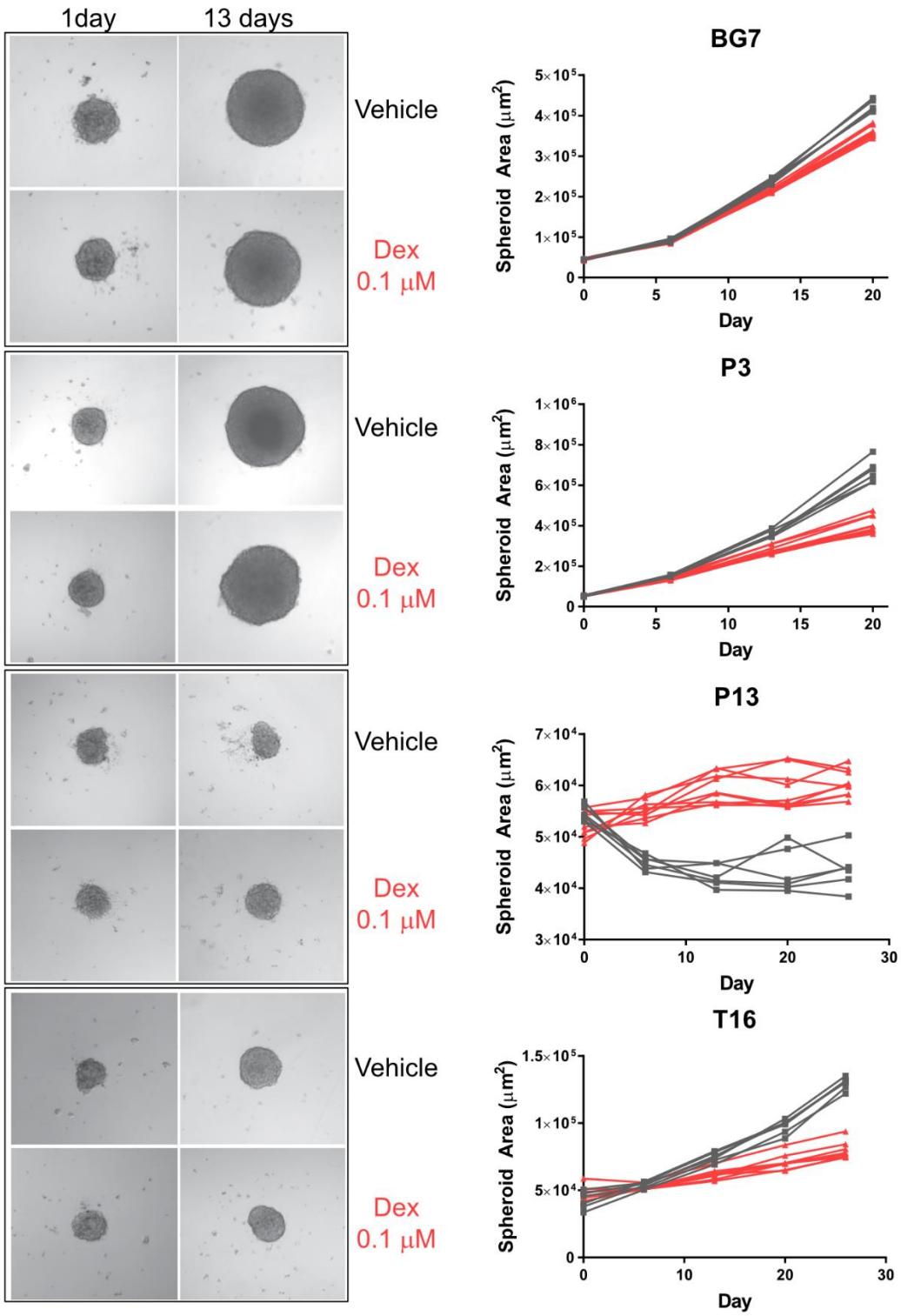

Figure 3-5 PDOX-derived spheroids and dexamethasone treatment

500 cells/well have been seeded in 96-well plates with round-bottom low-adherence wells. Images of the spheroids have been acquired at day 0, 6, 13, 20 for BG7 and P3, and at day 0, 6, 13, 20, 27 for P13 and T16. The area of the spheroids has been quantified using Fiji software. Representative images of the spheroids are shown on the left side of the panel, while the quantification of the spheroids areas is shown on the right side. Graphs are representative of one experiment (n=2 independent experiments; each line represents an individual spheroid). Data were analysed by multiple t-tests.

3.3 Glioblastoma cells express a functional glucocorticoid receptor

As explained in the introduction section, the main target of glucocorticoids is the glucocorticoid receptor (GR) that after ligand binding dimerizes and enters the nucleus where it functions as a transcription factor. Within the gene encoding the receptor (*NR3C1*) is found a functional glucocorticoid responsive element (GRE) that negatively regulates its own expression closing a feedback loop functional in different tissues [158]. First, we tested if glioblastoma cells express GR. We performed a Western blotting to assess the levels of the receptor at different time points after being exposed to increasing concentrations of dexamethasone (Figure 3-6, Panel A). The receptor was expressed in all the cells and the dexamethasone treatment caused a reduction in its expression levels. It has been reported that dexamethasone promotes the expression of stem cells markers, and chemoresistance in glioblastoma cells [116]. In our culture conditions stem cell markers were expressed by all cell lines. BG7 cells expressed less Nestin and more Sox2 protein compared to the other cells, while T16 appeared to express less Sox2. Dexamethasone treatment slightly reduced the expression of Nestin in P13 and T16 cells and of Sox2 in P3 and P13, while CD133 levels were not altered in any cell line (Figure 3-6, Panel B). To assess the functionality of the dexamethasone binding to GR, we employed an immunofluorescence staining in P3 and T16 cells. The results show that upon dexamethasone treatment GR translocates from the cytosol to the nucleus (Figure 3-6, Panel C).

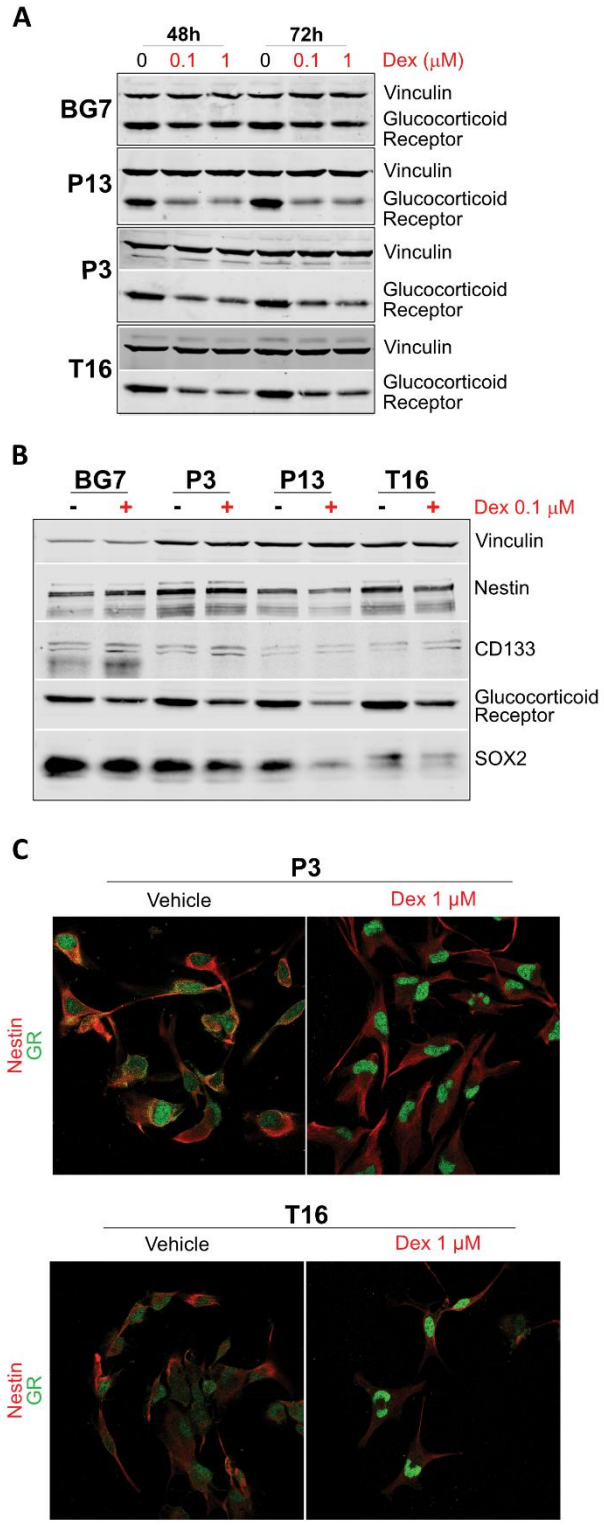

Figure 3-6 Glioblastoma cells express a functional glucocorticoid receptor

Cells have been cultured for 72 h as adherent monolayers in Plasmax medium containing vehicle (ethanol) or the indicated concentration of dexamethasone (0.1 or 1 μM). A, B) After 48 or 72 hours, the cells were lysated in RIPA buffer and the protein content quantified. Equal protein amounts were loaded and analyzed by Western blotting. Vinculin was used as a loading control. C) After 72 h, the cells were fixed with a solution of paraformaldehyde (4% V/V in PBS), permeabilized with PBS-Triton and incubated with antibodies anti-Glucocorticoid Receptor and anti-Nestin.

3.4 Chapter discussion and results limitations

Together with other aspects discussed in the introductory section, the unique structure of the blood-brain-barrier makes an almost impossible challenge to recapitulate the *in vivo* pathophysiology of glioblastoma through *in vitro* models. Moreover, glioblastoma is characterized by a high degree of intra- and inter-tumoural heterogeneity adding another layer of complexity to the system. Differently from other tumour types, knowledge about the exact nature of the glioblastoma initiating cells is still limited. This also limits the availability of genetically engineered mouse models for this type of cancer. Therefore, patient-derived orthotopic xenografts (PDOX) represent nowadays a valid model for the disease. Nonetheless, the Three Rs guidelines – Replacement, Reduction, Refinement – and the cost of animal-based experiments still advocate for *in vitro* models to produce solid hypotheses to further test *in vivo*. The cells we decided to use for this project derive from PDOX models that have been demonstrated to retain the same histopathological features of the originating tumours [26]. Furthermore, they were cultured for a limited number of passages to avoid further genomic aberrations to arise. These cellular models were therefore chosen to investigate the effects of glucocorticoids, in particular dexamethasone, on the proliferation of naïve glioblastoma cells. In these 60 years since the introduction of dexamethasone in glioblastoma standard-of-care, several laboratories have looked at its effects on glioma cells, obtaining variable *in vitro* and *in vivo* results. The factors that could possibly explain this variability are the presence or absence of serum in the culture media, the levels of glucocorticoid receptor (GR) expression in the cellular model, the cell density and the dose of glucocorticoids used. Part of this variability could be also explained by the supra-physiological culture media widely used in cancer research and the fact that the relevance of serum-free media for glioma research has been recognized relatively recently.

We tested dexamethasone concentrations ranging from 0.1 to 1 μM and within this clinically relevant range we could not detect a dose-dependent effect on cell proliferation. This prompted us to use the lowest dose for the future experiments. In order to investigate the dexamethasone effects on proliferation, the cells were cultured in both two- and three-dimensional systems. Collectively, the proliferation of BG7 adherent monolayers was not altered by dexamethasone, while P3 and P13 were slightly inhibited and T16 were consistently over-

proliferating upon glucocorticoids treatment. When analysed as three-dimensional spheroids, the cells produced different results. Surprisingly, P13 cells were forming spheres more efficiently after being treated with dexamethasone while BG7, P3 and T16 spheroids size was reduced by glucocorticoids. Mackie et al. showed that glucocorticoids can reduce the distribution of hyaluronic acid and increase sulphated glycosaminoglycans (GAGs) on the cellular membrane of glioma cells [159]. The dexamethasone-mediated effect on the P13 spheres and the discrepancy between adherent monolayers and spheroids suggest that glucocorticoids could affect cell-cell interaction and production of extra-cellular matrix (ECM). The matrigel used to coat the plates for culturing adherent monolayers partially releases the cells from the need of synthetizing ECM components. Moreover, the two-dimensional culturing allows an equal exposure to the nutrients present in the media, while in the spheroids multiple cellular layers produce areas where oxygen concentration and access to nutrients are limited. Dexamethasone might exacerbate these effects, explaining the diverging results obtained in the two systems. Moreover, we observed that P3 cells cultured at higher cellular density are more susceptible to the antiproliferative effect of glucocorticoids. This is consistent with the reduced growth observed in spheroids, multicellular structures with high cell density, raising the possibility that the same inhibitory effect could be observed in tumours. In fact, neurospheres are usually considered to retain the tumorigenic features of glioma stem cells, therefore the *in vitro* results might translate in an *in vivo* reduction of tumorigenicity. In colonies of human anaplastic astrocytoma cells, Freshney et al. have observed a similar over-proliferating phenotype as the one we could consistently measure in T16 cells upon dexamethasone treatment. Despite the biological explanation for this effect is still under investigation, the fact that it cannot be recapitulated when the same cells are cultured as spheroids suggests that it might be mediated by factors such as cellular adherence and cell-cell contacts.

To test if the effects of dexamethasone were on target in glioblastoma cells we evaluated and confirmed that the receptor was expressed in the four lines employed. Moreover, we could observe the negative feedback mechanism through which glucocorticoids down-regulate the receptor levels. Coherently with the discovery that the serum used for cell culture promotes the differentiation of glioblastoma cells and depletes the stem cells population [28], all the experiments

shown so far have been performed in serum-free media. In order to evaluate stem cells features of the GBM naïve cells, we investigated the expression levels of the accepted neural stem cells markers Nestin, CD133 and Sox2. The variability in the expression levels of these markers might point at a different tumorigenic capacity of each cell line. Furthermore, the fact that overall the markers were not greatly altered by dexamethasone treatment suggests that in our settings dexamethasone did not affect the stemness capacity of the glioblastoma cells.

3.5 Summary

In this chapter, we elucidated the models we selected for studying dexamethasone-mediated effects on glioblastoma cells proliferation. To this aim, we used two main methods, i.e. manual cell counting and a machine learning-based approach with the IncuCyte® machine measuring cell confluence. We selected a range of clinically relevant concentrations of dexamethasone and, not being able to detect any concentration-dependent effect, proceeded on using the lowest concentration. Each cell line responded to dexamethasone treatment differently with the glucocorticoids-treated T16 cells strikingly and consistently over-proliferating. The cells were then cultured as spheroids to investigate the impact of three-dimensional culturing. This approach highlighted an important discrepancy, especially regarding the T16 dexamethasone-treated spheroids, which grew to smaller sizes than the vehicle-treated ones. Finally, through Western blotting and confocal microscopy we observed that glioblastoma cells express high levels of glucocorticoid receptor and its expression decreased, as expected, upon exposure to dexamethasone. The cells were also analysed for stem cells markers whose levels were different in each cell line but not greatly altered by dexamethasone treatment.

Chapter 4. Transcriptomic characterization of dexamethasone-mediated effects on glioblastoma *in vitro* models

4.1 Introduction

The glucocorticoids-mediated signalling can be divided in transcriptional and non-transcriptional effects, with the transcriptional effects being the most characterized. As aforementioned, once bound to the glucocorticoids the receptor is able to dimerize and enter the nucleus where it acts as a transcription factor, binding to genes containing Glucocorticoid Responsive Elements (GREs) in their promoters. The GREs can be 'simple' when the binding of GR is sufficient to regulate transcription, 'composite' when GR directly binds the GRE together with other transcription factors and in a 'tethering' fashion when the GR binding to the GRE is indirect and mediated by other transcription factors. This type of regulation can be positive or negative, depending on the sequence of the GRE [160]. Even though the effects mediated by physiological glucocorticoids largely depend on the tissue considered, synthetic glucocorticoids are clinically employed for their systemic anti-inflammatory and immunosuppressive properties. As shown in the previous chapter, naïve glioblastoma cells express high levels of the glucocorticoid receptor, translocating to the nucleus upon exposure to dexamethasone. To characterize the transcriptional effects of dexamethasone on GBM cells, we carried out an experiment of whole transcriptome sequencing.

4.2 Dexamethasone induces a transcriptional signature common to all cell lines

The RNA-sequencing data has been deposited in the ArrayExpress database at EMBL-EBI (www.ebi.ac.uk/arrayexpress) under accession number E-MTAB-12007. The passcode to access it is available upon request to Dr Saverio Tardito (s.tardito@beatson.gla.ac.uk).

As shown in Figure 4-1, we performed a Principal Components Analysis (PCA) on the RNA sequencing results and observed that the first PC was able to segregate the four naïve GBM cell lines between vehicle- and dexamethasone treated-cells.

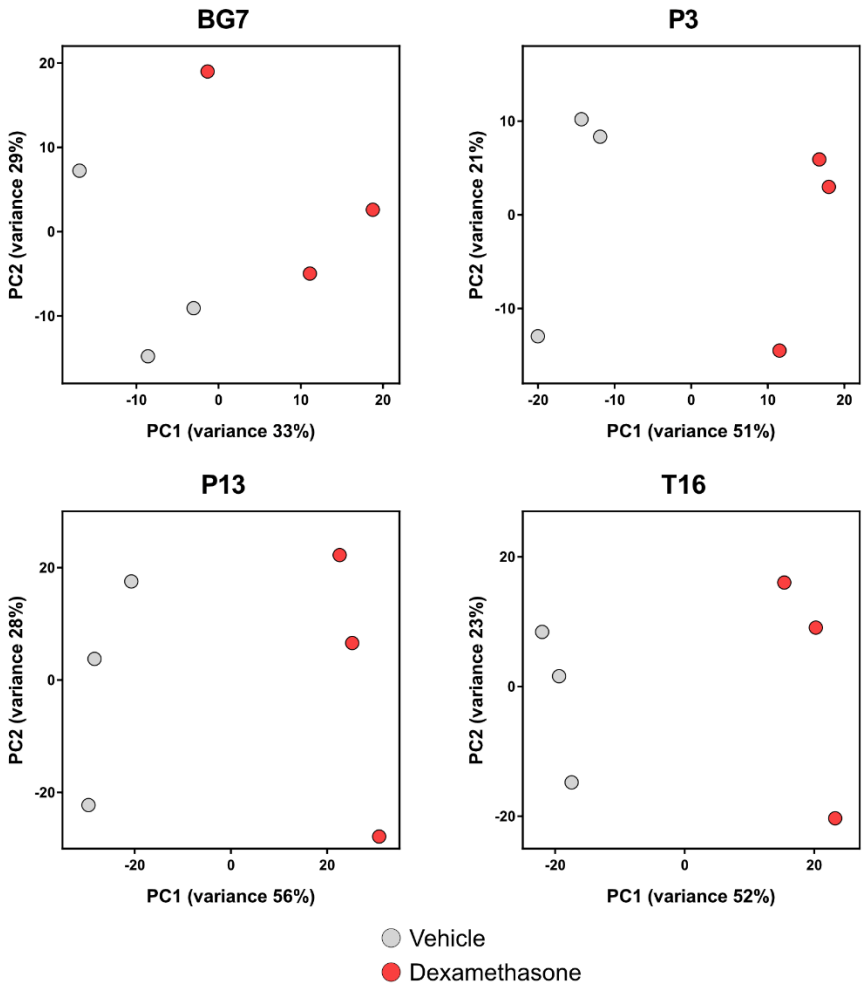

Figure 4-1 Principal Component Analysis of the whole transcriptome sequencing of naïve GBM cells upon dexamethasone treatment

Cell were cultured as adherent monolayers in Plasmax containing vehicle (ethanol) or 0.1 μM dexamethasone for three days. After three days the culture medium was refreshed and 24 h later cell number was determined using a Coulter counter, cells were then harvested for whole RNA extraction. Subsequently, the samples were analysed by poly-A RNA sequencing. Each dot represents an independent experiment (n=3 independent experiments).

As shown in the previous results chapter, the cell line-dependent proliferation response to dexamethasone is indicative of glioblastoma heterogeneity. To overcome the cell-line specific effects of dexamethasone we analysed the RNA sequencing data to identify gene sets significantly regulated in all four cell lines. The intersection of the dexamethasone-induced transcriptional changes common to all the GBM lines highlighted a group of 81 genes (Figure 4-2, panel A). The volcano plots highlight the distribution of these 81 genes, of which 79 were consistently upregulated in all GBM lines (Figure 4-2, panel B). Among these 79 genes we found known targets of glucocorticoids, such as FKBP prolyl isomerase 5 (*FKBP5*) and Krüppel like factor 9 (*KLF9*) [161, 162].

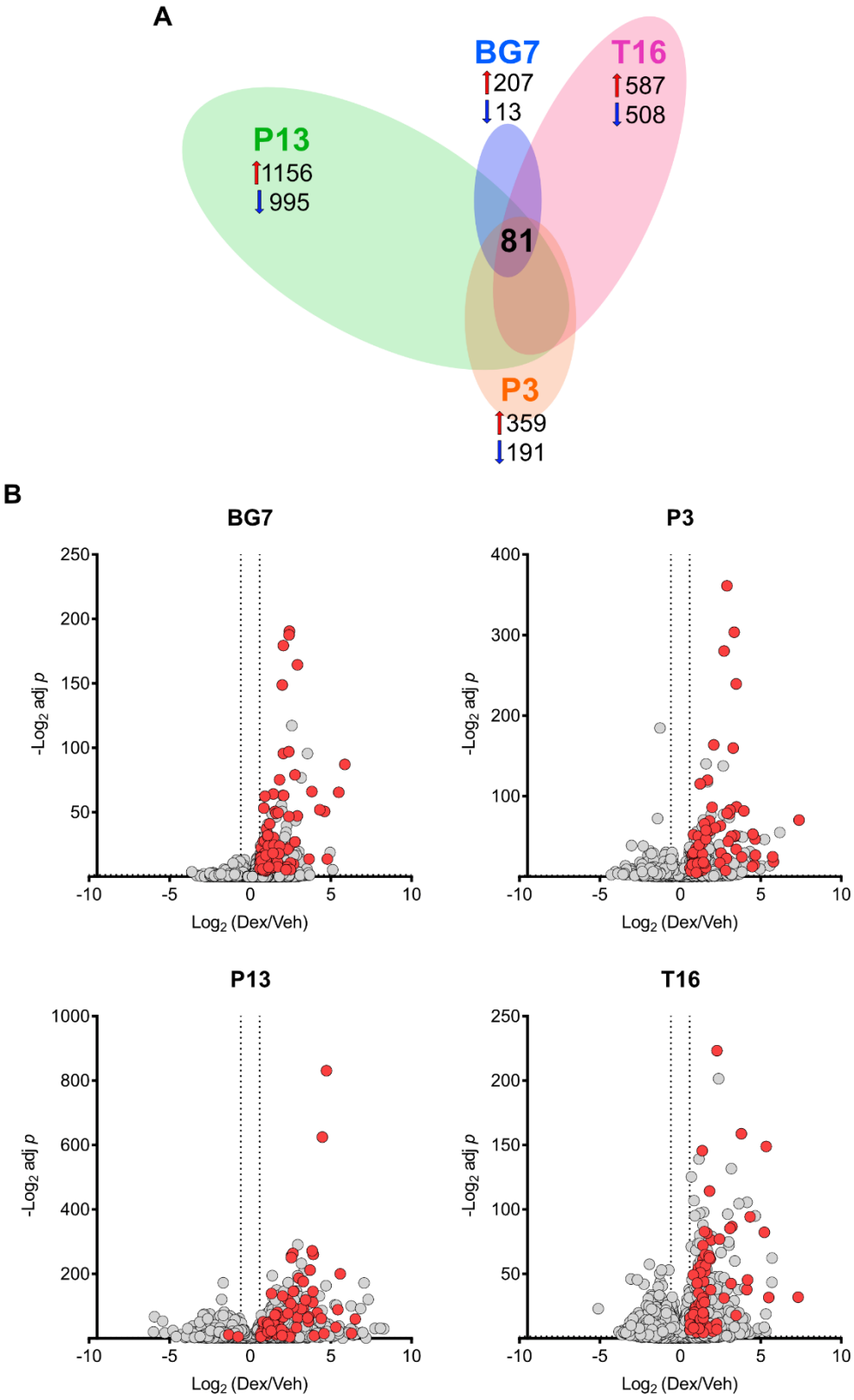

Figure 4-2 Transcriptomic characterization of dexamethasone treatment in GBM naïve cells

A) Venn diagram showing the transcriptional changes caused by dexamethasone in the four GBM cell lines. The size of the circle indicates the relative number of genes whose expression was changing upon dexamethasone treatment. Within each circle, the number of upregulated (red arrow) and downregulated (blue arrow) genes upon dexamethasone treatment is shown (n=3 independent experiments). B) Volcano plots summarizing the transcriptional changes caused by dexamethasone in each GBM cell lines. The red dots indicate the 81 genes significantly changing upon dexamethasone treatment in all cell lines (n=3 independent experiments).

4.3 Growth effects of Glucocorticoid Receptor targets

We proceeded targeting a selection of genes whose expression was upregulated by dexamethasone, and assessed the effects on the proliferation of glioblastoma cells.

4.3.1 Combining dexamethasone and BCL2 like 1 inhibitors does not sensitize GBM cells to apoptosis

One of the hits significantly and coherently upregulated in all four GBM lines was *BCL2 like 1 (BCL2L1)* (Figure 4-3, Panel A), encoding for Bcl-xL, a known antiapoptotic member of the Blc-2 family proteins [163]. Firstly, we confirmed by Western blotting that the increase in mRNA levels led to the an increase at the protein levels (Figure 4-3, Panel B). Synthetic steroids are strong pro-apoptotic agents used to treat acute lymphoblastic leukemia (ALL). Glucocorticoids have been shown to be highly cytotoxic for ALL cells due to their ability to induce apoptosis [164], and a synergizing effect between dexamethasone and venetoclax (ABY-199), a specific BCL-2 inhibitor, has been shown in multiple myeloma [165]. The increase in BCL-xL expression raised the possibility that dexamethasone might alter the sensitivity of cells to apoptosis inducers, therefore we decided to challenge GBM cells with ABT737, inhibiting both Bcl-2 and Bcl-xL proteins, and A-1155463, a highly potent and selective Bcl-xL inhibitor (Figure 4-3, Panel C). The GBM cells showed different levels of sensitivity to the drugs, with ABT737 reducing cell growth in 3 out of 4 cell lines. A-1155463 was effective at reducing cell proliferation only in P3 and P13. Collectively, the addition of dexamethasone did not significantly affect cell growth compared to the apoptosis inducers as single agents, except for P13 cells where the combination of dexamethasone with either inhibitor had an additive inhibitory effect on cell growth.

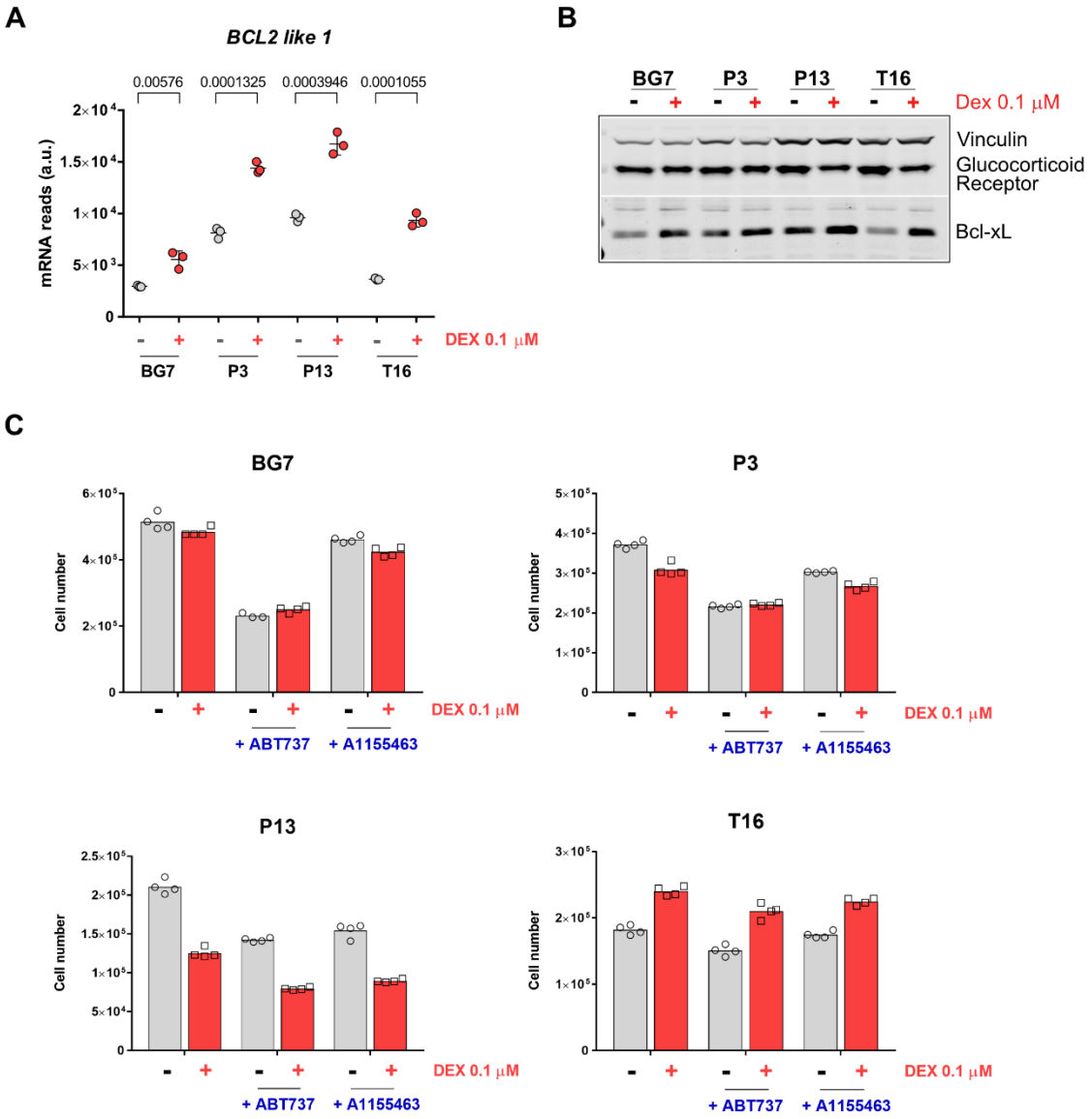

Figure 4-3 BCL2 like 1 is overexpressed upon dexamethasone treatment but the combination of dexamethasone with BCL2 inhibitors does not sensitize the cells to apoptosis

A) Cell were cultured as adherent monolayers in Plasmax containing vehicle (ethanol) or 0.1 µM dexamethasone for three days. After three days, the culture medium was refreshed and 24 h later cell number was determined using a Coulter counter, and cells were then harvested for whole RNA extraction. Subsequently, the samples were analysed by poly-A RNA sequencing. Each dot represents an independent experiment (n=3 independent experiments). B) Cells have been cultured for 72 h as adherent monolayers in Plasmax medium containing vehicle (ethanol) or dexamethasone (0.1 µM). The cells were lysated in RIPA buffer and the protein content quantified. Equal protein amounts were loaded and analysed by Western blotting. Vinculin was used as a loading control. C) The four PDX-derived cell lines have been cultured as adherent monolayers in Plasmax medium containing vehicle (ethanol) or 0.1 µM dexamethasone for three days. After 72 hours, the culture medium was replaced and the cells were cultured in Plasmax medium containing vehicle (ethanol), 0.1 µM dexamethasone, 1 µM ABT737 or 1 µM A-1155463 for four days. The cells were counted after seven days to assess cell growth (n=1 independent experiment, each dot represents data from a well).

4.3.2 Dexamethasone increases the expression of genes involved in polyunsaturated fatty acid synthesis

Among the 79 genes that dexamethasone significantly upregulated in naïve GBM cells, we found the elongation of very long chain fatty acids protein 2 (*ELOVL2*), a member of the ELOVL superfamily of proteins involved in the synthesis of fatty acids. In addition, another member of the superfamily, *ELOVL5*, was upregulated by dexamethasone treatment (Figure 4-4, Panel A). Interestingly, a research published in 2019 identified *ELOVL2* as a superenhancer-associated target gene in glioblastoma stem cells (GSC) which drive its overexpression in tumour tissue compared to normal brain through a superenhancer region, i.e. a regulatory region transcription factors have a very high affinity for [166]. ELOVL2 is responsible for the synthesis of long-chain ω3 and ω6 polyunsaturated fatty acids (LC-PUFA), and was shown to be essential for maintaining the cell membrane phospholipids composition and consequently sustaining a functional EGFR signalling. For this project naïve GBM cells were cultured in serum-free media to preserve their stemness features and avoid differentiation. In order to replace the lipids normally supplemented by serum, the culture medium was supplemented with AlbuMAX™ II Lipid-Rich BSA. To investigate if *ELOVL2* and *ELOVL5* overexpression upon dexamethasone treatment resulted in a different susceptibility of GBM cells to externally supplied fatty acids, AlbuMAX was replaced with a fatty acid-free albumin. As shown in Figure 4-4 (Panel B), the withdrawal of fatty acids caused a slight defect in the growth of the fast-growing BG7 cells but did not alter the proliferation of the other cell lines. Moreover, dexamethasone treatment did not sensitize the cells to the reduced amount of supplemented fatty acids.

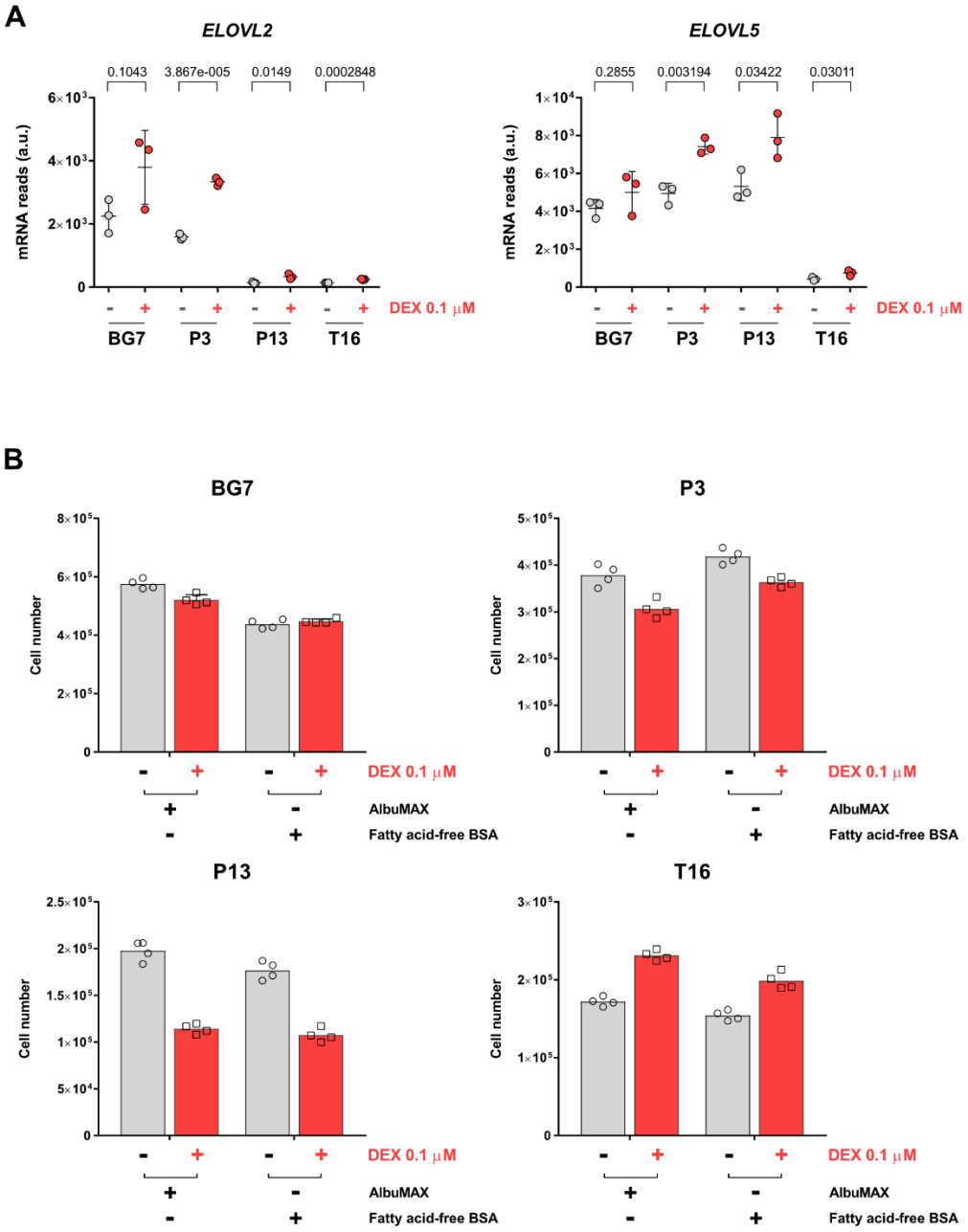

Figure 4-4 GBM cells overexpress genes encoding for fatty-acids elongases but dexamethasone does not sensitize their proliferation to limited fatty acids supplementation

A) Cell were cultured as adherent monolayers in Plasmax containing vehicle (ethanol) or 0.1 µM dexamethasone for three days. After three days, the culture medium was refreshed and 24 h later cell number was determined using a Coulter counter, and cells were harvested for whole RNA extraction. Subsequently, the samples were analysed by poly-A RNA sequencing. Each dot represents an independent experiment (n=3 independent experiments). B) The four PDX-derived cell lines have been cultured as adherent monolayers in Plasmax medium containing AlbuMAX™ II Lipid-Rich BSA or fatty acid-free BSA for seven days. Plasmax was supplemented with vehicle (ethanol) or 0.1 µM dexamethasone. After three days, the culture medium was refreshed to avoid nutrient exhaustion. The cells were counted after seven days to assess cell growth (n=1 independent experiment, each dot represents data from a well).

4.3.3 *MGMT* promoter methylation sensitizes GBM cells to temozolomide

There are several reasons why glioblastoma represents a clinically challenging cancer type; not only clinical symptoms start arising in patients when the tumour has already reached an advanced stage, but also very few prognostic factors are used to inform clinical decisions. The promoter methylation of the gene encoding for O^6-methylguanine-DNA methyltransferase (*MGMT*) represents a marker used for patients stratification. MGMT is a 'suicide' enzyme that removes the carcinogenic lesion O^6-alkylguanine while repairing DNA, transferring the methyl group to one of its cysteine residues [167]. The discovery that the *MGMT* gene is silenced in ~40% of GBM cases and that these patients are more susceptible to alkylating agents-based therapies represented a significant advancement in the clinical management of this tumour [18]. Once MGMT has been alkylated to repair the damage caused by alkylating drugs, such as temozolomide, it must be replenished by the cells. The *MGMT* silencing results in diminished MGMT activity and consequently more DNA damage and cell death upon treatment with temozolomide. From the RNAseq data we could observe that among the naïve GBM cells used for this project BG7 do not express *MGMT*, in contrast to the other three lines (Figure 4-5, Panel A). In order to test if dexamethasone could affect sensitivity to temozolomide, we treated cells with temozolomide (10-1000 μM) in the presence or absence of dexamethasone. Temozolomide at 25 μM was effective at halving BG7 cell number while for P3, P13, T16 cells a 10-fold higher concentration (250 μM) of temozolomide was required to produce a similar effect (Figure 4-5, Panel B). Dexamethasone had a slightly protective effect in P3 and P13 cells when treated with 250 μM temozolomide, whereas BG7 and T16 cells did not exhibit any dexamethasone-dependent response to temozolomide treatment.

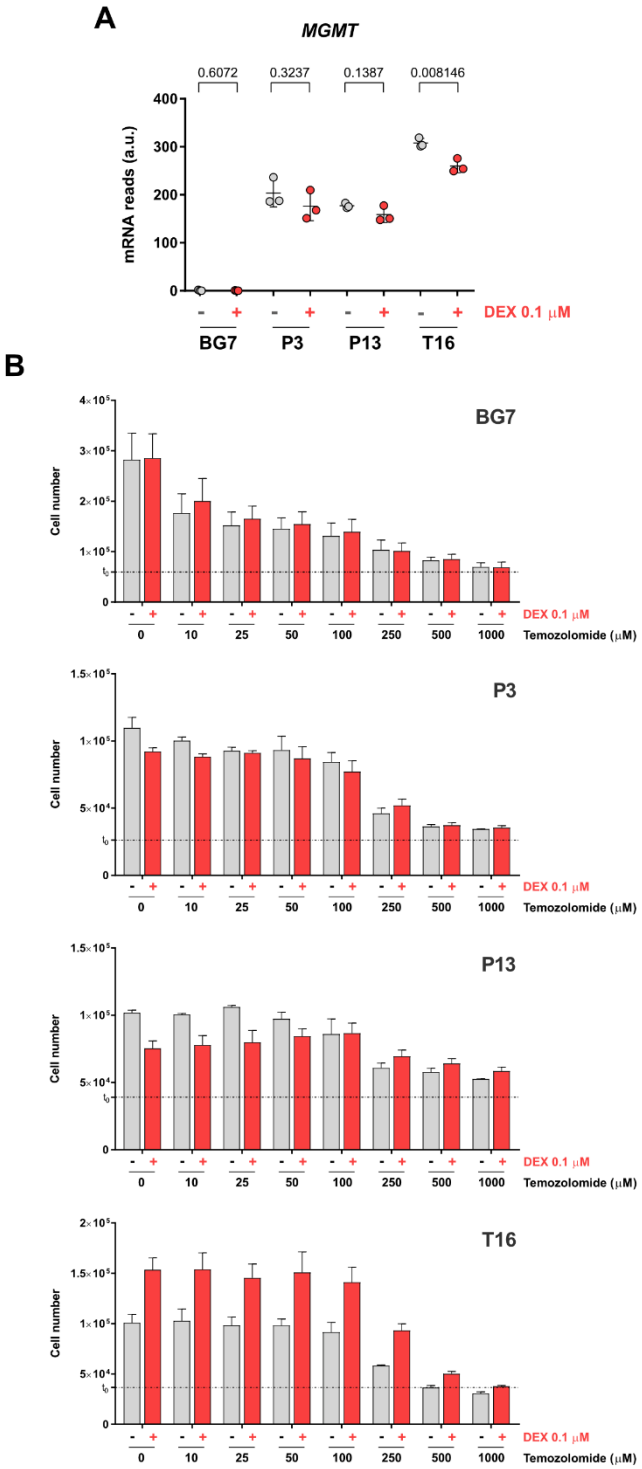

Figure 4-5 *MGMT* expression levels inversely correlate with sensitivity to temozolomide

A) Cell were cultured as adherent monolayers in Plasmax containing vehicle (ethanol) or 0.1 µM dexamethasone for three days. Three days later, the culture medium was refreshed and 24 h later cell number was determined using a Coulter counter, and cells were harvested for whole RNA extraction. Subsequently, the samples were analysed by poly-A RNA sequencing. Each dot represents an independent experiment (n=3 independent experiments). *P* values result from two-tailed unpaired t-tests. B) The four PDX-derived cell lines have been cultured as adherent monolayers in Plasmax medium containing vehicle (ethanol), 0.1 µM dexamethasone for 24 hours. After 24 hours, the indicated concentration of temozolomide (0-1000 µM) has been added to the culture medium. The cells were counted after four days to assess cell growth (n=2 independent experiments, four wells have been counted for each condition in each experiment). T_0 indicates the number of cells when the treatment started.

4.3.4 *β-catenin* and *Wnt5A* are upregulated upon dexamethasone treatment

Next, we interrogated the T16 dataset from the RNAseq analysis to understand the mechanism behind the pro-proliferative effect of dexamethasone. Cell cycle regulation and WNT signalling-related pathways emerged as altered by dexamethasone. The evolutionarily conserved WNT—ß-catenin pathway is involved in a plethora of processes essential for both developing and adult tissues, through the regulation of cell proliferation, differentiation, and tissue homeostasis. WNT signalling has also been found to be highly deregulated in many cancer types, therefore many therapeutic agents have been developed in the attempt to target this pathway [168]. The mRNA levels of *CTNNB1*, encoding for ß-catenin, and *WNT5A* were significantly upregulated by the glucocorticoids treatment in 3 out of 4 cell lines (Figure 4-6, Panel A). We then investigated by Western blotting if the total levels of ß-catenin were changing upon dexamethasone treatment but we could not detect any significant difference (Figure 4-6, Panel B). Although, upon Wnt signalling activation, ß-catenin can translocate to the nucleus where it will drive target genes expression through the recruitment of transcriptional coactivators and histone modifiers [169]. In order to evaluate if dexamethasone was causing ß-catenin translocation to the nucleus, we performed a cellular fractionation experiment on T16 cells and measured ß-catenin levels in different cellular compartments. As shown in Panel C of Figure 4-6, ß-catenin levels were unaltered. We investigated if targeting this pathway would affect differently the vehicle- and dexamethasone-treated GBM cells. To this aim, we employed LGK974, an inhibitor of Porcupine, a membrane bound O-acyl transferase that is responsible for the palmitoylation of Wnt ligands before their secretion in the extracellular space [170]. In order to test if the dexamethasone-mediated upregulation of *WNT5A* in GBM naïve cells contributed to proliferation, we pre-cultured the cells in dexamethasone for four days and then treated them with LGK974. BG7 and P13 cells proliferation was reduced upon treatment with the Porcupine inhibitor, however dexamethasone did not significantly alter cell growth in these conditions (Figure 4-6, Panel D).

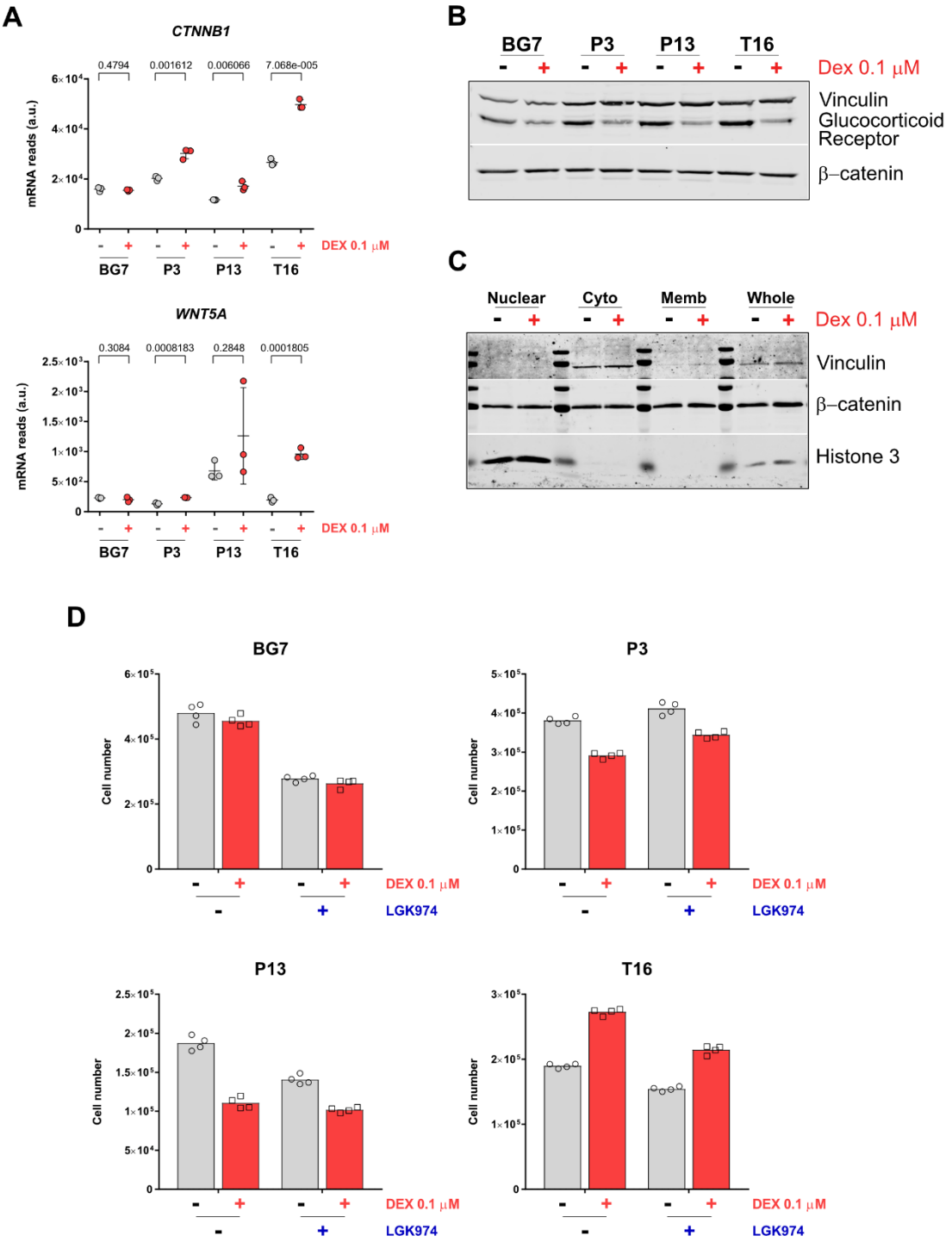

Figure 4-6 Dexamethasone causes *β-catenin* and *Wnt5A* overexpression but Porcupine inhibition does not affect GBM cells growth

A) Cells were cultured as adherent monolayers in Plasmax containing vehicle (ethanol) or 0.1 μM dexamethasone for three days. After three days, the culture medium was refreshed and 24 h later the cell number was determined using a Coulter counter, and cells were harvested for whole RNA extraction. Subsequently, the samples were analysed by poly-A RNA sequencing. Each dot represents an independent experiment (n=3 independent experiments). B) Cells were cultured for 72 h as adherent monolayers in Plasmax medium containing vehicle (ethanol) or dexamethasone (0.1 μM). The cells were lysated in RIPA buffer and the protein content quantified. Equal protein amounts were loaded and analysed by Western blotting. Vinculin was used as a loading control. C) T16 cells were cultured for 72 h as adherent monolayers in Plasmax medium containing vehicle (ethanol) or dexamethasone (0.1 μM). The Cell Fractionation Kit from Cell Signaling Technology was used to show nuclear, cytoplasmic, and organellular/membrane localization. Whole cell lysates were used to represent the total protein content. Equal protein amounts were loaded and analysed by

Western blotting. Vinculin and histone 3 were used as a loading control for the cytoplasmic and nuclear compartment, respectively. D) The four PDX-derived cell lines have been cultured as adherent monolayers in Plasmax medium containing vehicle (ethanol) or 0.1 µM dexamethasone for four days. After four days, the culture medium was refreshed and the cells were cultured in Plasmax medium containing vehicle (ethanol) or 0.1 µM dexamethasone with and without 5 µM LGK974 for three days. The cells were counted at the end of the seven days to assess cell growth (n=1, each dot represents data from a well).

4.4 Chapter discussion and results limitations

In order to define the transcriptional consequences of dexamethasone treatment in naïve GBM cells, we treated the cells with dexamethasone and then extracted and sequenced their whole transcriptome. The Principal Component Analysis following the RNA sequencing was able to discriminate between vehicle- and dexamethasone-treated GBM cells. BG7 cells were less segregated by the treatment possibly because dexamethasone caused fewer transcriptional changes than in the other three cell lines. In line with the variability and cell line-specificity we observed when analysing the cells proliferative response to dexamethasone, also the amount of transcriptional changes caused by the treatment was different in each cell line. The human glioblastoma tumours used to establish P3, P13 and T16 lines carried distinct chromosomal aberrations [26], and this difference might partially explain the unique transcriptional response of each cell line to dexamethasone. With a whole transcriptome analysis we identified genes that were significantly regulated by dexamethasone in four out of four GBM lines. This dexamethasone-specific transcriptional signature consisted of only 81 genes, of which 79 were consistently upregulated in all GBM lines. Some of these are known targets of dexamethasone, such as *KLF9* and *FKBP5*. We performed a series of exploratory experiments to test if selected transcriptional targets of dexamethasone could have an impact on cell proliferation and survival of glioblastoma cells and could underpin the pro-proliferative dexamethasone effects observed in T16 cells. Dexamethasone induced the expression of the anti-apoptotic protein Bcl-xL. We validated this upregulation at the protein level, and evaluated the effects of Bcl-xL pharmacologic inhibition. When we treated the GBM cells with ABT737, inhibiting both Bcl-2 and Bcl-xL, and A-1155463, a specific inhibitor of Bcl-xL, we observed a cell-line dependent inhibitory effect on proliferation, suggesting that cells might express and rely on different Bcl-2 proteins. Interestingly, in P3 and P13 cells upon treatment with the alkylating agent temozolomide, dexamethasone had a protective effect, possibly corroborating previous research showing that dexamethasone antagonizes temozolomide-induced apoptosis by decreasing the Bax—Bcl-2 ratio [119]. Given the clinical relevance of both dexamethasone and temozolomide in GBM standard-of-care, the impact of dexamethasone on apoptosis-inducing therapies needs more in-depth investigation. Moreover, in addition to the cell counting that we performed to assess the effect of dexamethasone combination with the Bcl2

inhibitors, it would be sensible to measure more direct indexes of apoptosis and cell death.

Another gene whose expression was significantly upregulated in the four GBM lines was *ELOVL2 (*Elongation Of Very Long Chain Fatty Acids-Like 2). The members of the ELOVL superfamily are membrane-bound enzymes responsible for the rate-limiting condensation step in the fatty acids elongation cycle. Specifically ELOVL2, ELOVL4 and ELOVL5 are responsible for the elongation of polyunsaturated fatty acids (PUFA) [171]. Fatty acids can be either taken up from diet or synthesized by the cytosolic enzyme fatty acid synthase (FASN) and then further elongated. All GBM lines tested exhibited a significant dexamethasone-mediated *ELOVL2* overexpression, and three of them also displayed a significant increase in *ELOVL5* levels. To investigate if limiting the amount of externally provided fatty acids would differently affect vehicle- and dexamethasone-treated cells, we supplemented GBM cells with either a lipid rich supplement (AlbuMAX™ II) or fatty acids-free albumin. Unexpectedly, fatty acids withdrawal did not markedly inhibit cell proliferation possibly due to the high expression levels of fatty acid synthase (*FASN*) and Fatty acid desaturase 2 (*FASN2*) (Figure 4-7), ensuring an endogenous source of fatty acids. Given the study from Gimple et al. [166], highlighting the impact of ELOVL2 overexpression on glioblastoma stem cells, the dexamethasone-mediated induction of *ELOVL2* should be tested *in vivo*. Moreover, lipidomic analyses would shed light on the hypothesis that dexamethasone treatment could alter the lipid profile of glioblastoma cells possibly allowing them to adapt to the dynamic tumour microenvironment.

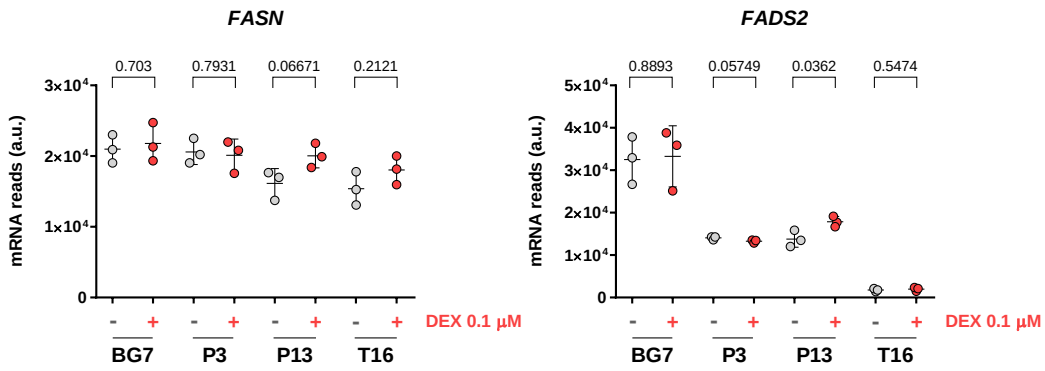

Figure 4-7 GBM cells expression levels of the genes encoding for some of the enzymes involved in fatty acids biosynthesis

Cell were cultured as adherent monolayers in Plasmax containing vehicle (ethanol) or 0.1 µM dexamethasone for three days. After three days, the culture medium was refreshed and 24 h later the cell number was determined using a Coulter counter, and cells were harvested for whole RNA extraction. Subsequently, the samples were analysed by poly-A RNA sequencing. Each dot represents an independent experiment (n=3 independent experiments). *P* values result from unpaired two-tailed t-tests.

We observed that among the four GBM lines employed for this project, BG7 cells carried the *MGMT* silencing that characterizes ~40% of glioblastoma cases, making the patients more responsive to temozolomide-based therapeutic regimens [18]. A dose-response experiment confirmed that BG7 cells have a much higher sensitivity to temozolomide than the other cell lines. Moreover, in P3 and P13 cells upon combination of high concentrations of temozolomide and dexamethasone, we could not observe anymore the decrease in proliferation usually obtained with dexamethasone alone, suggesting that dexamethasone partially protected the cells from the cytotoxic effects of the alkylating agent. These results are consistent with a study performed in glioblastoma T98G cells showing that dexamethasone (200 µM) counteracted the temozolomide-induced apoptosis [172]. Moreover, a retrospective analysis of newly diagnosed GBM patients showed that administering both dexamethasone and temozolomide during radiotherapy correlated with a reduced overall survival and progression-free survival, a detrimental effect counteracted by Bevacizumab [123]. We can speculate that the hypermethylation of MGMT observed in BG7 cells is associated with the reduced responsiveness to dexamethasone, as indicated by the fewer transcriptional changes compared to the other cell lines.

Finally, we investigated if the RNA sequencing results could provide an explanation for the over-proliferative behaviour of T16 cells upon dexamethasone treatment. We observed a significant increase in the mRNA levels of the genes encoding for ß-catenin and Wnt5A, a ligand of the non-canonical WNT signalling. Dexamethasone-mediated effects on ß-catenin and Wnt5A have been observed at the protein level in mammary epithelial tumour cells [173, 174], but in our conditions ß-catenin levels were not significantly affected by dexamethasone. Through cellular fractionation we tested if ß-catenin translocation to the nucleus was favoured by dexamethasone, a hypothesis that we could not confirm. In glioma and other cancer models a correlation between MGMT expression and ß-catenin has been shown [175], potentially explaining why in BG7 cells

dexamethasone does not cause any alteration of Wnt5A/ß-catenin. Furthermore, the exposure of GBM cells to LGK974, a Porcupine inhibitor used to prevent Wnt ligand secretion, showed a cell line-dependent but dexamethasone-independent effect on proliferation, suggesting that the transcriptional increase of Wnt5A and ß-catenin does not have an impact on GBM cell proliferation.

Finally, the *in vitro* settings of this experiment leave the door open to the possibility that these changes might not be recapitulated *in vivo*, therefore it would be relevant to define dexamethasone-induced transcriptional changes when these cells are orthotopically injected and allowed to form tumours in animal models.

4.5 Summary

We performed an experiment of RNA sequencing on the GBM cells upon 72 hours of dexamethasone treatment. This highlighted that dexamethasone has a glioblastoma-specific transcriptional signature, including already known targets such as *FKBP5* and *KLF9*, but also genes whose glucocorticoids-mediated regulation has not been observed before in glioblastoma models. Among these genes, dexamethasone caused an increase in the levels of *Bcl-xL*, an anti-apoptotic protein part of the Bcl-2 family proteins, *ELOVL2*, encoding a polyunsaturated fatty acids elongase shown to be a potential target for glioblastoma therapy, and *β-catenin* and *Wnt5A*. We then investigated if interfering with these pathways upon dexamethasone treatment would differently alter GBM cells growth but dexamethasone did not alter their proliferation in any of the conditions considered.

Chapter 5. Metabolic characterization of dexamethasone-mediated effects in glioblastoma *in vitro* models

5.1 Introduction

As suggested by their name, glucocorticoids have a role in regulating glucose metabolism. Their impact on metabolism becomes evident in individuals with pathological hypersecretion of glucocorticoids or patients undergoing glucocorticoids-based therapies, exhibiting medical conditions such as obesity, hyperglycaemia, elevated cholesterol, and insulin resistance [176]. Despite the molecular mechanisms through which glucocorticoids regulate cellular metabolism are not fully understood, several studies have shown that they are responsible for the hepatic induction of gluconeogenesis and downregulation of glucose uptake [177]. Most of these mechanisms have been investigated in normal organs, such as liver and adipose tissues, while our understanding of the glucocorticoids-mediated effects on cancer cells metabolism is much more limited. The results collected in the previous chapters have highlighted the heterogeneous response of GBM cells to dexamethasone in terms of proliferation and transcriptional response. In order to identify dexamethasone-induced phenotypes reproducible in all four GBM lines, we decided to focus on the alterations induced by dexamethasone on cellular metabolism.

5.2 Profiling the metabolic state of GBM cells

5.2.1 Dexamethasone does not affect Oxygen Consumption Rate in GBM cells

Firstly, we employed the Seahorse XF Analyzer to measure the Oxygen Consumption Rate (OCR) of GBM cells upon dexamethasone administration. As observable in Figure 5-1 (Panel A), dexamethasone treatment did not alter the OCR of any of the cell lines tested. Given the bicarbonate presence in Plasmax medium, the ECAR values obtained from this experiment were discarded. Therefore, the glycolytic index of the cells was analysed through the YSI Biochemistry Analyzer as shown in Figure 5-1 (Panel B). Only in P13 cells dexamethasone significantly reduced the glycolytic flux.

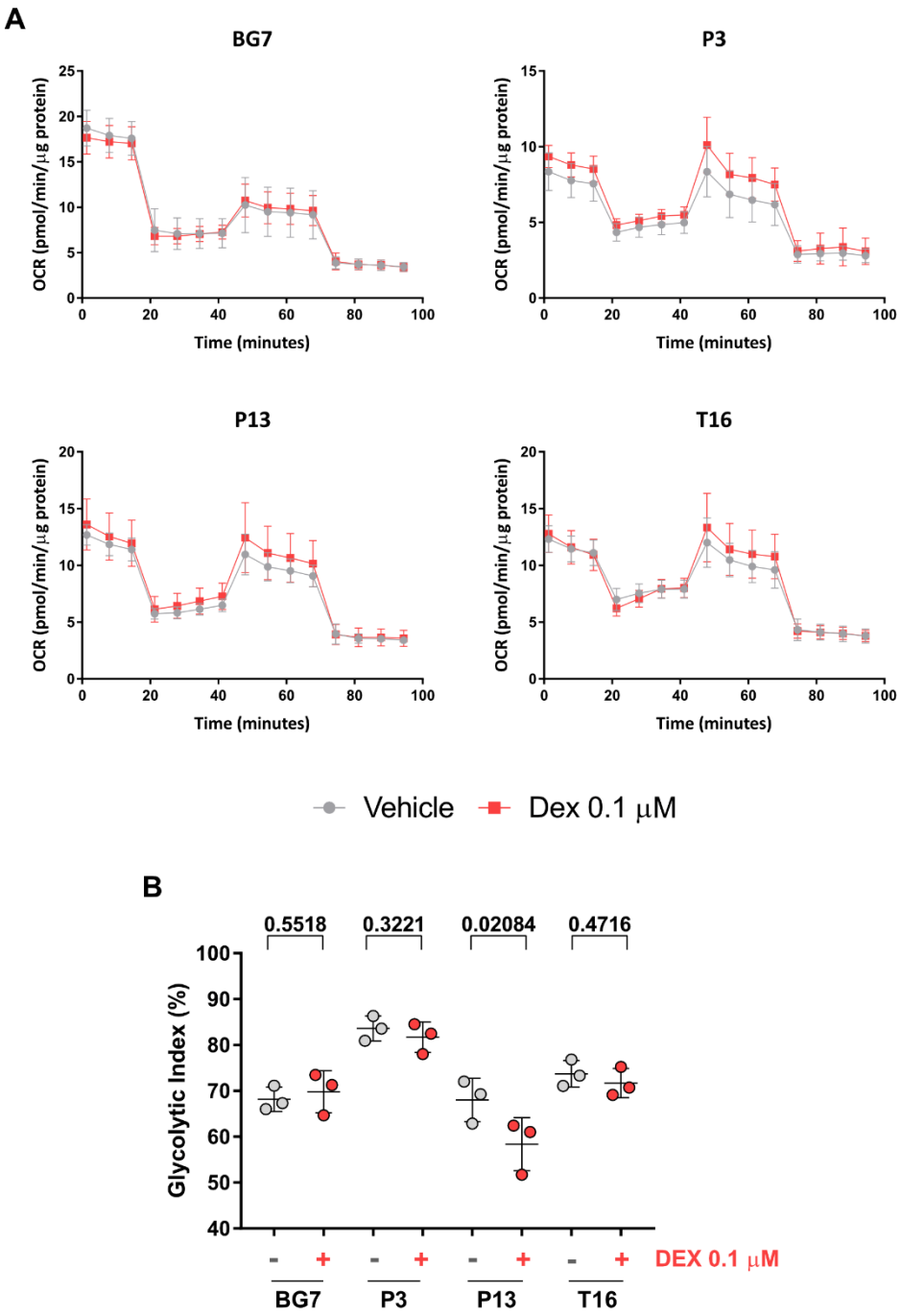

Figure 5-1 The oxygen consumption rate of GBM cells is not affected by dexamethasone treatment

A) Cells have been cultured as adherent monolayers in Plasmax medium containing vehicle (ethanol) or 0.1 µM dexamethasone. After 72 h, the medium was replaced with fresh Plasmax. After 3 hours, cellular respiration was measured with the Seahorse XF96 Analyzer using the Seahorse Cell Mito Stress Test Kit (Seahorse Bioscience). The assay was performed injecting sequentially 1 µM of Oligomycin, 2 µM of FCCP and 0.5 µM of Rotenone and Antimycin A. The oxygen consumption rate was recorded and normalized to protein content (n=1 independent experiment, for each condition 8 wells have been measured). B) Cells were cultured in 24-well plates as adherent monolayers in Plasmax medium (400 µL/well). After 72 h, the medium was refreshed (time 0) and samples of medium were collected at different time points and transferred to an YSI Biochemistry Analyzer 96-wells plate where glucose and lactate concentrations were measured. For each well the glycolytic index (x) was calculated as x= (secreted lactate*0.5)/(consumed glucose). The measurements were normalized to protein content/well (n=3 independent experiments, 3 wells were analysed for each condition). *P* values result from paired two-tailed t-tests.

5.2.2 Hypoxia has a cell line-dependent effect on GBM cells growth

Within the tumour mass there are less oxygenated hypoxic areas, where the hypoxia-inducible factors (HIFs) orchestrate a transcriptional response [178]. In order to investigate how hypoxic conditions affected the growth of GBM cells and if dexamethasone had an impact on this response, we cultured the cells as monolayers in a normoxic (21% O_2) or hypoxic (1% O_2) environment treating them with dexamethasone (Figure 5-2). Dexamethasone had a cell-line specific effect on the proliferation of GBM cells cultured in hypoxic conditions, consistent with the results obtained at 21% oxygen levels. More specifically, we observed that the growth of BG7 cells was significantly impaired at 1% oxygen concentrations, but not significantly affected by dexamethasone. P3 cells proliferation was slowed down by hypoxia that also abrogated dexamethasone antiproliferative effects. A comparable result was observable in P13 cells where hypoxia appeared to blunt the dexamethasone-mediated inhibitory effect. Finally, we observed that hypoxia did not have any effect on the growth of T16 cells in the presence or absence of dexamethasone (Figure 5-2).

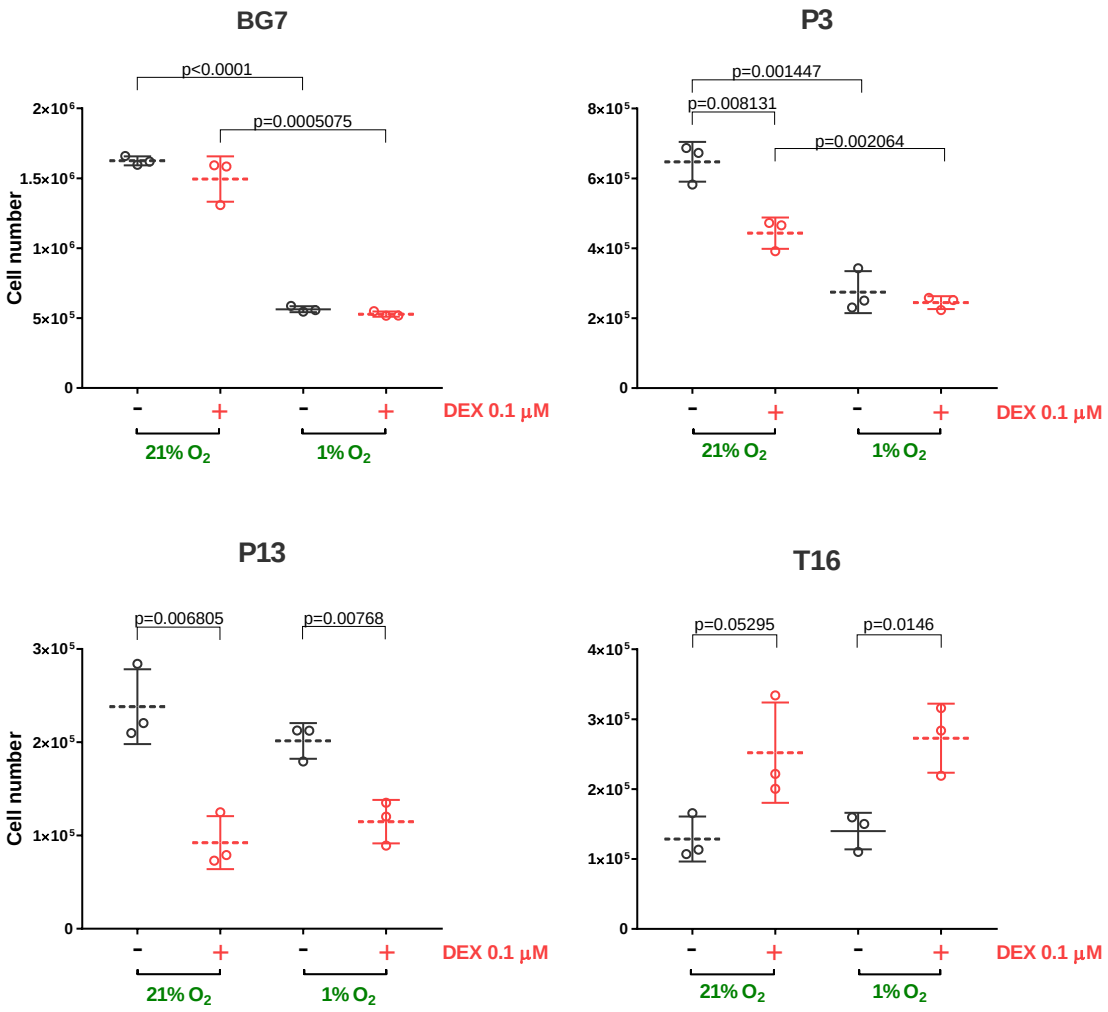

Figure 5-2 Dexamethasone has a cell-line specific effect on GBM cells growth upon hypoxic conditions

Cells have been cultured as adherent monolayers in Plasmax medium containing vehicle (ethanol) or 0.1 µM dexamethasone at physiological (21% O_2) or hypoxic (1% O_2) oxygen concentrations for 12 days. The medium was refreshed every 4 days to avoid nutrient exhaustion. The cells were counted to assess cell growth after 12 days (n=3 independent experiments, 4 wells have been counted for each condition). *P* values result from unpaired two-tailed t-tests.

5.2.3 Glioblastoma cells avidly consume glutamate

As previously anticipated in order to characterize further the metabolic profile of GBM cells, we used the YSI Biochemistry Analyzer to obtain a quantitative readout of glucose, lactate, glutamine and glutamate concentrations in the media sampled at different time points (Figure 5-3). The results highlighted the glycolytic behaviour of P3 cells, which compared to the other cell lines, consumed the entire amount of glucose (5.5 mM) present in 0.4 ml of Plasmax in 24 hours. Moreover, this experiment revealed that T16 cells secreted glutamine in the medium, suggesting that these cancer cells retain high glutamine synthetase (GS) activity, a metabolic hallmark of normal astrocytes. It has been shown that in the tumour microenvironment, GS-positive GBM cells supports the growth of GS-negative cells requiring exogenous supply of glutamine for growth [148]. Furthermore, and irrespectively of glutamine release, all GBM cells entirely cleared the whole pool of glutamate (98 μM) present in the media within 6 hours. This metabolic behaviour is consistent with high affinity glutamate uptake, another astrocytic hallmark. Among the four metabolites whose changes in uptake/secretion were measured through the YSI Biochemistry Analyzer, dexamethasone had a significant effect on P3 and P13 cells glutamine uptake. Particularly, at 12 and 24 h the glutamine consumption by dexamethasone-treated cells was significantly less than glutamine consumption by vehicle-treated cells. Moreover, in P13 cells dexamethasone had a slight but significant effect also on the consumption of glucose (24 h) and glutamate (1 and 3 h), and the secretion of lactate (12 and 24 h).

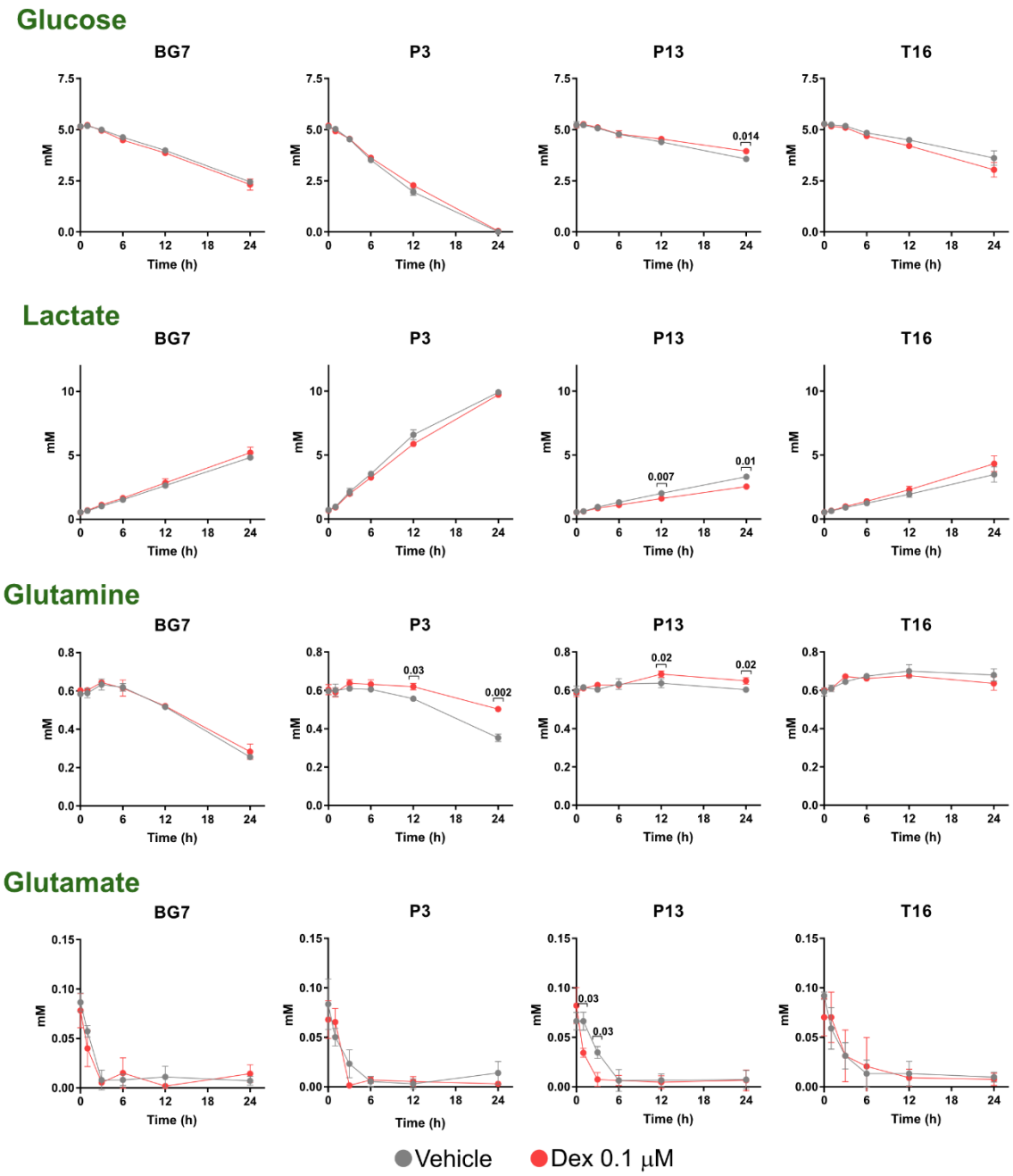

Figure 5-3 Glioblastoma cells differently consume glucose, lactate, glutamine and glutamate within 24 hours

Cells were cultured in 24-well plates as adherent monolayers in Plasmax medium (400 µL/well). After 72 h, the medium was refreshed (time 0) and samples of medium were collected at 0, 1, 3, 6, 12, 24 hours. The media samples were then transferred to an YSI Biochemistry Analyzer 96-wells plate and glucose, lactate, glutamine and glutamate concentrations were measured. The measurements were normalized to protein content/well (n=3 independent experiments, for each condition 3 wells were averaged). *P* values are adjusted *p* values resulting from multiple t-tests.

5.3 Untargeted LC-MS analysis identifies new dexamethasone-dependent metabolic alterations

We employed liquid chromatography-mass spectrometry (LC-MS) to characterize the metabolome of GBM cells and identify metabolites whose levels were significantly affected by dexamethasone treatment. Firstly we designed an experimental plan (Figure 5-4, Panel A) suitable to analyse the intracellular metabolome and the exchange rates of nutrients and metabolites between GBM cells and media upon dexamethasone treatment (Figure 5-4, Panel B). The exchange rates analysis farther corroborated the results we had obtained from the YSI Biochemistry Analyzer, showing that glucose was the most consumed nutrient and glutamate the second most consumed metabolite for all GBM cells. Moreover, pyruvate and lactate were the most secreted nutrients, and GBM cells were either consuming or releasing glutamine. We observed some differences among the four cell lines in the consumption of few amino acids, such as alanine and proline, but dexamethasone treatment did not significantly and consistently affect the exchange rates of any of the most highly consumed/secreted metabolites (Figure 5-4, Panel B).

The analysis of the extracellular media curiously highlighted a difference between the four GBM lines. Looking at the levels of 5'-methylthioadenosine (MTA) in the extracellular media, we found that BG7 cells expressed 5'-Methylthioadenosine Phosphorylase (MTAP), i.e. the enzyme responsible for the phosphorylation of MTA to adenine and 5-methylthioribose-1-phosphate, while the other three GBM lines lacked the enzyme and were accumulating the metabolite in the extracellular milieu (Figure 5-4, Panel C). This was also confirmed by the mRNA levels analysis that showed reduced levels of *MTAP* in all GBM lines excluding BG7 cells (Figure 5-4, Panel D). Dexamethasone treatment did not have any effect on MTA metabolism.

Then, we proceeded with an untargeted approach to pinpoint metabolic *features* consistently regulated by dexamethasone in all cell lines. As shown in Figure 5-5 (Panel A) this analysis was performed through the software Compound Discoverer, and allowed us to find several features that were significantly accumulating upon dexamethasone treatment. One of the features that we identified with this analysis was dexamethasone itself. In order to determine the identity of other

features that were increased in dexamethasone-treated cells, we compared the fragmentation spectra of the cellular extracts with the spectra found on the public database mzCloud™. Moreover, analysing commercially available standards, through their retention times we found that two of the compounds coherently and significantly accumulating in the dexamethasone-treated GBM cells were *N*1-methylnicotinamide and UDP-α-glucuronic acid (Figure 5-5, Panel B).

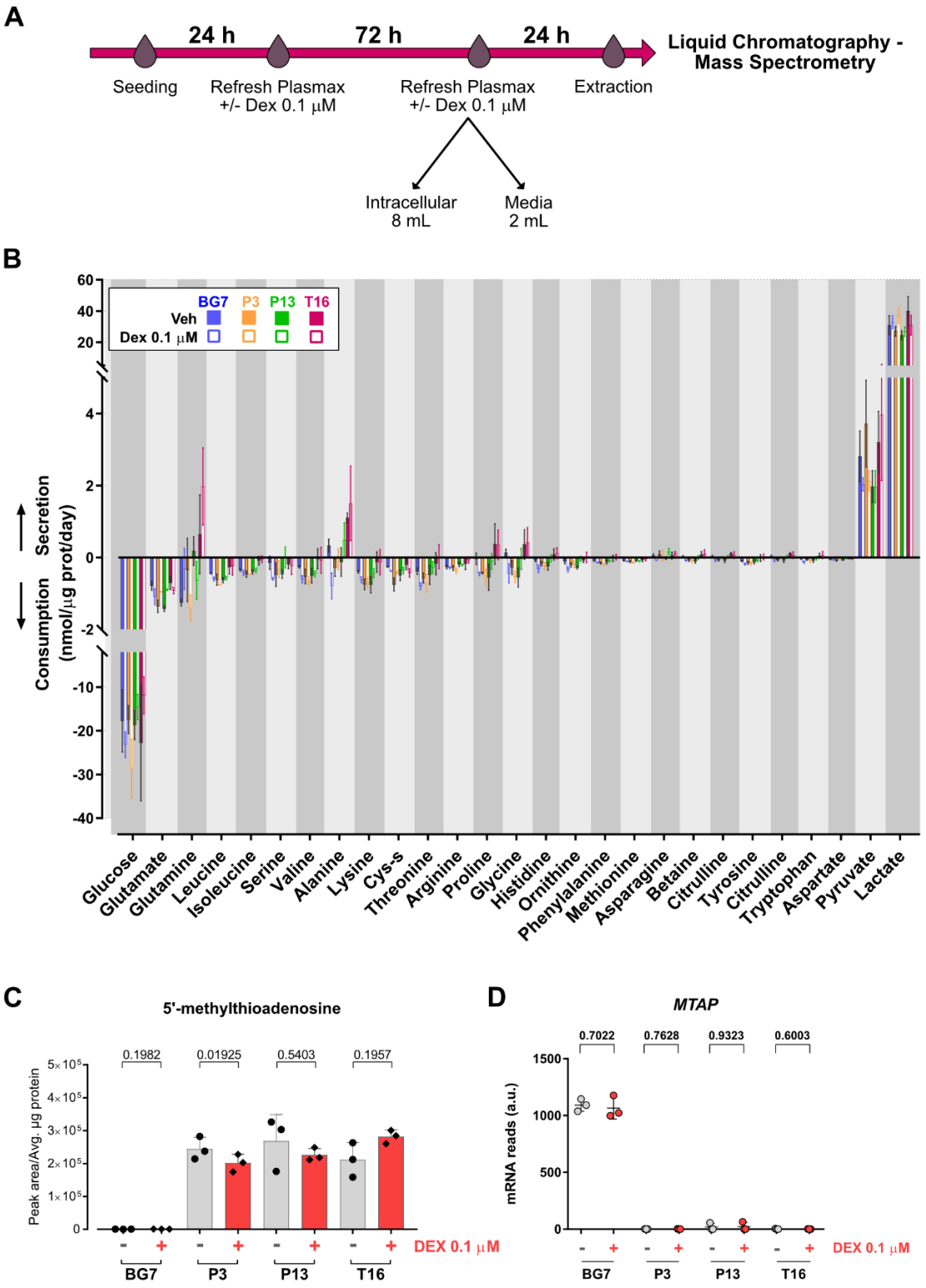

Figure 5-4 Metabolites exchange rates of GBM cells upon dexamethasone treatment

A) This experimental plan was used to investigate the intracellular metabolome and the metabolites exchange rate of the cells upon dexamethasone treatment. Cells were cultured for 72 h as adherent monolayers in Plasmax containing vehicle (ethanol) or 0.1 µM dexamethasone. The culture medium was replaced by 8 mL for the intracellular metabolome (panel C) and 2 mL for the metabolites exchange rates (panel B) and 24 h later the metabolites were extracted with extraction solution and the samples analysed by LC-MS (n=3 independent experiments, for each condition 3 wells were averaged). D) Cells were cultured as adherent monolayers in Plasmax medium containing vehicle (ethanol) or 0.1 µM dexamethasone (DEX) for 72 h. The culture medium was replaced and 24 h later cells were counted and harvested for RNA extraction and sequencing (n=3 independent experiments). *P* values result from paired two-tailed t-tests.

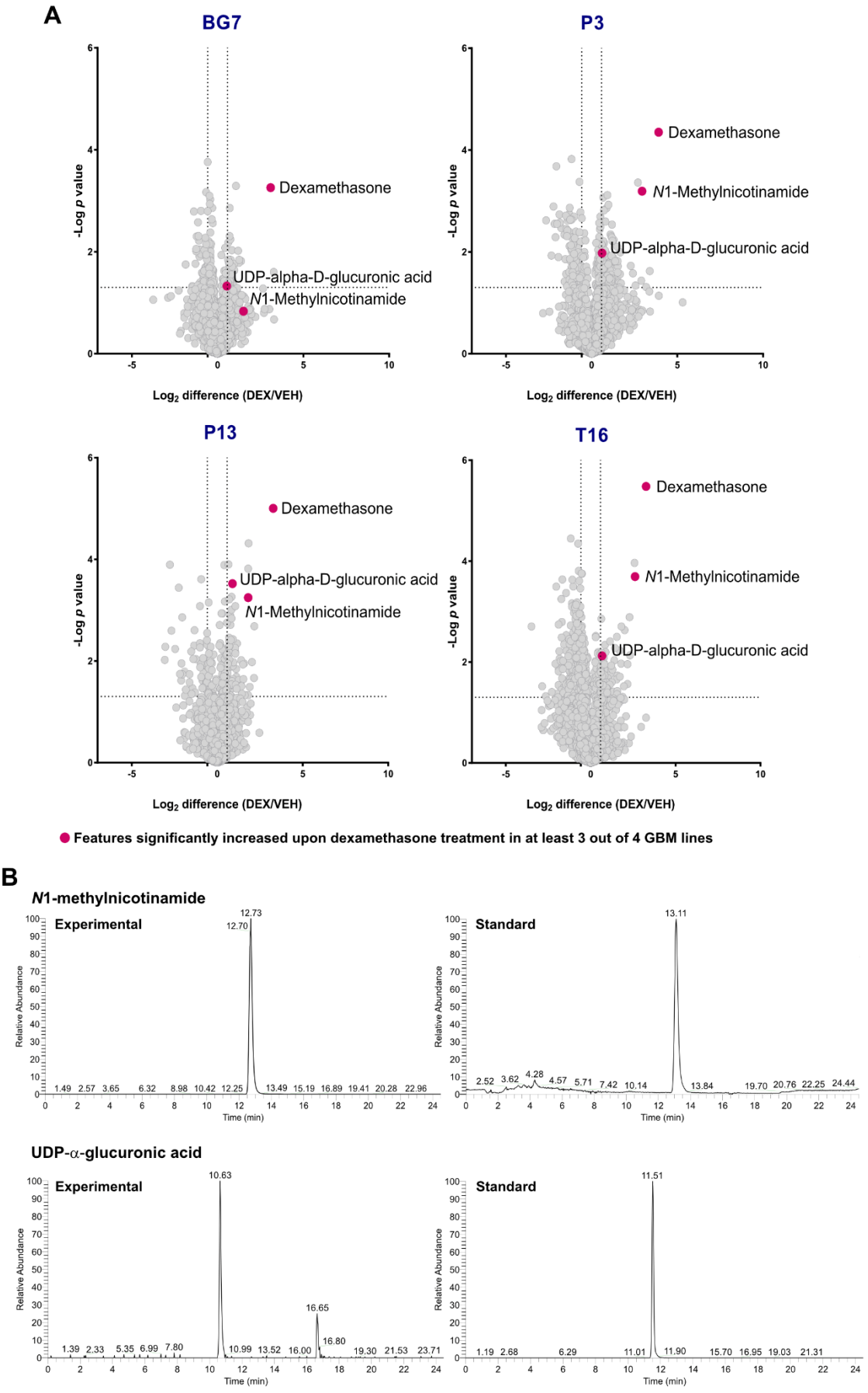

Figure 5-5 Untargeted metabolomics approach identifies metabolic *features* accumulating in dexamethasone-treated GBM naïve cells

A) The untargeted analysis was performed through the software Compound Discoverer and the metabolites that were changing upon dexamethasone treatment in GBM cells are shown in the volcano plots. The fuchsia dots indicate the metabolic features that were significantly accumulating in at least 3 out of 4 GBM cell lines upon dexamethasone administration (n=3 independent experiments; 3 wells were extracted for each condition). B) *N*1-methylnicotinamide and UDP-α-glucuronic were identified by comparing the mass and retention time of experimental peaks to an in-house library generated using commercial standards.

5.4 Dexamethasone regulates *NNMT* expression

As a further validation of the identity of these metabolites, we turned to a targeted metabolomics approach and used the TraceFinder software to confirm the pattern of *N*1-methylnicotinamide and UDP-α-glucuronic acid upon dexamethasone treatment. We confirmed that dexamethasone was only found in treated GBM cells (Figure 5-6, Panel A), and that consistently with the untargeted analysis, the dexamethasone-induced increase in *N*1-methylnicotinamide and UDP-α-glucuronic acid levels was statistically significant in three out of four GBM lines while the trend was comparable in all cell lines (Figure 5-6, Panel A). In order to explain the build-up of these metabolites upon DEX treatment, we focused on the enzymes responsible for their synthesis. *N*1-methylnicotinamide represents the methylated form of nicotinamide (NAM), one of the essential precursors for the synthesis of Nicotinamide Adenine Dinucleotide (NAD+). *N*1-methylnicotinamide is synthesized by nicotinamide-*N*-methyltransferase (NNMT), a cytosolic enzyme that transfers methyl groups from the methyl donor *S*-adenosyl-L-methionine (SAM) to nicotinamide (a schematic of this reaction can be found in Figure 5-9). In parallel, we investigated the accumulation of UDP-α-glucuronic acid in dexamethasone-treated cells. UDP-α-glucuronic acid, synthesized by the enzyme UDP-glucose-6-dehydrogenase (UGDH), represents the precursor for the biosynthesis of glycosaminoglycans and proteoglycans, i.e. components of the extracellular matrix [179]. To investigate if dexamethasone was upregulating NNMT at the transcriptional level, we went back to the RNA sequencing analysis and observed an accumulation of *NNMT* mRNA in the dexamethasone-treated cells. Indeed, *NNMT* was one of the 79 genes that we had identified as the dexamethasone-specific transcriptional signature in GBM cells. On the other hand, there was no difference in the levels of *UGDH* mRNA (Figure 5-6, Panel B). Moreover, NNMT levels were tested by Western blotting that revealed that dexamethasone was boosting the expression of the enzyme in all four GBM lines (Figure 5-6, Panel C). However, consistently with the unchanged transcriptional levels, UGDH expression was not affected by dexamethasone treatment in our experimental model, suggesting that dexamethasone might regulate metabolic reactions downstream of UDP-α-glucuronate (Figure 5-6, Panel C).

The analysis of the extracellular metabolome of GBM cells allowed us to observe *N*1-methylnicotinamide accumulation also in the extracellular media of the dexamethasone-treated cells (Figure 5-6, Panel D). However, extracellular UDP-α-glucuronic acid was not detectable in any of the conditions tested.

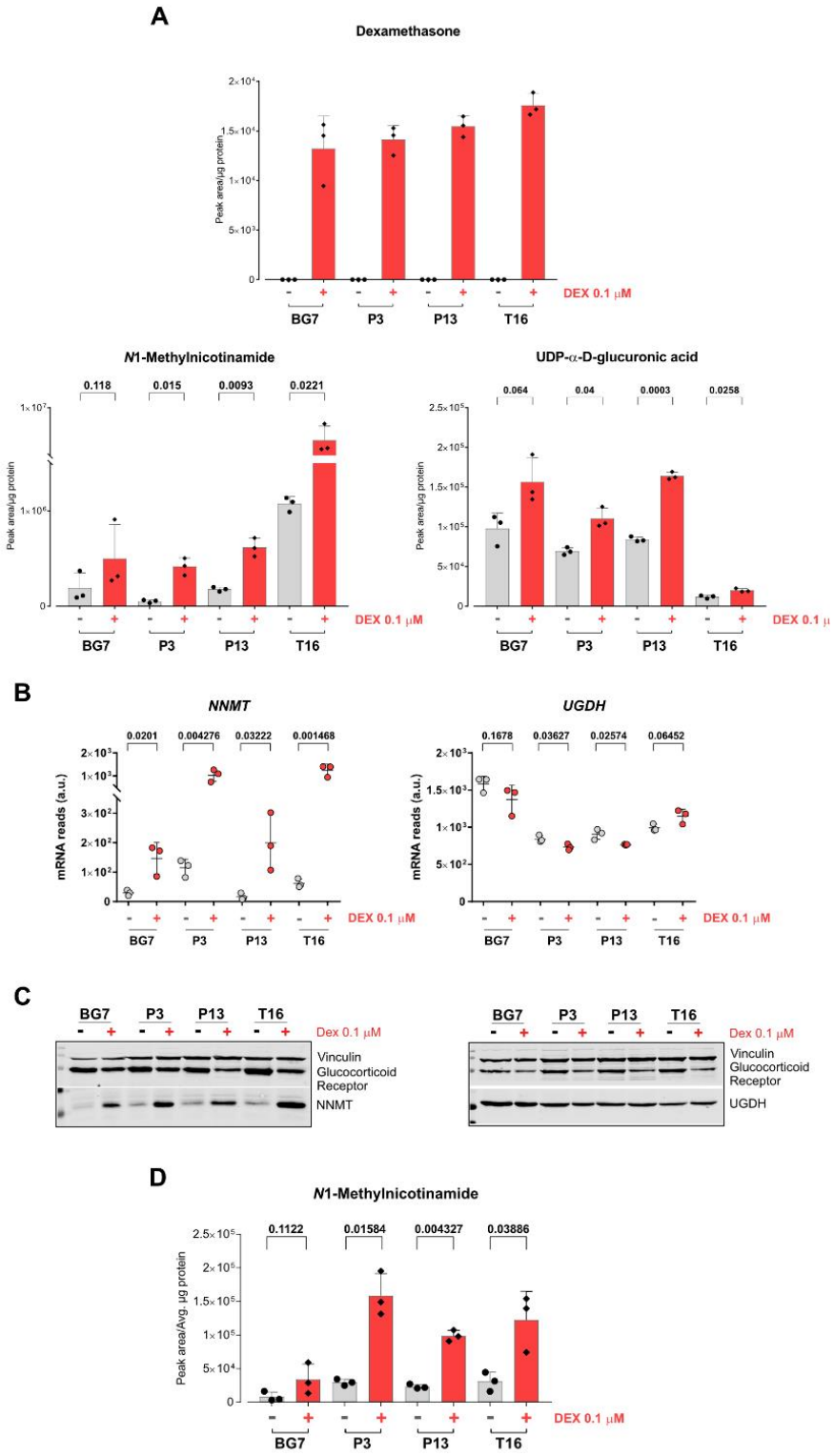

Figure 5-6 Dexamethasone causes accumulation of *N*1-methylnicotinamide and UDP-α-glucuronic acid in GBM cells

A) GBM cells were cultured for 72 h as adherent monolayers in Plasmax medium containing vehicle (ethanol) or 0.1 µM dexamethasone (DEX). After three days, Plasmax medium was refreshed and 24 h later the intracellular metabolites were extracted with extraction solution. The bar plots represent the peak areas of the metabolites normalized for the protein content (n=3 independent experiments; 3 wells have been averaged for each condition). B) Cells were cultured as adherent monolayers in Plasmax medium containing vehicle (ethanol) or 0.1 µM dexamethasone (DEX) for 72 h. The cell culture medium was refreshed and 24 h later cells were counted and harvested for RNA extraction and sequencing (n=3 independent experiments). C) Cells have been cultured for 72 h as adherent monolayers in Plasmax medium containing vehicle (ethanol) or 0.1 µM dexamethasone (DEX). The cells were lysated in RIPA buffer and the protein content quantified. Equal protein amounts were loaded and analysed by Western blotting. Vinculin was used as a loading control. D) GBM cells were cultured for 72 h as adherent monolayers in Plasmax medium containing vehicle (ethanol) or 0.1 µM dexamethasone (DEX). After three days, Plasmax medium was refreshed and 24 h later the extracellular metabolites were extracted with extraction solution. The bar plots represent the peak areas of *N*1-methylnicotinamide normalized for the protein content (n=3 independent experiments; 3 wells have been averaged for each condition). *P* values result from paired two-tailed t-tests.

5.4.1 Dexamethasone-mediated NNMT induction is conserved across a wide panel of naïve GBM lines and in 3D cultures

In order to test the generality of dexamethasone-mediated NNMT induction observed in GBM cells we expanded the panel with 6 more naïve GBM lines obtained from Prof Steve Pollard, University of Edinburgh. In these cells we measured the intracellular levels of *N*1-methylnicotinamide upon dexamethasone treatment (Figure 5-7, Panel A), and found that in five out of six lines, dexamethasone significantly increased the levels of *N*1-methylnicotinamide. Moreover, also in these cells we could prove that the metabolic effect was the consequence of a dexamethasone-mediated increase in NNMT expression (Figure 5-7, Panel B). Also in this panel of GBM cells dexamethasone exerted cell line-dependent effects on proliferation (Figure 5-7, Panel C).

In the first chapter of the results of this project, we showed that GBM cells responded differently to dexamethasone if grown as a monolayer or as three-dimensional spheroids. The organoids architecture is believed to recapitulate some *in vivo* tumour features such as a heterogeneous access to nutrients, therefore these three-dimensional models have been employed to study GBM metabolism [180]. We investigated if the dexamethasone induced metabolic hallmarks were maintained in three-dimensional settings. To this aim, we extracted GBM spheroids metabolites and measured the levels of *N*1-methylnicotinamide and UDP-α-glucuronic acid. The levels of UDP-α-glucoronate were not altered by dexamethasone in GBM spheroids, but we observed a trend towards an increase in *N*1-methylnicotinamide levels upon dexamethasone treatment in three out of four cell lines (Figure 5-7, Panel D).

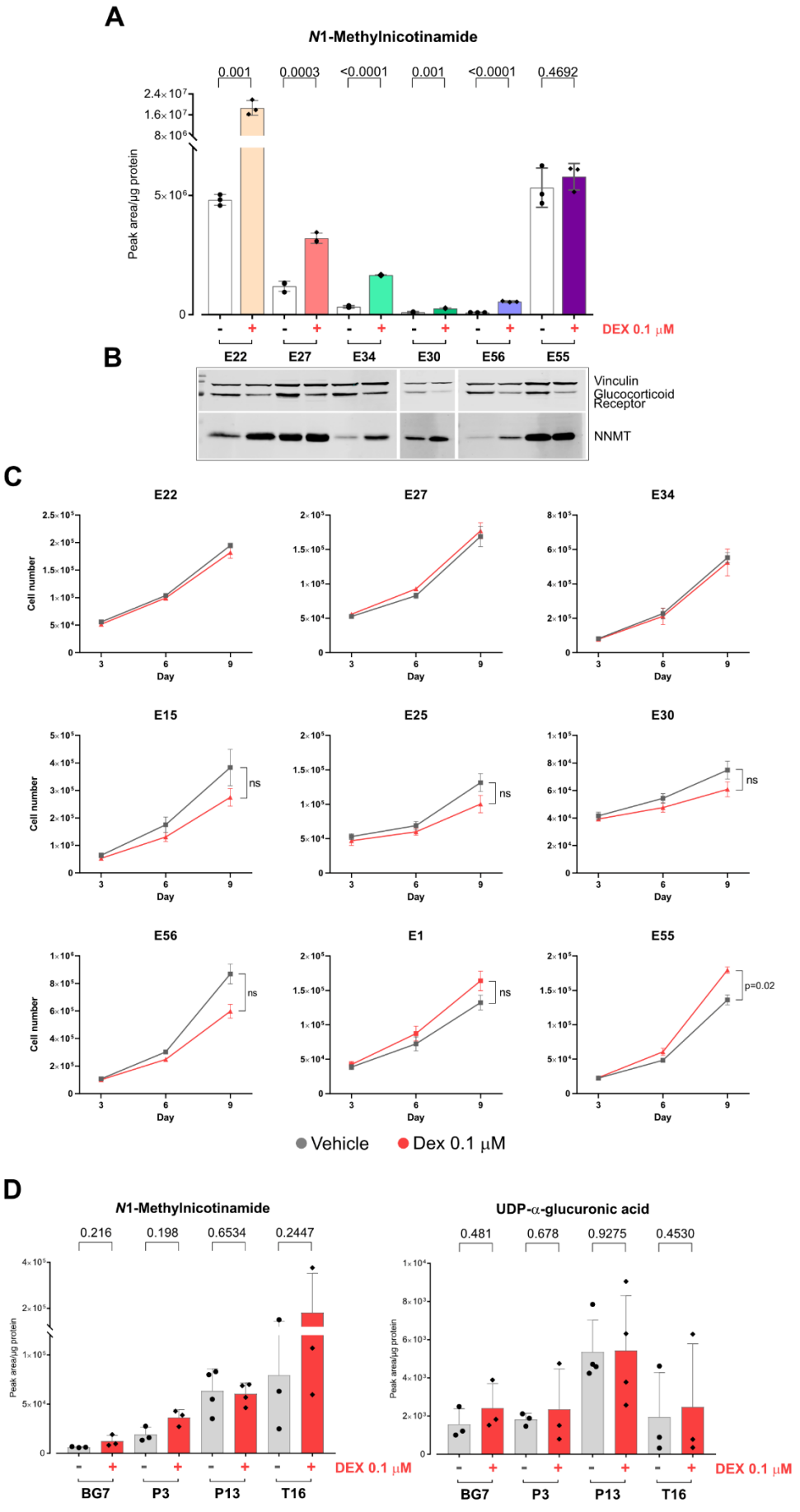

Figure 5-7 Dexamethasone-mediated NNMT induction is consistent across naïve GBM lines

A) Naïve GBM cells were cultured for 72 h as adherent monolayers in Plasmax containing vehicle (ethanol) or 0.1 µM dexamethasone. The culture medium was refreshed and 24 h later the intracellular metabolites were extracted with extraction solution. The bar plots represent the peak area of the metabolites normalized for the protein content (n=1 independent experiment; 3 wells have been extracted for each condition). B) Cells were cultured for 72 h as adherent monolayers in Plasmax medium containing vehicle (ethanol) or 0.1 µM dexamethasone (DEX). The cells were lysated in RIPA buffer and the protein content quantified. Equal protein amounts were loaded and analysed by Western blotting. Vinculin was used as a loading control. C) GBM cells were cultured as adherent monolayers in Plasmax medium containing vehicle (ethanol) or 0.1 µM dexamethasone (Dex) up to 9 days. The cells were counted every three days to assess cell growth and every 3 days, the culture medium was replaced to avoid nutrient exhaustion (n=3 independent experiments, 4 wells were counted for each condition). *P* values are adjusted *p* values resulting from multiple t-tests. D) GBM cells were cultured as spheroids in low-adherence flasks and treated for 72 h with vehicle (ethanol) or 0.1 µM dexamethasone. After three days, the culture medium was refreshed to avoid nutrient exhaustion and 24 h later the spheroids were extracted in extraction solution. The bar plots represent the peak area of the metabolites normalized for the protein content (n=3 independent experiments; 1 flask was extracted for each condition). *P* values result from paired two-tailed t-tests.

5.5 Chapter discussion and results limitations

In 2000, Douglas Hanahan and Robert Weinberg defined the 'cancer hallmarks' concept [181]. Since then, this idea has been revisited and refined to include the progressively discovered adaptations that cancer cells acquire to successfully grow in the tumour microenvironment. Ten years later the reprogramming of energy metabolism has been introduced as part of the hallmarks "next generation" [47]. The clinical relevance of glioma metabolism is demonstrated by the WHO brain tumour classification, where gliomas are divided in Isocitrate Dehydrogenase (IDH) wild-type and mutant [50]. The reason why this metabolic mutation is so relevant for glioma patients lies with the discovery of IDH-mutant tumours that have a better prognosis compared to patients with wild-type IDH1/IDH2 [19]. The higher aggressiveness and plasticity of IDH wild-type cells is also observed *in vitro* where these cells grow more easily than IDH-mutant counterparts. In the context of this project, we employed all IDH wild-type primary GBM cells derived from the most aggressive and common type of high grade glioma.

As illustrated in the introductory section, the centrality of glucocorticoids in the regulation of cellular metabolism has been known for a long time. Therefore, after characterizing how dexamethasone affects GBM lines growth and their transcriptional response, we focused on the metabolic effects of dexamethasone on GBM cells. With the aim of investigating the interaction between tricyclic antidepressant drugs and dexamethasone in anaplastic astrocytoma cells, Higgins et al. observed that pre-treating the cells with dexamethasone was able to amplify in a dose-dependent manner the inhibition of cellular respiration caused by clomipramine hydrochloride [182]. Nevertheless, in our conditions dexamethasone did not have an impact on the OCR of any of the GBM lines tested. This parameter is routinely used to determine how much cells rely on oxidative phosphorylation for biosynthetic and energetic purposes. In our experimental conditions, P3 cells appeared to have the lowest OCR suggesting that this GBM line relies comparatively more on the glycolytic flux than the other GBM cells. In 1924, Otto Warburg proposed what has been since called the "Warburg effect", theorizing that mitochondrial defects were forcing cancer cells to engage with glycolysis even in normoxic conditions [183]. The glycolytic pathway alone produces only 2 adenosine 5′-triphosphate (ATP) molecules for each glucose molecule *versus* the 38 ATP molecules synthetized when glucose metabolism is coupled with the

oxidative phosphorylation. The energetic inefficiency of glycolysis led Warburg to explain this behaviour with mitochondrial abnormalities, but we know today that cancer cells with perfectly functional mitochondria perform glycolysis in aerobic environment for yet to be fully understood reasons. The fast rate of glycolysis in a glucose-rich environment compensates for a lower ATP production, moreover several glycolytic intermediates represent building blocks for cancer biomass, and glycolysis allows production of NAD+ and lactate [184]. As mentioned at the beginning of this chapter, one of the known consequences of corticotherapy is the increase of circulating glucose levels. We hypothesized that the proliferation response of GBM cells to dexamethasone might reflect major alterations in the central carbon metabolism. To this aim, we measured the consumption/secretion of glucose, lactate, glutamine and glutamate with the Biochemistry YSI Analyser that highlighted the high glucose consumption of GBM naïve cells, with P3 cells clearing the entire pool of glucose available within 24 hours. Dexamethasone reduced the glycolytic expenditure of P13 cells only, while leaving unaltered the other three lines' glycolytic capacity. Moreover, dexamethasone did not affect the lactate dehydrogenase (LDH)-mediated conversion of pyruvate to lactate molecules. In the tumour context, lactate secretion has a crucial role as this metabolite acidifies the extracellular microenvironment, and in hypoxic conditions enables tumour growth and angiogenesis [185]. Moreover, *in vivo* research has shown that inhibiting the monocarboxylate transporters (MCTs) that are responsible for the transport of pyruvate and lactate across the plasma membrane disrupts viability and invasiveness of glioblastoma tumours [186]. In the normal brain, through the lactate shuttle astrocytes secrete lactate that is taken up by neurons and converted to pyruvate for fuelling the tricarboxylic acid (TCA) cycle or producing the neurotransmitter glutamate [187].

With the aim of recapitulating the hypoxic tumour microenvironment, we exposed the GBM cells to atmospheric high (21%) or hypoxic (1%) oxygen concentrations and followed their growth over time. This experiment highlighted the well-known GBM heterogeneity and showed a cell-line dependent susceptibility to a hypoxic environment. We observed that hypoxia partially rescued the dexamethasone-mediated inhibitory effect on P3 and P13 cells growth. It has been previously observed that in hypoxic conditions glucocorticoids can further upregulate HIF1α-dependent genes expression [188], furthermore in T-cell acute lymphoblastic

leukaemia cells hypoxia has been shown to induce glucocorticoids resistance [189]. Our results suggest a reduced sensitivity to glucocorticoids in hypoxic conditions, but this effect was cell line-dependent and observed only in two out of four cell lines.

Similarly to the aforementioned lactate shuttle, another metabolic feature of glioblastoma cells that is reminiscent of their glial origin is represented by the ability to consume glutamate. In the normal brain, astrocytes are responsible for taking up the glutamate released by synaptic neurons and failure to do so causes excitotoxicity and neuronal damage [190]. When we performed a time-course experiment to analyse the nutrients levels in spent medium, we observed that all GBM cells were consuming the entire pool of glutamate present in the culture medium. *SLC1A2,* encoding for the excitatory amino acid transporter 2 (EAAT2), was among the list of dexamethasone transcriptional targets coherently upregulated in all GBM lines (Figure 5-8, Panel A). EAAT2 represents one of the most abundant glutamate transporters in the brain, mainly expressed on the surface of glial cells that are responsible for clearing the glutamate present in the synapse, thus modulating the glutamatergic signalling and avoiding glutamate excitoxicity [191]. Physiological glucocorticoids are also produced upon exposure to various stressors and the impact of this stress response on glutamate-mediated neurotransmission has been partially understood [192]. We were expecting the dexamethasone-mediated *SLC1A2* overexpression to have an impact on the glutamate uptake capacity of GBM cells and indeed in P13 cells dexamethasone increased glutamate uptake at early points of the time course experiment.

The data we obtained regarding the glutamine consumption/uptake was remarkably cell line-dependent. In fact, while BG7 and P3 cells were actively consuming glutamine, P13 and T16 were producing it and releasing it in the media. Moreover, in the case of P3 and P13 cells we observed that dexamethasone-treated cells were consuming significantly less glutamine, suggestive of a dexamethasone-induced increased expression of glutamine synthetase (GS). From the RNA sequencing data, we could appreciate a statistically significant increase of mRNA levels of GLUL, the gene encoding for GS, upon dexamethasone treatment in P3 and P13 cells (Figure 5-8, Panel B), and by Western blotting we observed that GS protein was increased also in BG7 cells (Figure 5-8, Panel C).

This is in line with previous research showing that GS expression is regulated by physiological glucocorticoids [193].

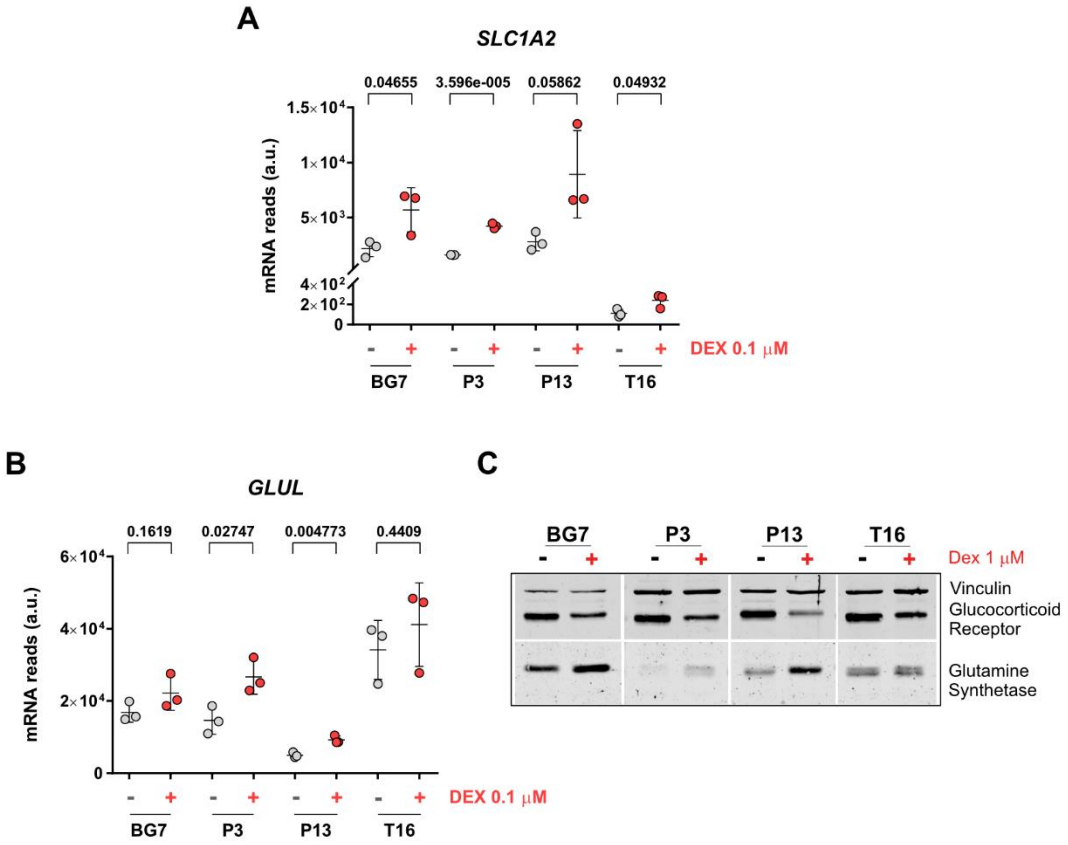

Figure 5-8 Glutamate and glutamine metabolism are differently affected by dexamethasone

A, B) Cells have been cultured as adherent monolayers in Plasmax medium containing vehicle (ethanol) or 0.1 μM dexamethasone (DEX) for 72 h. After three days, the culture medium was refreshed and 24 h later cells were counted and harvested for RNA extraction and sequencing (n=3 independent experiments). *P* values result from paired two-tailed t-tests. C) Cells were cultured for 72 h as adherent monolayers in Plasmax medium containing vehicle (ethanol) or 1 μM dexamethasone (DEX). The cells were lysated in RIPA buffer and the protein content quantified. Equal protein amounts were loaded and analysed by Western blotting. Vinculin was used as a loading control.

When P3, P13 and T16 cell lines were established from GBM patients tumour samples, their chromosomal aberrations were characterized and mapped [26]. Therefore, we knew that all three lines exhibited the homozygous deletion of p16/*CDKN2A*, an event occurring in ~50% of glioblastoma cases [194]. *CDKN2A* encodes for crucial tumour suppressors, but the relevance of its loss is also due to the co-deletion of proximal genes, such as *MTAP*, occurring in 80-90% of *CDKN2A*-deleted tumours [195]. MTAP is a metabolic enzyme responsible for the conversion of MTA to adenine and 5'-methylthioribose-1-phosphate, an essential reaction for the methionine salvage pathway and the polyamine pathway [196]. In GBM, MTAP loss has been shown to promote stemness features and render cells more susceptible to L-alanosine, an inhibitor of the *de novo* purines biosynthetic pathway [197]. MTAP-deleted cancer cells accumulate and start secreting MTA *in vitro*, and this accumulation has been demonstrated to inhibit Protein arginine N-methyltransferase 5 (PRMT5) and make cells sensitive to its targeting [198]. Despite the accumulation of MTA has been observed and exploited in several *in vitro* contexts, it has been recently established that this metabolic behaviour is not recapitulated in *in vivo* GBM models. In fact, Barekatain et al. validated the *in vitro* significant elevation of MTA in MTAP-deleted glioma cells, but showed that this increase is not displayed by human GBM tumour samples potentially because of the clearing effects of MTAP-proficient neighbouring cells [199]. MTA accumulation can be measured through mass spectrometry and the metabolic characterization of the GBM cells used in this project highlighted that BG7 cells did not exhibit high levels of extracellular MTA, while P3, P13 and T16 cells – as expected due to the CDKN2A homozygous deletion – did. The RNA sequencing results confirmed that BG7 are *MTAP*-proficient cells, while the other three lines lack *MTAP* expression. Similarly to the *MGMT* downregulation mentioned in the previous chapter of this thesis, it would be interesting to investigate if this metabolic difference among the GBM lines might explain the reduced responsiveness of BG7 cells to dexamethasone treatment.

The results obtained measuring GBM cells growth upon dexamethasone treatment gave us the chance to appreciate the well-known intra- and inter- tumour heterogeneity typical of GBM. To overcome the variability in the response to dexamethasone we focused on metabolic features common to all GBM lines. To this aim, we extracted the intra- and extra-cellular metabolome of the GBM cells

upon dexamethasone treatment and analysed it through liquid chromatography-mass spectrometry. Then, we used the software Compound Discoverer to perform an untargeted analysis that highlighted the significant accumulation of three features, one of which was identified as dexamethasone. In order to identify the other two features we analysed the intracellular samples using tandem mass spectrometry (MS/MS). The comparison of the fragmentation patterns with the fragmentation spectra available on mzCloud™, an extensive online advanced mass spectral fragmentation database, led to the identification of UDP-α-glucuronic acid and *N*1-methylnicotinamide as metabolites significantly accumulating upon dexamethasone treatment in the four GBM cell lines. The identity of these compounds was further confirmed by comparing the mass and retention time of experimental peaks to commercially available standards. UDP-α-glucuronic acid is an essential precursor of glycosaminoglycans (GAGs), representing the building blocks for the ECM, and is produced from UDP-glucose oxidation mediated by the enzyme UDP-glucose dehydrogenase (UGDH) [200]. A research by Oyinlade et al. showed that *UGDH* knockdown reduced the migratory and clonogenic capacities of GBM cells, moreover *UGDH* silencing repressed tumour growth in xenograft GBM models [179]. Therefore, we were interested in assessing UGDH as a potential therapeutic target exacerbated by dexamethasone treatment. However, neither UGDH mRNA nor protein levels were altered upon dexamethasone treatment in our GBM models. We hypothesized that the reason why UDP-α-glucuronic acid levels were increased by dexamethasone lies downstream of UGDH but we did not further investigate this aspect. Besides, we could not recapitulate the dexamethasone-induced UDP-α-glucuronic acid accumulation in GBM three-dimensional spheroids, suggesting that the dexamethasone potential impact on ECM production might be relevant solely in a two-dimensional setting. Next we focused on *N*1-methylnicotinamide, which is the product of a methylation reaction catalysed by nicotinamide *N*-methyltransferase (NNMT) [201]. This enzyme was initially characterized in liver tissue as a drug-metabolizing methyltransferase using *S*-adenosyl methionine (SAM) as methyl donor [202]. Indeed, looking at the transcriptomic data on the open access Genotype-Tissue Expression (GTEx) portal that collects tissue-specific gene expression from 54 non-diseased tissue sites, we found that NNMT is mostly expressed in liver tissue and scarcely present in the normal brain (Figure 5-9, Panel A). Nonetheless, the comparison of normal cerebral tissue to GBM tissue has revealed a significant increase in expression in

the tumour tissue. Indeed, *NNMT* has been identified in several gene expression analyses looking at genes overexpressed in GBM tissue when compared to normal brain tissue [203, 204]. Although NNMT is able to methylate compounds other than nicotinamide (NAM), NAM represents the best-characterized endogenous substrate, and this methylation reaction is considered irreversible. Panel B in Figure 5-9 schematically represents the nicotinamide cycle that includes NNMT. Since its discovery, NNMT-catalysed reaction has been considered as a nicotinamide clearing reaction. Therefore, *N*1-methylnicotinamide and the products of its metabolism - *N*1-methyl-2pyridone-5-carboxamide (2py) and *N*1-methyl-4-pyridone-3-carboxamide (4py), resulting from *N*1-methylnicotinamide oxidation by aldehyde oxidase (AOX) - were believed to be waste products excreted through urine [205]. More recently, the finding that NNMT is overexpressed in several cancer types [206-208] has attracted more research on the possible functions of this methyltransferase. In particular, it has been proposed that its SAM-depleting activity could impair the cellular methylation capacity, creating a methyl sink through its main product *N*1-methylnicotinamide, and eventually alter DNA and histones methylation [209]. The relevance of NNMT in GBM biology has been investigated by Jung et al. that analysed several publicly available GBM datasets to show NNMT overexpression in GBM tissue compared to normal brain. In addition the study associated high NNMT expression with worse patients prognosis. They speculated that NNMT would become crucial in the context of mesenchymal glioma stem cells, where low methionine availability would paradoxically promote NNMT expression and *N*1-methylnicotinamide production. Although, the reason why NNMT is more expressed in GBM cells is still unknown [210]. In the context of ovarian cancer, Eckert et al. performed a proteomics-based screen in ovarian cancer patients and identified NNMT as a driver of the cancer-associated fibroblasts (CAF) phenotype, i.e. sustaining ovarian cancer cells migration and proliferation through the secretion of cytokines and oncogenic ECM components. Again, they suggested that stromal NNMT expression was modulating cancer cells behaviour through alteration of the cellular methylation potential [211]. Looking at both mRNA and protein levels, we reasoned that dexamethasone-mediated *NNMT* overexpression explains the intracellular accumulation of *N*1-methylnicotinamide in GBM cells. The glucocorticoid-treated cells were secreting *N*1-methylnicotinamide in the culture medium and we observed a trend towards its build-up also when the GBM cells

were cultured as three-dimensional spheroids. Moreover, we showed that *NNMT* transcriptional activation by dexamethasone was significant and conserved across the panel of 10 GBM naïve cells. We think that our results disclose a novel direct link between dexamethasone and NNMT. In a recent paper about the impact of stress-induced physiological glucocorticoids on breast cancer cells, Obradovic et al. performed a proteome network analysis comparing dexamethasone-treated and vehicle-treated MDA-MB-231 breast cancer cells. One of the highest-ranking biological pathway was 'Nicotinamide nucleotide metabolic process', and NNMT appeared as one of the dexamethasone top-regulated proteins [212]. Altogether, this data suggests that NNMT represents a previously unrecognized dexamethasone target but the impact of this regulation on GBM cells biology requires further investigation.

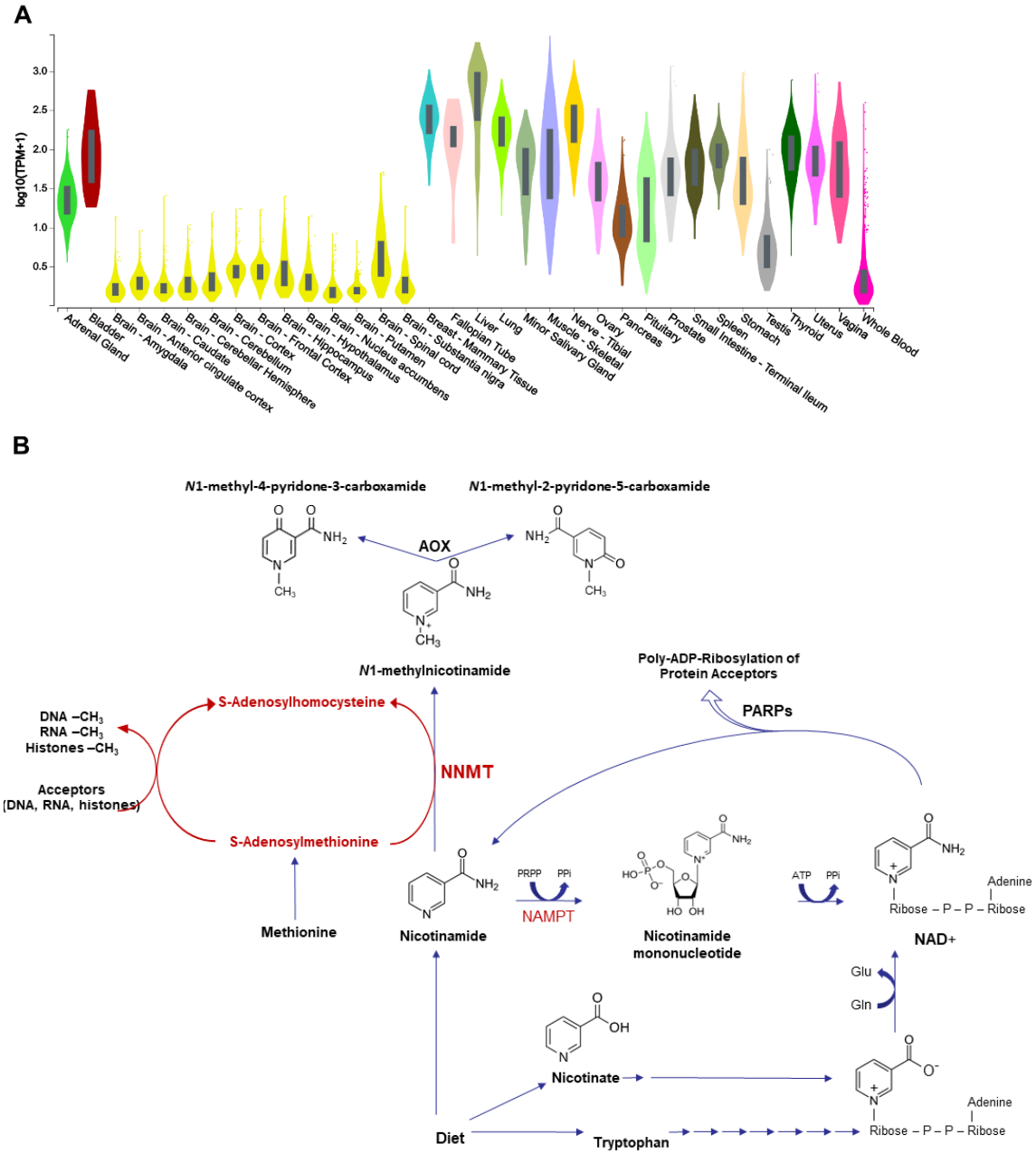

Figure 5-9 NNMT is mainly expressed in the liver and responsible for the methylation of nicotinamide

A) *NNMT* expression across non-diseased tissue site has been obtained from the publicly available GTEx Portal. B) Schematic representing the NAD+ biosynthetic pathways. Nicotinamide, nicotinic acid and tryptophan can be obtained from the diet. Through different enzymatic ways, the three compounds are converted to NAD+ that is converted back to nicotinamide from PARP proteins activity. *N*1-methylnicotinamide represents the product of an irreversible reaction catalysed by nicotinamide N-methyltransferase (NNMT) using S-adenosylmethionine (SAM) as a methyl donor and generating S-adenosylhomocysteine (SAH). *N*1-methylnicotinamide can be further metabolized to *N*1-methyl-2-pyridone-5-carboxamide (2py) and *N*1-methyl-4-pyridone-3-carboxamide (4py). All three metabolites are eventually excreted in the urine.

5.6 Summary

In order to profile GBM cells metabolic features, we measured their OCR and analysed the consumption/secretion of glucose, lactate, glutamine and glutamate through the YSI Biochemistry Analyzer. Reminiscent of their astrocytic origin, all GBM cells were able to clear up the glutamate pool present in the media and some of the cells secreted glutamine. By LC-MS-based metabolomics, we characterized the metabolism of GBM cells upon dexamethasone treatment. An untargeted analysis highlighted the consistent accumulation of metabolites, whose identity were confirmed through targeted approaches. Particularly, we observed that dexamethasone caused the accumulation of *N*1-methylnicotinamide, the methylated form of nicotinamide, i.e. one of the main precursors of NAD+, in GBM cells cultured both as adherent monolayers and three-dimensional spheroids. We demonstrated that dexamethasone induces the expression of nicotinamide *N*-methyltransferase, the enzyme responsible for *N*1-methylnicotinamide synthesis, in a panel of naïve GBM cells.

Chapter 6. Dexamethasone increases nicotinamide methylation in GBM cells

6.1 Introduction

In the previous chapter, we found through an untargeted metabolomics approach that dexamethasone treatment causes the overexpression of NNMT in GBM cells, a metabolic enzyme responsible of the methylation of nicotinamide (Figure 6-1, Panel A). Several groups have shown that alterations in NNMT activity and consequently in N1-methylnicotinamide production lead to epigenetic changes, specifically in DNA and histones methylation levels. We have highlighted the relevance of epigenetics for GBM biology when we discussed the *MGMT* promoter hypermethylation and consequent *MGMT* silencing as one of the few available parameters for GBM patients stratification. Moreover, a glioma-CpG island methylator phenotype (G-CIMP) has been identified in patients with a longer survival [21], and IDH mutations have been shown to be responsible for the establishment of this phenotype [20]. Therefore, given the centrality of epigenetic markers in GBM biology, we decided to investigate if dexamethasone could regulate the epigenome through the induction of NNMT expression. Nicotinamide is a substrate of nicotinamide phosphoribosyltransferase (NAMPT), the rate-limiting enzyme responsible for the synthesis of NAD+, an essential cofactor for a multitude of reactions that overall maintain the cellular redox and energy balance. We reasoned that NAMPT and NNMT compete for the same substrate, and we tested the possibility that altering nicotinamide levels in the culture medium could affect NAD+ availability and proliferation capacity of GBM cells.

6.2 Investigating dexamethasone effects on GBM cells epigenome

6.2.1 SAM/SAH ratio is decreased upon dexamethasone treatment

The methyl donor used by NNMT to methylate nicotinamide is S-adenosylmethionine (SAM), whose demethylation produces S-adenosylhomocysteine (SAH) [213]. SAM provides methyl groups to several methyltransferases and the SAM/SAH ratio is considered a good representation of the cellular methylation capacity. Given the increased activity of NNMT upon

dexamethasone treatment, we hypothesized that dexamethasone could decrease the SAM/SAH ratio in GBM cells. Therefore, we measured the levels of both SAM and SAH and calculated their ratio. In line with our hypothesis we observed that upon dexamethasone treatment the SAM/SAH ratio significantly decreased in all GBM cells cultured as adherent monolayers (Figure 6-1, Panel B). As showed in the previous chapter, *N*1-methylnicotinamide accumulated also in GBM cells cultured as spheroids and treated with dexamethasone. Consistently, the SAM/SAH ratio in dexamethasone-treated GBM spheroids was also decreased (Figure 6-1, Panel B).

6.2.2 Global DNA methylation is not affected by dexamethasone

We employed a liquid chromatography-mass spectrometry-based method to analyse the whole-genome methylation levels [149]. Briefly, we isolated the DNA from GBM cells, processed it through acid hydrolysis and analysed the single nucleobases by LC-MS. Then, the peak areas of cytosine and methyl cytosine were analysed through a targeted approach and the percentage of 5-methylcytosine over total cytosine calculated. As biological and technical control, we treated the cells with 5-azacytidine, an inhibitor of DNA methyltransferases [214], and compared the DNA methylation levels of vehicle- and dexamethasone-treated GBM cells. As shown in Figure 6-1 (Panel C), GBM cells treated with 5-azacytidine had total DNA methylation levels halved compared with vehicle-treated cells, demonstrating that the method was sufficiently sensitive to detect such marked alterations in DNA methylation. On the contrary, we could not detect significant differences in DNA methylation in cells treated with dexamethasone.

6.2.3 Dexamethasone treatment alters histones methylation marks in GBM cells

Ulanovskaya et al. have proposed that *N*1-methylnicotinamide could represent a methylation sink used by cells to regulate SAM levels. They highlighted that NNMT overexpression or silencing in cells grown in culture medium containing 10 or 20 μM methionine (‘low methionine’) caused changes in the levels of specific histones methylation markers [209]. The impact of NNMT on histones methylation has been shown to be relevant also for naïve-to-primed transition of human embryonic stem cells (hESCs) [215]. In fact, Sperber et al. demonstrated that in naïve hESCs high NNMT activity and consequent high *N*1-methylnicotinamide, and low SAM

availability, correlated with reduced H3K27me3 levels, whereas in primed hESCs the reduction in NNMT activity was sparing SAM and favouring DNA and histones methylation. The relevance of NNMT for glioblastoma stem cells was highlighted also from Engstrom et al. who performed a gene expression analysis comparing patient-derived glioma neural stem cells to neural stem cells. NNMT was upregulated in GBM tissue *versus* non-neoplastic brain and grade III astrocytoma tissue [216]. Therefore, we tested if in our conditions NNMT overactivity was modulating histone methylation, by assessing a panel of histone methylation marks through Western blotting. Figure 6-1 (Panel D) shows that dexamethasone treatment caused cell line specific changes in the levels of H3K27me3. In P13 cells dexamethasone reduced H3K27me3 levels, whereas in the other three GBM lines H3K27me3 levels were increased.

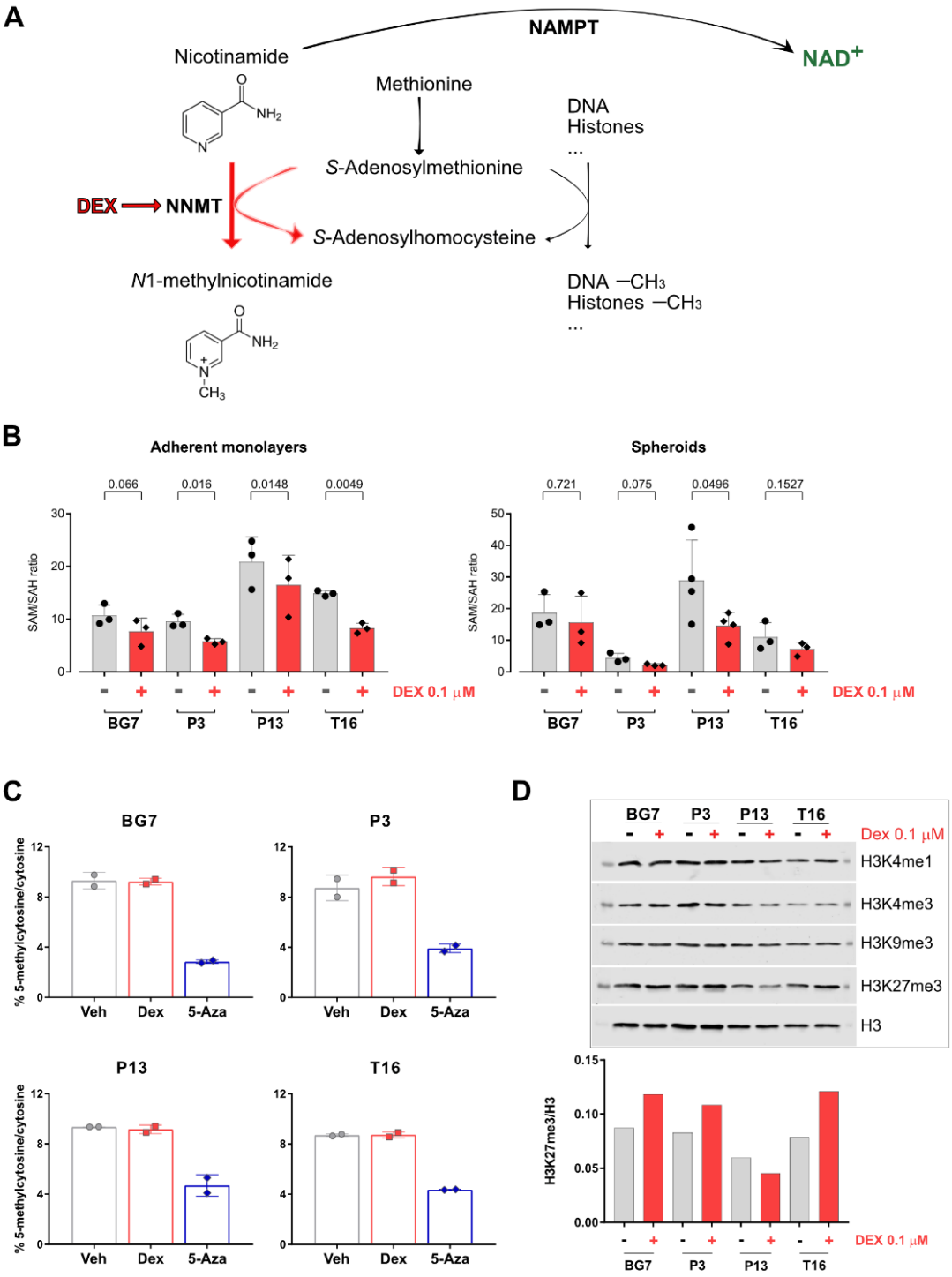

Figure 6-1 Investigating the effects of dexamethasone treatment on GBM cells epigenome

A) Schematic representing the dexamethasone-mediated induction of the NNMT reaction. B) Left: cells were cultured for 72 h as adherent monolayers in Plasmax containing vehicle (ethanol) or 0.1 µM dexamethasone (DEX). After three days, the medium was refreshed and 24 h later the intracellular metabolites were extracted with extraction solution. The bar plots represent the SAM/SAH ratio (n=3 independent experiment; n=3 wells extracted for each condition). Right: GBM cells were cultured as spheroids in low-adherence flasks in Plasmax medium containing vehicle (ethanol) or 0.1 µM dexamethasone for 72 h. After three days, the culture medium was refreshed to avoid nutrient exhaustion and 24 h later the spheroids were extracted in extraction solution. The bar plots represent the peak area of the metabolites normalized for the protein content (n=3 independent experiments; 1 flask was extracted for each condition). *P* values result from paired two-tailed t-tests. C) GBM cells have been cultured for 72 h as adherent monolayers in Plasmax medium containing vehicle (ethanol), 0.1 µM dexamethasone (Dex), or 5 uM 5-azacytidine (5-Aza). After 72 hours, the medium was refreshed to avoid nutrient exhaustion. 5-azacytidine was supplemented every day to

ensure effective inhibition of DNA methyltransferases. 6 days after seeding the DNA was extracted, hydrolysed and run through LC-MS. The graphs show the percentage of 5-methylcytosine over the total cytosine (n=2 independent experiments, 3 wells have been extracted for each condition). D) Cells have been cultured for 72 h as adherent monolayers in Plasmax medium containing vehicle (ethanol) or 0.1 µM dexamethasone. A cell fractionation kit (Cell Signaling Technology) was used to separate nuclear, cytoplasmic, and organellular/membrane compartments. The fractions were analysed by Western blotting and probed for histone methylation markers. Equal protein amounts were loaded and Histone 3 was used as loading control.

6.3 Metabolic restriction approaches to target GBM cells growth

6.3.1 GBM cells growth requires externally supplied methionine

To exacerbate the effects of NNMT activity on histone methylation, Ulanovskaya et al. lowered the methionine concentration in the medium from 100 to 10-20 μM [209]. Plasmax medium contains physiological concentrations of methionine, i.e. 30 μM, and methionine is a precursor for SAM biosynthesis (Figure 6-1, Panel A). Therefore, we wanted to investigate if dexamethasone-treated cells were more susceptible to methionine restriction because of their increased SAM usage for nicotinamide methylation. Methionine is an essential amino acid for most cancer cells that cannot synthetize it *de novo* at a rate compatible with their anabolism. Also, the methionine cycle lies at the crossroad of three different metabolic pathways, the polyamines cycle, the folate cycle and the transsulfuration pathway [217]. The methionine dependency of transformed and cancer cells has been known since the 80s, when the comparison between tumour and non-transformed cells highlighted that homocysteine, the immediate methionine precursor, does not sustain the proliferation of transformed cells [218]. Among the cancer cells tested, A172, a glioblastoma-derived cell line, was classified as 'slightly independent' from methionine [219]. In order to investigate the methionine dependence of GBM cells, we modified Plasmax formulation and decreased methionine levels from 30 μM to 10 and 3 μM. Unexpectedly, after 4 days in culture with 10 μM methionine cells did not show any significant reduction in the growth rate. Even at 3μM methionine, all the cell lines sustained proliferation as showed by the greater number of cells at endpoint compared to the treatment start. Moreover, dexamethasone treatment did not sensitize GBM cells to the methionine restriction (Figure 6-2, Panel A). To test if the presence of homocysteine could compensate for methionine restriction we combined methionine and homocysteine deprivation. Plasmax medium normally contains 9 μM homocysteine; we formulated a homocysteine-free Plasmax and supplemented it with 3 μM methionine. After 8 days of culture, homocysteine deprivation in the presence of physiological methionine levels (30 μM) did not affect GBM cells proliferation. However, the presence of homocysteine partially rescued the effect of methionine restriction in 3 out of 4 cell lines, suggesting that methionine synthase supports GBM growth under methionine restriction. Finally, the

combination of homocysteine removal and low methionine levels did not markedly alter the effect of dexamethasone on GBM cells proliferation (Figure 6-2, Panel B).

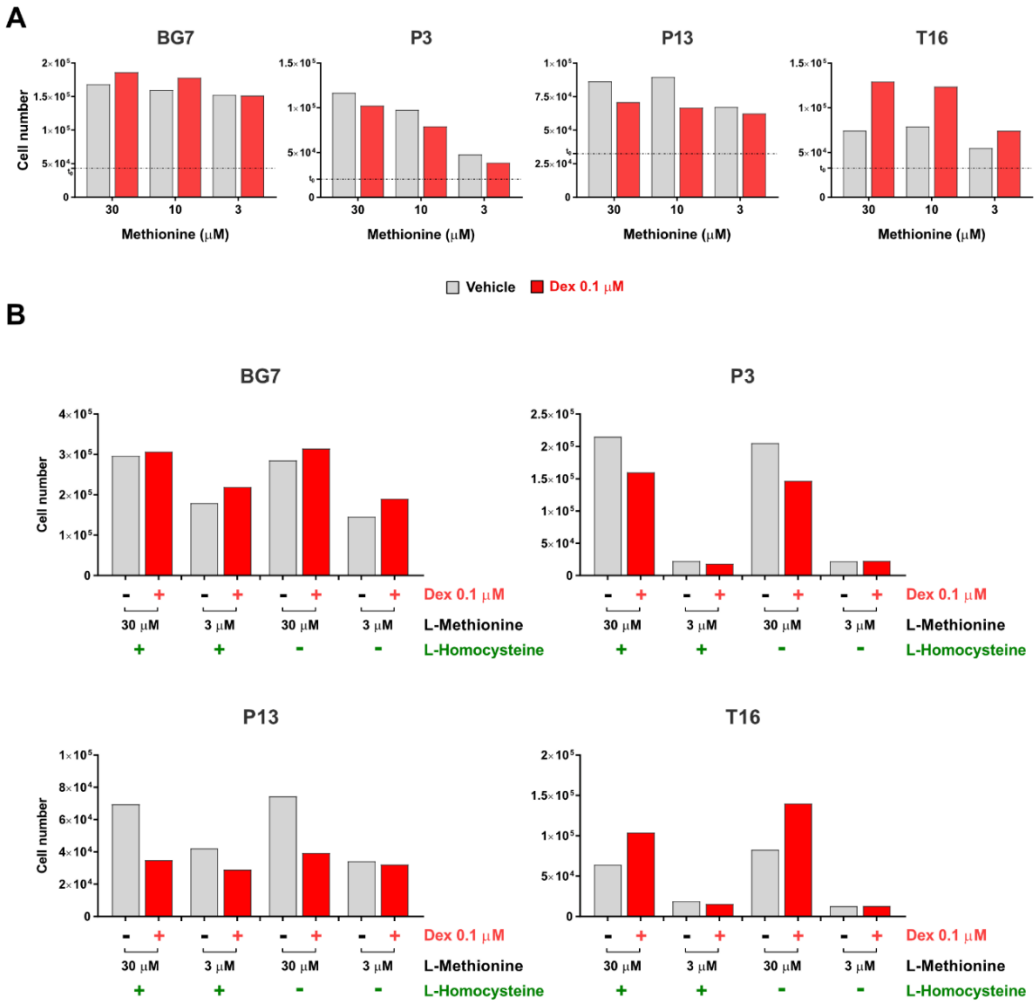

Figure 6-2 Methionine restriction impairs GBM cells growth but homocysteine does not fully rescue the growth reduction due to methionine deprivation

A) GBM cells have been cultured as adherent monolayers in Plasmax medium containing vehicle (ethanol) or 0.1 μM dexamethasone (Dex) for 24 hours. After 24 hours, full Plasmax medium was replaced with Plasmax containing 30, 10 or 3 μM methionine. 48 hours later, the medium was refreshed to avoid nutrient exhaustion and cells were counted after 4 days from seeding (n=1 independent experiment, 4 wells have been counted for each condition). B) GBM cells have been cultured as in Panel A) in Plasmax supplemented with the indicated concentrations of methionine and homocysteine. Every 3 days, the medium was refreshed to avoid nutrient exhaustion and after 8 days the cells were counted to assess cell growth (n=1 independent experiment, 4 wells have been counted for each condition).

6.3.2 Nicotinamide availability does not challenge GBM cells proliferation

Nicotinamide, nicotinic acid and nicotinamide riboside, collectively known as vitamin B3 complex, are crucial for NAD+ synthesis. NAD+ representing one of the most abundant molecules within the human body, is required for ~500 enzymatic reactions and its synthesis can occur either through *de novo* biosynthesis from tryptophan through the kynurenine pathway or *via* salvage pathways (a schematic of NAD+ biosynthetic pathway has been shown in the previous chapter of this thesis, Figure 5-9). From the transcriptomic data emerged that GBM cells do not express the enzymes required for the conversion of tryptophan to NAD+, such as indoleamine 2,3-dioxygenase 1 (IDO1) and tryptophan 2,3-dioxygenase (TDO2), suggesting that the maintenance of an optimal NAD+ concentration is achieved through the salvage pathways [220]. The metabolomics analyses showed that dexamethasone did not affect tryptophan, nicotinamide and NAD+ levels (Figure 6-3, Panel A). Plasmax nicotinamide concentration is 8.2 μM. The Human Metabolome Database reports concentrations of nicotinic acid of 50 uM in blood and 0.8-4 uM in cerebrospinal fluid (CSF), while nicotinamide is reported to be between 0.03 and 0.44 μM in blood (not reported in CSF) [221]. We decided to investigate if nicotinamide restriction would become critical for dexamethasone-treated GBM cells proliferation. Moreover, we tested the ability of GBM cells to use nicotinic acid as a NAD+ precursor, when nicotinamide is not available. To this aim, we prepared a nicotinamide-free Plasmax and measured GBM cells growth in this medium as such or supplemented with nicotinamide (8.2 μM) or different concentrations of nicotinic acid (15, 30, 90 μM). Surprisingly, after 4 days in nicotinamide-restricted medium GBM cells growth was not affected and dexamethasone treatment did not differently impact their proliferation. Moreover, the replacement of nicotinamide with nicotinic acid did not alter GBM cells proliferation (Figure 6-3, Panel B).

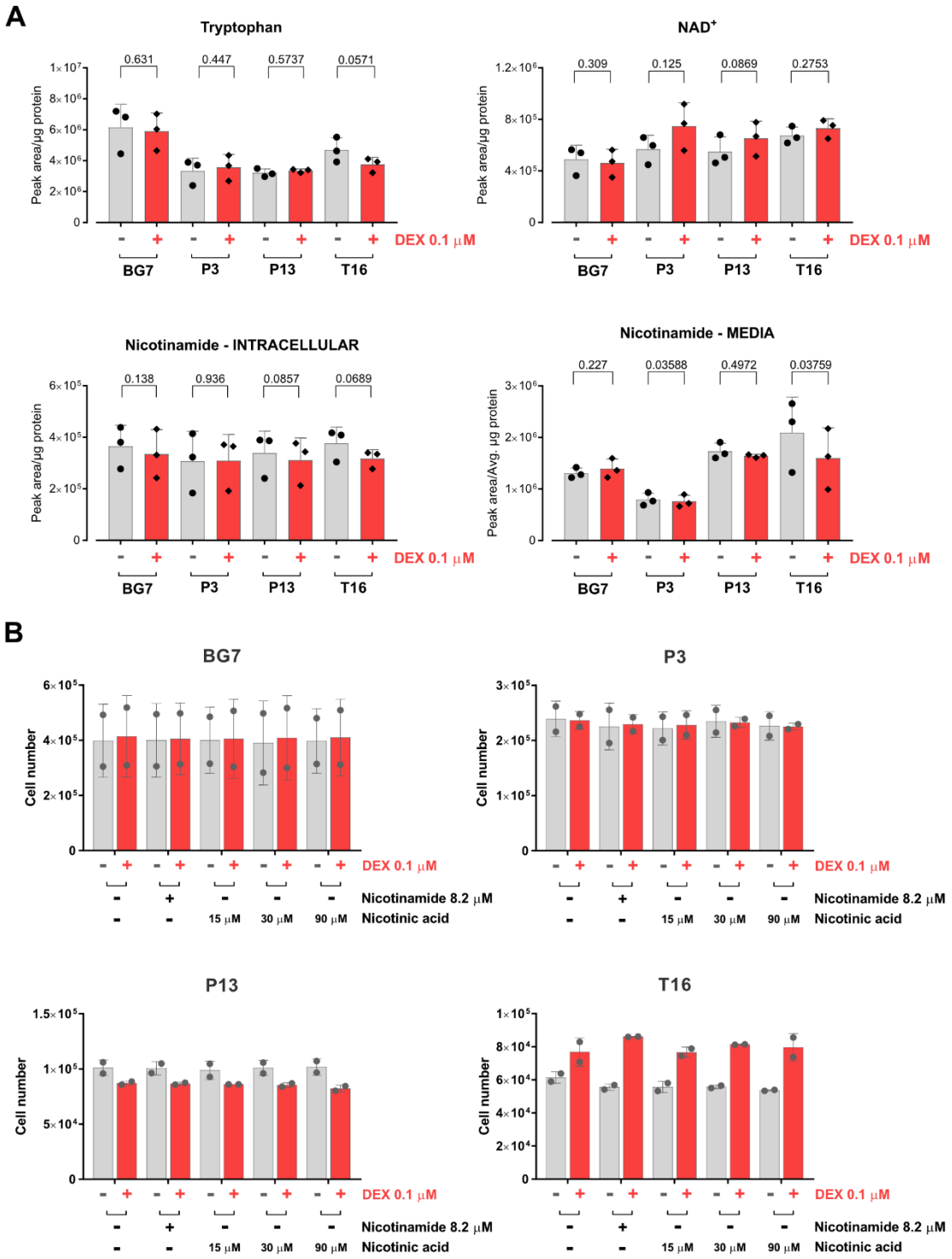

Figure 6-3 Nicotinamide levels are not altered by dexamethasone treatment and nicotinamide short-term restriction does not challenge GBM cells growth

A) GBM cells were cultured for 72 h as adherent monolayers in Plasmax medium containing vehicle (ethanol) or 0.1 µM dexamethasone (DEX). After three days, the medium was refreshed and 24 h later the intracellular metabolites were extracted with extraction solution. The bar plots represent the peak area of the metabolites normalized for the protein content (n=3 independent experiments; 3 wells were analysed for each condition). *P* values result from paired two-tailed t-tests. B) GBM cells were cultured as adherent monolayers in Plasmax medium containing vehicle (ethanol) or 0.1 µM dexamethasone (DEX) for 24 hours. After 24 hours, full Plasmax medium was replaced with nicotinamide-deprived Plasmax supplemented with nicotinamide 8.2 µM or the indicated concentrations of nicotinic acid. 48 hours later, the medium was refreshed to avoid nutrient exhaustion and after 4 days from seeding, the cells were counted to assess cell growth (n=2 independent experiments, 4 wells were counted for each condition).

Four days of culturing in nicotinamide-restricted Plasmax did not appear to be able at affecting GBM cells proliferation. We hypothesized that this effect was due to a considerable internal pool of nicotinamide, therefore we cultured the GBM cells in nicotinamide-free Plasmax for 12 days in an attempt to deplete the intracellular pool of nicotinamide. To our surprise, nicotinamide deprivation was decreasing the proliferation of the fast-growing BG7 and P3 cells but did not have any effect on P13 and T16 growth. Finally, dexamethasone treatment did not exacerbate the consequences of nicotinamide deprivation (Figure 6-4).

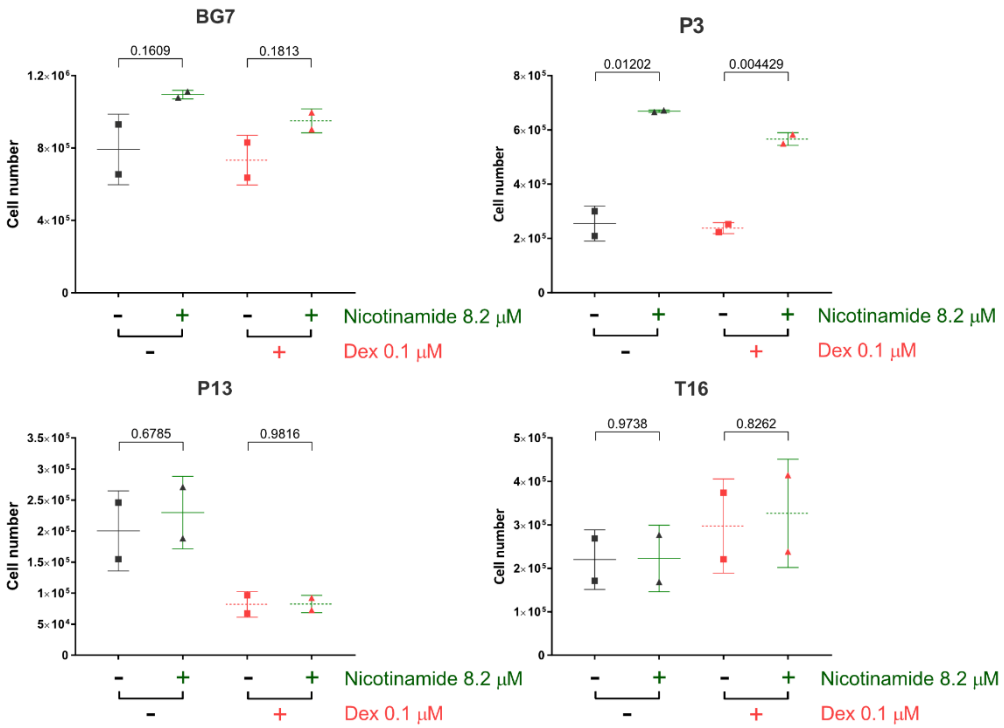

Figure 6-4 Long term nicotinamide deprivation does not consistently affect GBM cells proliferating capacity

GBM cells were cultured as adherent monolayers in Plasmax medium containing vehicle (ethanol) or 0.1 µM dexamethasone (Dex) for 24 hours. After 24 hours, full Plasmax medium was replaced with Plasmax deprived of nicotinamide or supplemented with 8.2 µM nicotinamide. Every 4 days the medium was refreshed to avoid nutrient exhaustion and after 12 days from seeding, the cells were counted to assess cell growth (n=2 independent experiments, 4 wells have been counted for each condition).

6.3.3 Nicotinamide withdrawal impairs NNMT activity

In order to further investigate the metabolic effects of nicotinamide withdrawal, we cultured the cells in nicotinamide-restricted Plasmax, and analysed their intracellular metabolome with LC-MS. The intracellular nicotinamide pool was markedly and consistently reduced by nicotinamide withdrawal and in these conditions dexamethasone did not increase the intracellular levels of *N*1-methylnicotinamide. Moreover, we observed that even in conditions of nicotinamide withdrawal, all GBM cells had residual levels of intracellular NAD+ (Figure 6-5).

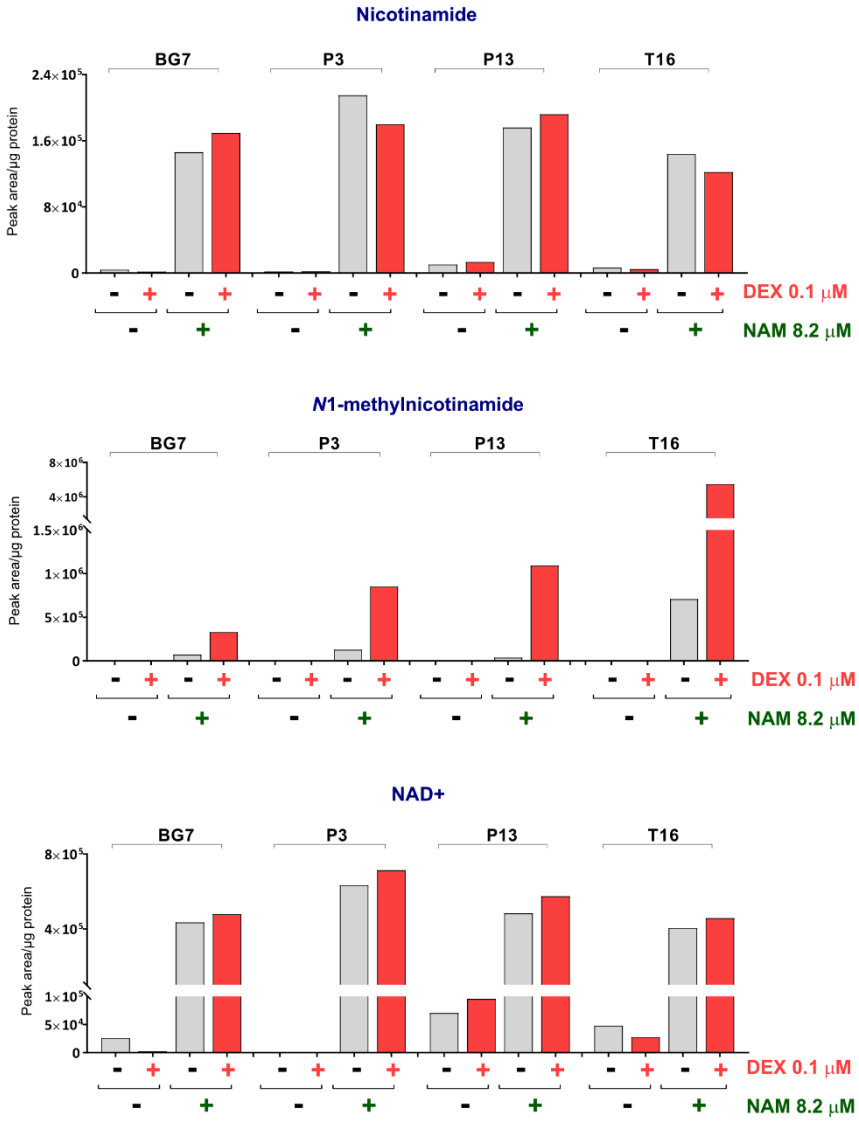

Figure 6-5 Nicotinamide restriction suppresses dexamethasone-induced *N*1-methylnicotianmide over production

Cells were cultured for 72 h as adherent monolayers in Plasmax medium containing vehicle (ethanol) or 0.1 µM dexamethasone (DEX), with or without 8.2 µM nicotinamide (NAM). Three days later, the medium was refreshed and 24 h later the intracellular metabolites were extracted with extraction solution. The bar plots represent the peak area of the metabolites normalized for the protein content (n=1 independent experiment, 3 wells were analysed for each condition).

6.3.4 Exhausting the methylation capacity of dexamethasone-treated GBM cells

We hypothesized that exposing dexamethasone-treated cells to methionine restriction and concomitantly to supra-physiological concentrations of nicotinamide could cause a shortage in SAM pool not compatible with cellular growth (Figure 6-6). We cultured cells for 12 days at supra-physiological nicotinamide concentrations (500 µm or 2 mM) with 30 µM or 3 µM methionine. The excess of nicotinamide did not markedly affect proliferation of GBM cells. In line with previous experiments, methionine restriction (3 µM) slowed the proliferation of all GBM cells, but in these conditions nicotinamide supplementation did not significantly alter the cell line-specific effect of dexamethasone on growth (Figure 6-7). Overall with this approach we could not demonstrate that the increased NNMT activity induced by dexamethasone treatment sensitizes GBM cells to methionine restriction and nicotinamide supplementation.

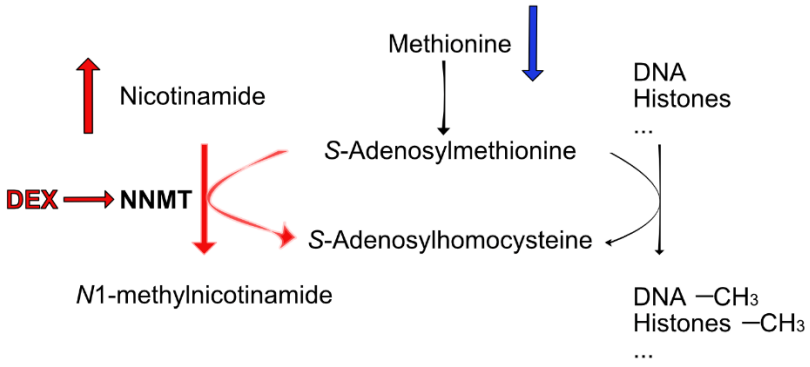

Figure 6-6 Supplementing methionine-restricted GBM cells with supra-physiological amounts of nicotinamide in the presence of dexamethasone treatment

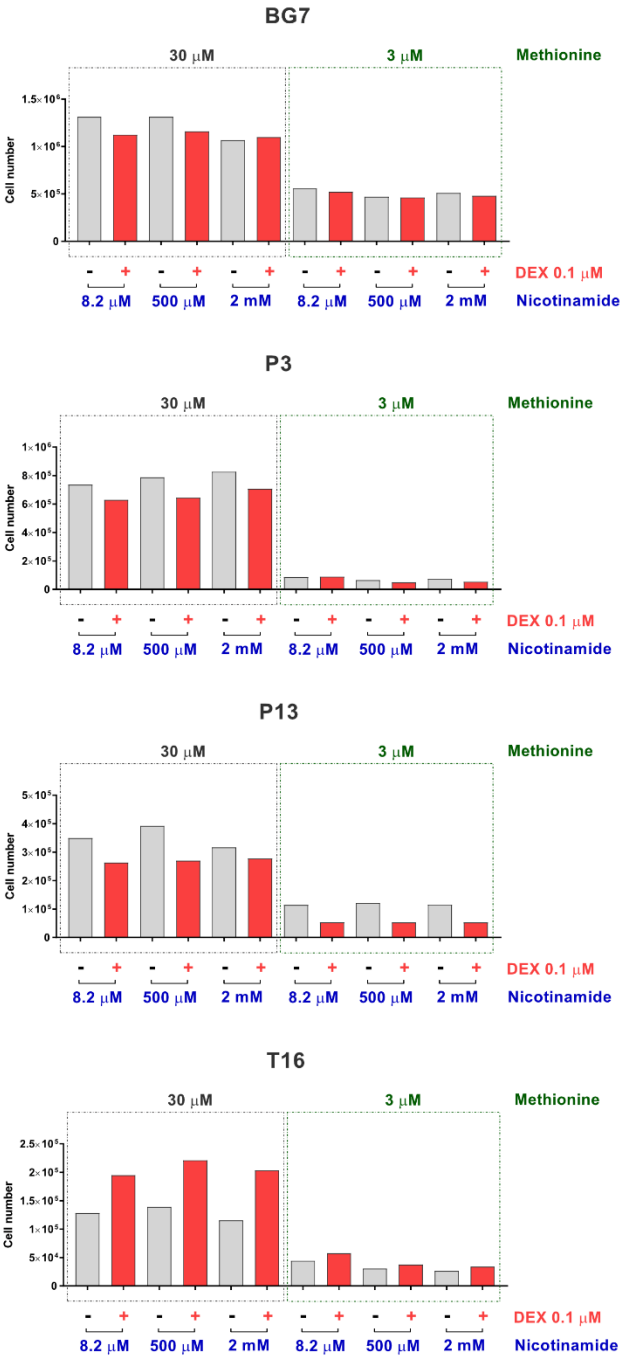

Figure 6-7 Combining supplementation of supra-physiological nicotinamide with methionine restriction does not alter GBM cells growth

GBM cells were cultured as adherent monolayers in Plasmax medium containing vehicle (ethanol) or 0.1 µM dexamethasone (DEX) for 24 hours. After 24 hours, full Plasmax medium was replaced with methionine-restricted Plasmax fully deprived of nicotinamide or supplemented with the indicated concentrations of nicotinamide. Every 4 days the medium was refreshed to avoid nutrient exhaustion and after 12 days from seeding, the cells were counted to assess cell growth (n=1 independent experiment, 4 wells were counted for each condition).

6.4 Exploiting dexamethasone-induced NNMT overactivity to interfere with GBM cells proliferation

6.4.1 NNMT inhibition does not impair GBM cells growth

We found that NNMT expression was induced coherently in all GBM cells by dexamethasone treatment. However, under the same dexamethasone treatment some cell lines proliferated faster and other slower than the controls demonstrating that NNMT levels did not correlate with proliferation rate. To directly address the NNMT role in controlling proliferation we treated GBM cells with the product of NNMT-catalysed reaction, *N*1-methylnicotinamide. *N*1-methylnicotinamide supplementation did not significantly affect GBM cells growth (Figure 6-8, Panel A). To further test the relevance of NNMT catalytic activity on GBM cells proliferation we treated the cells with the NNMT inhibitor 5-Amino-1-methylquinolinium iodide [222]. We observed that NNMT inhibition slowed down the proliferation of BG7 and T16 cells, but the combined treatment with dexamethasone and 5-Amino-1-methylquinolinium iodide did not show combinatorial effects in any of the GBM cell lines (Figure 6-8, Panel B).

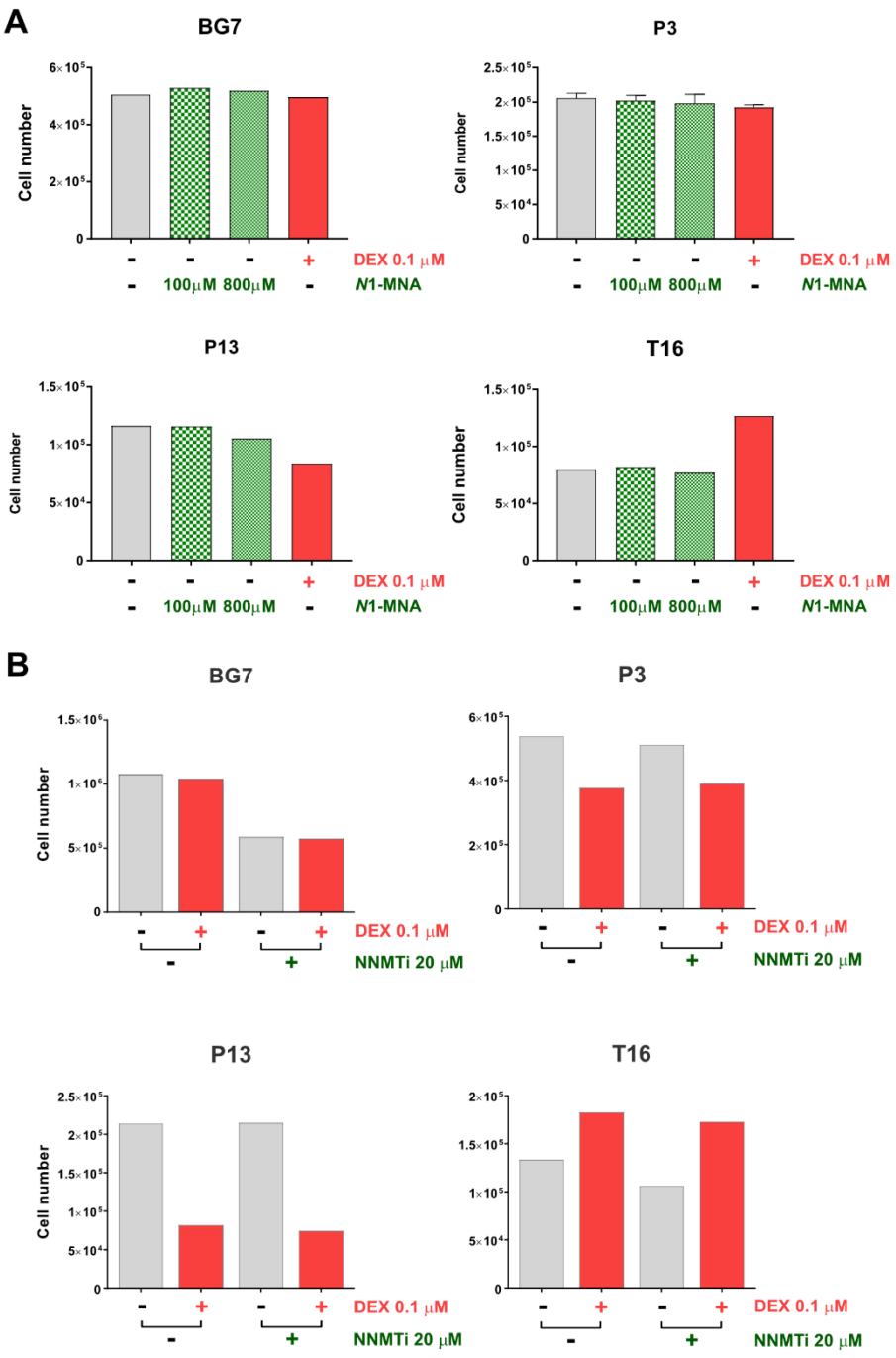

Figure 6-8 NNMT inhibition does not affect GBM cells growth

A) GBM cells were cultured as adherent monolayers in Plasmax medium containing vehicle (ethanol) or 0.1 μM dexamethasone (DEX) for 24 hours. After 24 hours, the culture medium was supplemented with the indicated concentrations of *N*1-methylnicotinamide (*N*1-MNA). After 4 days, the cells were counted to assess cell growth (n=1 independent experiment, 4 wells were counted for each condition). B) GBM cells were cultured as adherent monolayers in Plasmax medium containing vehicle (ethanol) or 0.1 μM dexamethasone (DEX) for 24 hours. After 24 hours, the culture medium was supplemented with the NNMT inhibitor 5-Amino-1-methylquinolinium iodide (NNMTi, 20 μM). Every 4 days the medium was refreshed to avoid nutrient exhaustion and after 12 days from seeding the cells were counted to assess cell growth (n=1 independent experiment, 4 wells were counted for each condition).

6.4.2 Exploiting NNMT ability to methylate compounds structurally related to nicotinamide to induce toxicity in GBM cells

NNMT enzymatic characterization revealed that the enzyme was able to methylate various compounds structurally related to nicotinamide [223]. At the time of NNMT discovery, methylation was considered a minor detoxification pathway, explaining why NNMT was classified as a detoxification enzyme [224]. Despite not much research has looked at the role of NNMT in the detoxification of xenobiotics, one of NNMT substrates was identified as 4-phenylpyridine, whose methylation produces 1-methyl-4-phenylpyridinium ion (MPP+). MPP+ is a neurotoxin especially toxic for the dopaminergic neurons in a specific area of the brain, i.e. the *substantia nigra* [225], widely studied in the context of Parkinson's disease [226]. We hypothesized that dexamethasone-induced NNMT overactivity could sensitize GBM cells to the toxic effects of MPP+ (Figure 6-9, Panel A). To this aim, we treated GBM cells to increasing concentration of 4-phenylpyridine and measured their proliferation. In all GBM cells, 4-phenylpyridine had a dose dependent antiproliferative effects however dexamethasone did not increase the sensitivity to this compound (Figure 6-9, Panel B).

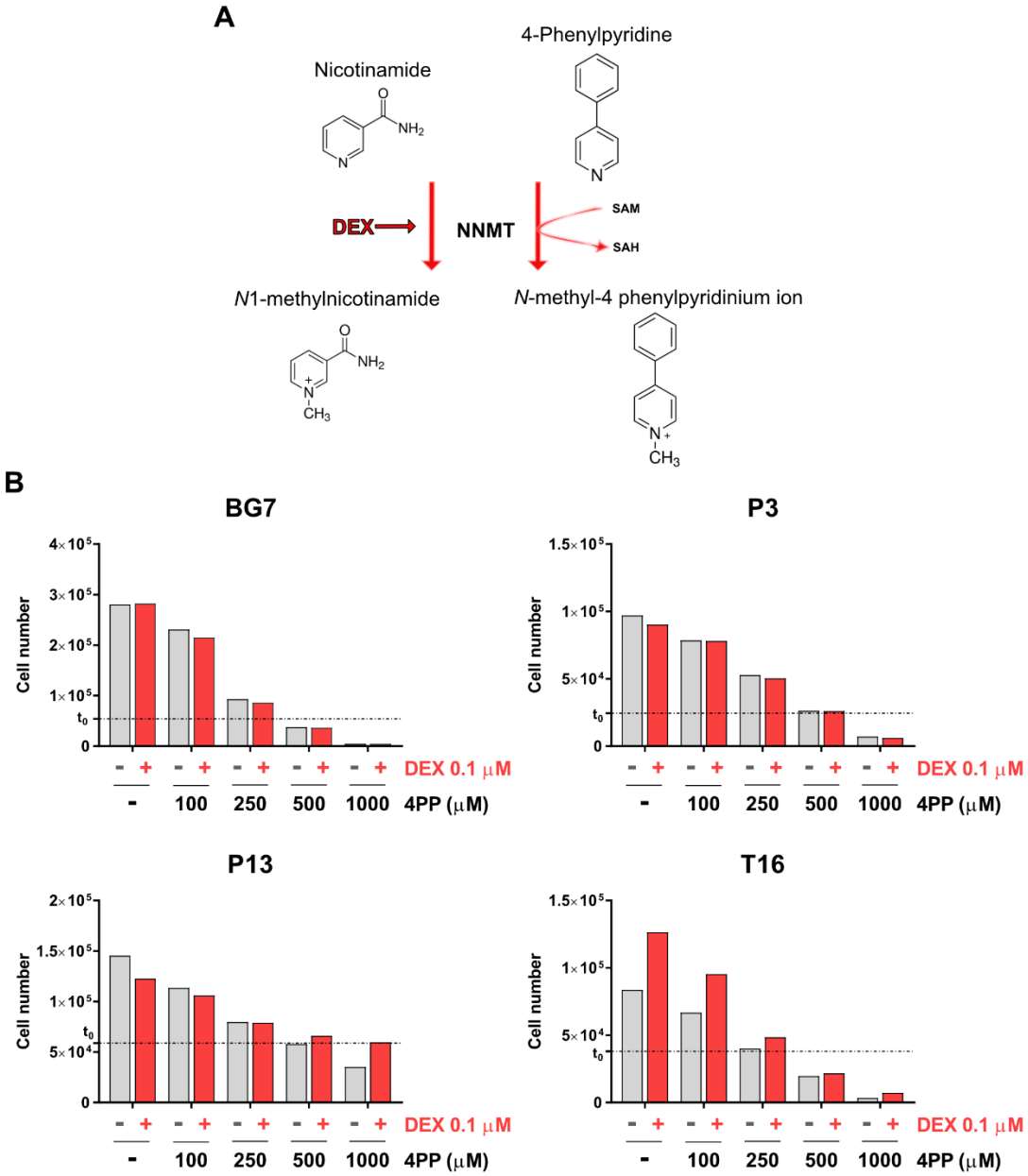

Figure 6-9 Exploiting NNMT ability to methylate compounds structurally related to nicotinamide to induce GBM cells toxicity

A) Scheme of NNMT activity towards nicotinamide and 4-phenylpyridine. B) GBM cells cultured as adherent monolayers in Plasmax containing vehicle (ethanol) or 0.1 µM dexamethasone for 24 hours. After 24 hours, the culture medium was supplemented with the indicated concentrations of 4-phenylpyridine (4PP). After 4 days, the cells were counted (n=1 independent experiment, four wells have been counted for each condition).

6.4.3 Combining dexamethasone and irradiation to target GBM cells

Together with surgery and chemotherapy, radiotherapy represents a mainstay of GBM patients' standard-of-care. In order to investigate if glucocorticoids treatment interferes with radiotherapy, we exposed vehicle- and dexamethasone-treated GBM cells to 5 Gy of radiation and measured the proliferation thereafter. As highlighted in Figure 6-10 (Panel A), upon irradiation all GBM cells exhibited a marked growth delay. In particular, irradiation worsened the dexamethasone-induced growth inhibition in P3 cells. DNA damage represents one of the main molecular consequences of irradiation, and requires activation of DNA damage repair pathways to be resolved. Poly(ADP-ribose) polymerase 1 (PARP1) senses DNA damage and uses NAD+ in order to modify itself and other target proteins [227]. PARP1-mediated utilization of NAD+ generates nicotinamide, therefore we investigated if the combination of irradiation and dexamethasone was differently altering the nicotinamide metabolism of GBM cells. We hypothesized that cells would be using more NAD+ upon irradiation treatment, and in T16 cells we observed a decrease in both nicotinamide and NAD+ upon combination of dexamethasone and irradiation. However, this effect was cell line-specific and the other GBM lines did not exhibit the same response (Figure 6-10, Panel B). Moreover, both control and irradiated cells had comparable levels of *N*1-methylnicotinamide upon dexamethasone treatment.

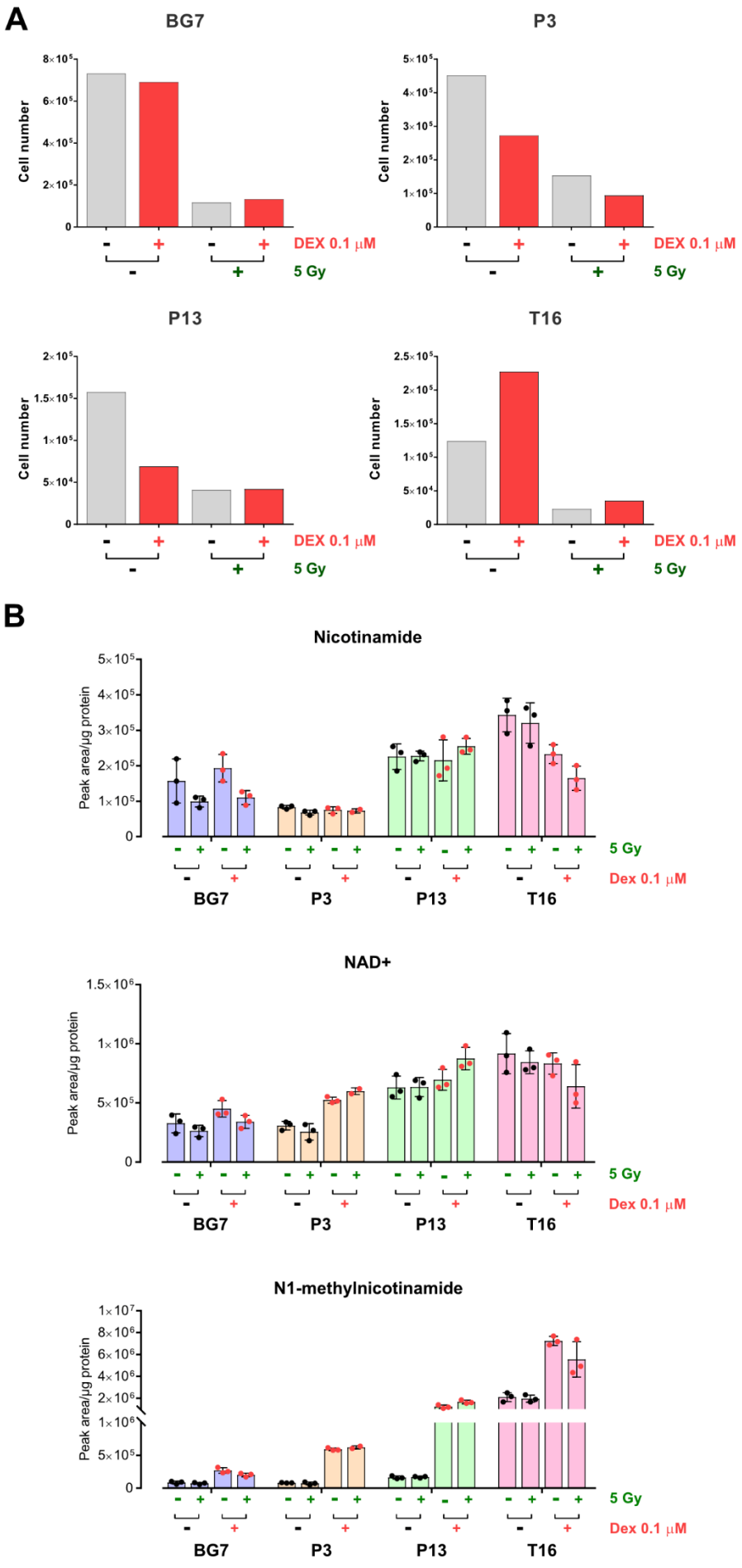

Figure 6-10 Investigating the effects of irradiation on GBM cells proliferation and metabolism

A) Cells were cultured for as adherent monolayers in Plasmax medium containing vehicle (ethanol) or 0.1 µM dexamethasone (DEX). 24 hours later the cells were exposed to a single dose of irradiation (5 Gy). After 4 days the cells were again treated with 5 Gy ionizing radiation and after 8 days, the cells were counted to assess cell growth (n=1 independent experiment, 4 wells were counted for each condition). B) Cells were cultured for 72 h as adherent monolayers in Plasmax medium containing vehicle (ethanol) or 0.1 µM dexamethasone (DEX). Three days later, the culture medium was refreshed and 24 h later the intracellular metabolites were extracted with extraction solution. The bar plots represent the peak area of the metabolites normalized for the protein content (n=1 independent experiment, 3 wells were extracted for each condition).

6.5 Chapter discussion and results limitations

An untargeted metabolomics approach combined with a whole transcriptome analysis revealed nicotinamide *N*-methyltransferase as a novel metabolic target of dexamethasone in GBM cells. In this chapter we showed the effects of NNMT activation upon dexamethasone treatment and investigated how to exploit it with the aim of impairing GBM cells growth. We could show that an increased NNMT expression and activity reflected in a reduced SAM/SAH ratio, pointing at an increased usage of this methyl donor in dexamethasone-treated cells. Therefore, we investigated if the NNMT-mediated depletion of SAM would change the methylation levels of DNA and histones. In order to analyse the DNA methylation levels, we isolated the DNA from vehicle- and dexamethasone-treated cells, hydrolysed it and then analysed it through LC-MS [149]. The ratio between 5-methyl cytosine and cytosine highlighted that dexamethasone did not alter the overall methylation status of the DNA within GBM cells. A limitation of this analytical method is that it would not detect differences in the methylation levels of *specific* genomic regions. Therefore, we cannot exclude that dexamethasone alters the methylation of selected DNA regions. In this regard, the Assay for Transposase-Accessible Chromatin with high-throughput sequencing (ATAC-seq) technique would be a suitable approach to investigate dexamethasone-mediated differences in chromatin accessibility [228]. On a similar note, the selection of histone methylation markers was based on the published literature linking NNMT and histone modifications. We acknowledge that a broader selection of methylation markers assessed either by Western blotting or by proteomics, would be more suitable to screen for NNMT-dependent modifications. Also, exploring how genome and histones methylation levels are affected by dexamethasone treatment in GBM tumours would add an important layer of knowledge about the relation between this drug and epigenetic changes, potentially impacting tumour progression and response to therapy. Ulanovskaya et al. showed that NNMT overexpression or silencing combined with methionine restriction (10-20 μM) was needed to obtain measurable changes in the histones methylation levels [209]. When we analysed DNA and histones methylation levels, we conducted the experiments in Plasmax medium, containing physiological methionine concentrations (30 μM), therefore it would be relevant investigating if lower methionine concentrations could modulate the DNA and histone methylation of dexamethasone-treated cells. Our findings demonstrating that dexamethasone

increases the expression of NNMT prompted us to investigate how this reaction could be exploited to impair GBM cells growth. We restricted methionine availability in otherwise physiological conditions and observed a reduction in GBM cells proliferation. However this antiproliferative effect was not different in the presence of dexamethasone. Methionine dependency has been shown in cancer cells from several tumour types. We found that in our model homocysteine supplementation did not compensate for methionine restriction. By comparing the CSF of malignant glioma patients and control patients, Locasale et al. showed that methionine is one of the most significantly enriched metabolites in the CSF of glioma patients [229]. Moreover, research from Shiraki et al. highlighted that undifferentiated human embryonic and induced pluripotent stem cells exhibit a high-methionine metabolic state, where high levels of SAM are needed to sustain self-renewal and maintain the cells undifferentiated state [230]. Methionine restriction has shown therapeutic responses in mouse models of chemo-resistant and radio-resistant tumours [231]. Interestingly, in the report from Gao et al. it is shown that a methionine-restricted diet in healthy individuals caused an increased plasma levels of *N*1-methylnicotinamide. In conditions of methionine deprivation, the observation that cells "waste" methyl donor for producing *N*1-methylnicotinamide calls for further investigation to better understand the mechanistic relation between methionine dependency and NNMT activity. Furthermore, our data shows that GBM cells do not efficiently use homocysteine as a methionine precursor, therefore it was unexpected that 3 μM methionine could sustain GBM cells growth.

Thanks to its ability to methylate nicotinamide, NNMT represents a link between methionine and the vitamin B3 metabolism. In our settings, dexamethasone appeared to affect both of these pathways in GBM cells, as highlighted from the transcriptional data. In fact, dexamethasone upregulated not only *NNMT* expression, but also methionine adenosyltransferase II (*MAT2A*), encoding for the enzyme responsible of SAM biosynthesis, and nicotinamide phosphoribosyltransferase (*NAMPT*), that we mentioned already as the rate-limiting enzyme in NAD+ synthesis (Figure 6-11).

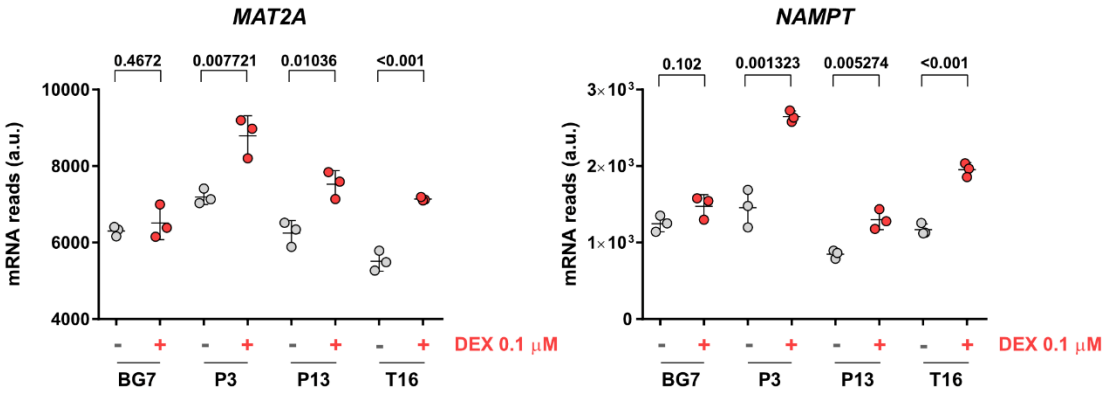

Figure 6-11 Dexamethasone transcriptionally upregulates enzymes of the methionine and nicotinamide pathways

Cell were cultured as adherent monolayers in Plasmax containing vehicle (ethanol) or 0.1 μM dexamethasone (DEX) for 72 h. After three days, the culture medium was refreshed and 24 h later cell number was determined using a Coulter counter, and cells were harvested for whole RNA extraction. Subsequently, the samples were analysed by poly-A RNA sequencing (n=3 independent experiments).

In the context of glioma, sensitivity to NAD+ biosynthesis blockage through NAMPT inhibition has been shown to correlate with IDH mutations [232]. We tested two NAMPT inhibitors and observed that also IDH wild-type cells proliferation is impaired by these inhibitors, highlighting how crucial NAD+ pool is for cellular viability (Figure 6-12). Similarly to NNMT, also NAMPT is overexpressed in GBM tissue compared to brain normal tissue and its overexpression correlates with worse overall survival in patients [233]. Previous research has shown NAMPT ability to drive stemness in glioblastoma [234], but effects of the dexamethasone-mediated *NAMPT* upregulation on stemness remain to be elucidated. Our results show that dexamethasone-treated cells are not more sensitive to the two NAMPT inhibitors, FK866 and CHS828 (Figure 6-12).

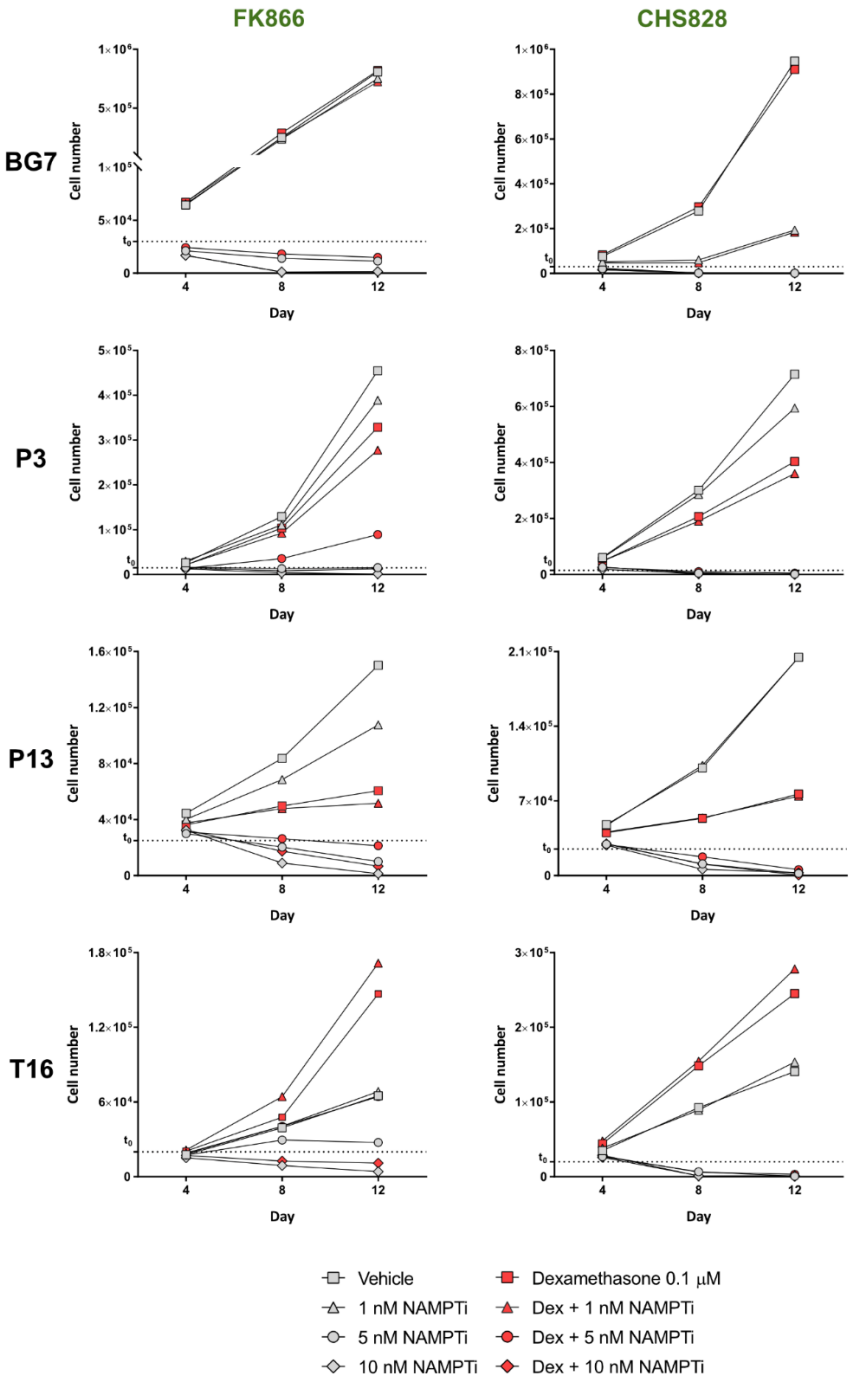

Figure 6-12 Inhibition of NAMPT is extremely potent at impairing GBM cell proliferation

Cell were cultured as adherent monolayers in Plasmax containing vehicle (ethanol) or 0.1 μM dexamethasone (Dex). 24 hours later, the indicated concentrations of FK866 or CHS828 (NAMPTi) was added to the culture medium and the medium was refreshed every 4 days to avoid nutrient exhaustion. The cells were counted at 4, 8 and 12 days (n=1 independent experiment, 4 wells were counted for each condition).

Next we interfered with the metabolism of nicotinamide, the *N*1-methylnicotinamide precursor. This nutrient is present in every commercially available vitamin mix, therefore we customized Plasmax to obtain a nicotinamide-free culture medium. Unexpectedly, GBM cells cultured in nicotinamide-free Plasmax for 12 days did not show growth impairment. In addition, dexamethasone did not impact their ability to proliferate under these conditions. Given the essentiality of NAD+, NAMPT has a much higher affinity for nicotinamide than NNMT. In fact, NAMPT affinity for nicotinamide is less than 1 μM [235], while the reported K_m of human NNMT for nicotinamide is around 430 μM [201], a value that is likely exceeding the intracellular levels of nicotinamide obtained upon nicotinamide withdrawal. These observations led us to conclude that the affinity of NNMT for nicotinamide is too low to efficiently catalyse *N*1-methylnicotinamide production in nicotinamide-starved GBM cells, even when NNMT expression is enhanced by dexamethasone. The analysis of GBM cells metabolome upon nicotinamide restriction confirmed this hypothesis, showing that removal of nicotinamide from Plasmax drastically reduced the intracellular nicotinamide content and consequently NNMT activity.

Based on these results we tested an alternative hypothesis to harness dexamethasone driven-NNMT overactivity. We reasoned that the combination of an excess of nicotinamide upon methionine restriction would constitute a “double hit” to the SAM cellular pool. The results showed that upon dexamethasone treatment, nicotinamide supplementation did not sensitize GBM cells to methionine restriction. A metabolic analysis of cell metabolism in these conditions would clarify if the intracellular levels of SAM were decreased upon combination of supra-physiological nicotinamide and low-methionine availability.

To directly study the role of NNMT in supporting GBM cells proliferation we inhibited NNMT activity by two complementary approaches. Firstly, we cultured the cells in the presence of increasing concentrations of *N*1-methylnicotinamide to obtain a product inhibition of NNMT. Then, we treated the cells with 5-amino-1-methylquinolium, a synthetic inhibitor of NNMT. *N*1-methylnicotinamide did not affect GBM cells growth, while 5-amino-1-methylquinolium slightly inhibited the proliferation of BG7 and T16 cells. Collectively, these experiments suggested that NNMT activity is not a prerequisite for GBM cells growth. The discovery that NNMT

is overexpressed in the adipose tissue of mouse models of obesity prompted the development of pharmacologic inhibitors [236]. The fact that in our context NNMT inhibition has limited and cell line-dependent effects on cell proliferation does not exclude the possibility that alterations in NNMT activity might have other cell-autonomous or paracrine consequences. For instance, a recent study looked at the metabolic differences between T cells derived from patient ascites with ovarian cancer and T cells isolated from tumour samples, and found *N*1-methylnicotinamide to be the most enriched metabolite in the ascites-derived T cells [237]. Kilgour et al. suggested that the high NNMT expressing-cancer associated fibroblasts produce *N*1-methylnicotinamide that is then taken up from the T cells, possibly reducing the T cells cytotoxic capacity. The role of *N*1-methylnicotinamide as an immune-modulatory metabolite has not been investigated in our study that was focused on the effects of dexamethasone, a drug with well-established immune-suppressive effects. Moreover, a novel role of *N*1-methylnicotinamide in mediating responses to inflammation has been unveiled by Chlopicki et al. who discovered the anti-thrombotic activity of *N*1-methylnicotinamide through the production of 6-Keto-prostaglandin F1α, the more stable but less active product of prostacyclin hydrolysis [238]. In line with the anti-metastatic properties of prostacyclin, *N*1-methylnicotinamide anti-metastatic capacity has been shown in an *in vivo* murine mammary gland cancer model [239].

We also tried to target dexamethasone-mediated NNMT overexpression treating cells with an alternative NNMT substrate, 4-phenylpyridine, whose methylation leads to the production of the neurotoxic 1-methyl-4-phenylpyridinium ion, particularly studied in the context of Parkinson's disease [226]. The finding that NNMT is overexpressed in the brain of patients with Parkinson's disease suggested that NNMT might represent a link between environmental and genetic factors of this disorder [240]. In culture dexamethasone-treated GBM cells did not exhibit higher sensitivity to 4-phenylpyridine, but this remains to be investigated *in vivo*.

In a recent screening aimed at finding small molecule inhibitors effective at killing GBM cells when combined with radiotherapy, Aldaz et al. found that in culture dexamethasone had a radio-protective effect on human GBM cells. They observed that dexamethasone was able to sustain the proliferation of irradiated GBM cells,

and hypothesized that this effect might be due to a downregulation of mitosis-regulators and upregulation of anti-apoptotic proteins [241]. In our hands, the combination of dexamethasone treatment with ionizing radiation produced cell line-dependent effects but we could not observe an obvious radio-protective effect of dexamethasone. Because of the centrality of both therapies for GBM patients, the potential interference of dexamethasone with radiotherapy deserves further investigation in pre-clinical and clinical settings. Glucocorticoids are known to induce hyperglycaemia, and not only it has been shown that hyperglycaemia is associated with shorter patients survival [71], but Adeberg et al. identified persistent hyperglycaemia as an unfavourable predictor of survival in glioblastoma patients during radiotherapy [242].

6.6 Summary

We identified nicotinamide *N*-methyltransferase (NNMT), the enzyme responsible for the methylation of nicotinamide, as a metabolic target of dexamethasone. Here, we show that upon NNMT activation, dexamethasone-treated GBM cells consume more methyl donor SAM, however the resulting decreased SAM/SAH ratio does not seem to significantly affect neither DNA nor histones methylation. By altering the levels of nicotinamide and methionine in the medium, we found that GBM cells can sustain proliferation even at sub-physiological (~10%) levels of methionine concentrations, and that culturing in a medium totally deprived of nicotinamide does not affect their growth capacity for 12 days. Further, we observed that NNMT inhibition does not have a marked effect on proliferation of GBM cells. Finally the combination of ionizing radiation and dexamethasone did not produce synergistic effects in the cell models employed.

Chapter 7. Effects of dexamethasone in orthotopic GBM xenografts

7.1 Introduction

In the previous chapters of this thesis, we characterized the effects of dexamethasone treatment in cell models of GBM. In cancer research, the discrepancies between *in vitro* and *in vivo* models limit the translation of basic discoveries to the clinic. Most cancers are hallmarked by intra- and inter-tumour heterogeneity, and to model this heterogeneity in cell culture is an actual research challenge. Moreover, compared to other cancer types where genetically engineered models are widely used for therapeutic studies, the genetic GBM models available are useful for studying tumour initiation but less reliable when it comes to faithfully reproducing response to therapy. In fact, despite allowing the dissection of the events following specific genetic alterations, genetic GBM models are not highly reproducible when it comes to time of tumour initiation, critical for therapeutic studies [46]. Therefore, orthotopic xenografts, obtained by the surgical implantation of glioblastoma cells in the brain, represent a useful experimental model. To investigate the dexamethasone effects *in vivo* we surgically injected T16 tumour cells in the brain of immunocompromised mice.

7.2 Pharmacokinetics of dexamethasone in NOD Scid Gamma mice

Firstly, we aimed to identify the optimal time to study dexamethasone effects on the target organ, the brain. Therefore, we injected intraperitoneally a small cohort of female and male NOD Scid Gamma mice with 2 mg/kg dexamethasone-21-phosphate. This compound represents a more soluble prodrug of dexamethasone, requiring the rapid dephosphorylating activity of intra-cellular esterases to be converted to a functional drug [243]. This dosage was based on scientific papers recently published in similar models [126]. We sacrificed the mice 1, 3, 6, 12 and 24 hours after the dexamethasone administration and collected serum, brain and liver tissues for LC-MS analysis and compared metabolites levels to tissues samples from control mice not injected with dexamethasone (time 0). As shown in Figure 7-1, despite with a different amplitude in the two sexes, females and males exhibited the same pharmacokinetic pattern in response to the dexamethasone-21-phosphate single-dose treatment, and every tissue analysed in both sexes showed a peak in dexamethasone concentration 1 hour after the injection time.

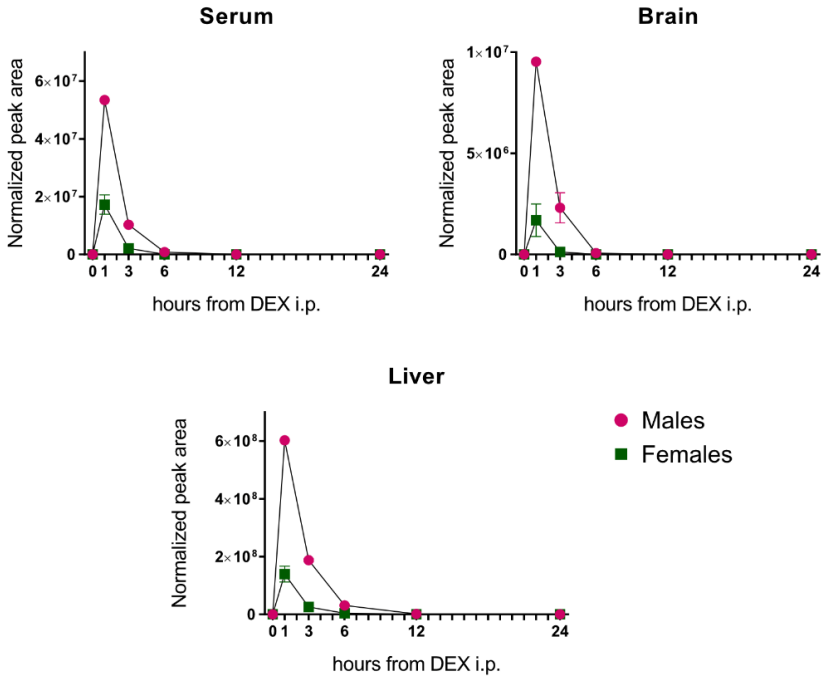

Figure 7-1 Pharmacokinetics of dexamethasone in NOD Scid Gamma mice

Ten female and ten male NOD Scid Gamma mice were injected intraperitoneally (i.p.) with 2 mg/kg dexamethasone-21-phosphate disodium salt and euthanized at the indicated time points from the injection time. Then, serum, brain and liver tissues were sampled and extracted in extraction solution for LC-MS analysis. For each time point, two female and two male mice were sampled and, as a control, two female and two male mice were sacrificed without being injected with dexamethasone (time 0). The peak areas have been normalized on the µg of serum and mg of brain and liver tissues extracted.

7.3 Intracranial injection of T16 cells in nude mice

In collaboration with the research group of Simone Niclou at the Luxembourg Institute of Health, we performed intracranial implantations of T16 tumour cells in Swiss Nu/Nu mice. Tumours formation was assessed by Magnetic resonance imaging (MRI) and tumour-bearing mice were randomized in two experimental arms: vehicle-treated (NaCl 0.9% solution) or treated with clinically relevant doses of dexamethasone-21-phosphate disodium salt (2 mg/kg) for five days/week through intraperitoneal injection. Despite the exact mechanism has not been established, glucocorticoids are known to induce muscle wasting, and therefore weight loss represents one of the expected side effects of dexamethasone treatment in mice [244]. This might represent an issue because some animal licences require the sacrifice of mice losing more than 20% of their pre-operative weight. For this reason, we closely monitored the weight of the mice after the surgery and during the course of the treatment. As shown in Figure 7-2, we observed some fluctuations in the weight of the mice, but none of them lost more than 10% of weight compared to the pre-operative weight.

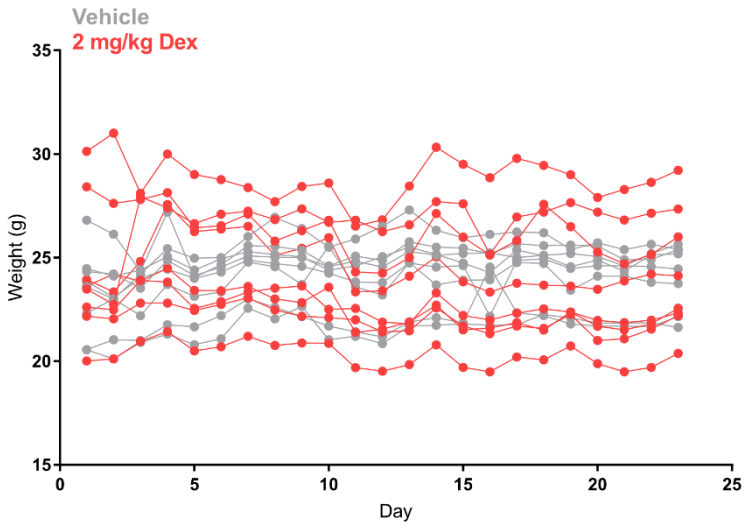

Figure 7-2 Weight measurements of T16 tumours-bearing nude mice treated with NaCl 0.9 % solution (vehicle) or dexamethasone-21-phosphate disodium salt (2 mg/kg Dex)

7.3.1 Dexamethasone causes a reduction of tumour growth

Tumour volume was followed by T2 MRI until the mice reached the experimental endpoint (Figure 7-3, Panel A). The treatment with dexamethasone significantly reduced the size of T16 tumours (Figure 7-3, Panel B). When the mice reached the experimental endpoint (tumour volume ≥80 mm^3), they were euthanized 4 hours after the last dexamethasone injection and samples of tumour tissue, contralateral brain, liver and serum were collected for metabolomics analyses and immunohistochemistry staining. Tumour sections were stained with hematoxylin and eosin (H&E) staining, and antibodies against Nestin, Ki67 and GR (Figure 7-4, Panel A). In order to investigate whether dexamethasone decreased the proliferation of GBM cells, HALO software was used to quantify the number of nuclei stained with the antibody against the proliferation marker Ki67 [245]. This quantification highlighted that the percentage of Ki67-positive tumour cells was significantly lower in the dexamethasone-treated tumours (Figure 7-4, Panel B). Therefore, in these settings dexamethasone caused a decrease in the T16 GBM cells proliferation *in vivo*.

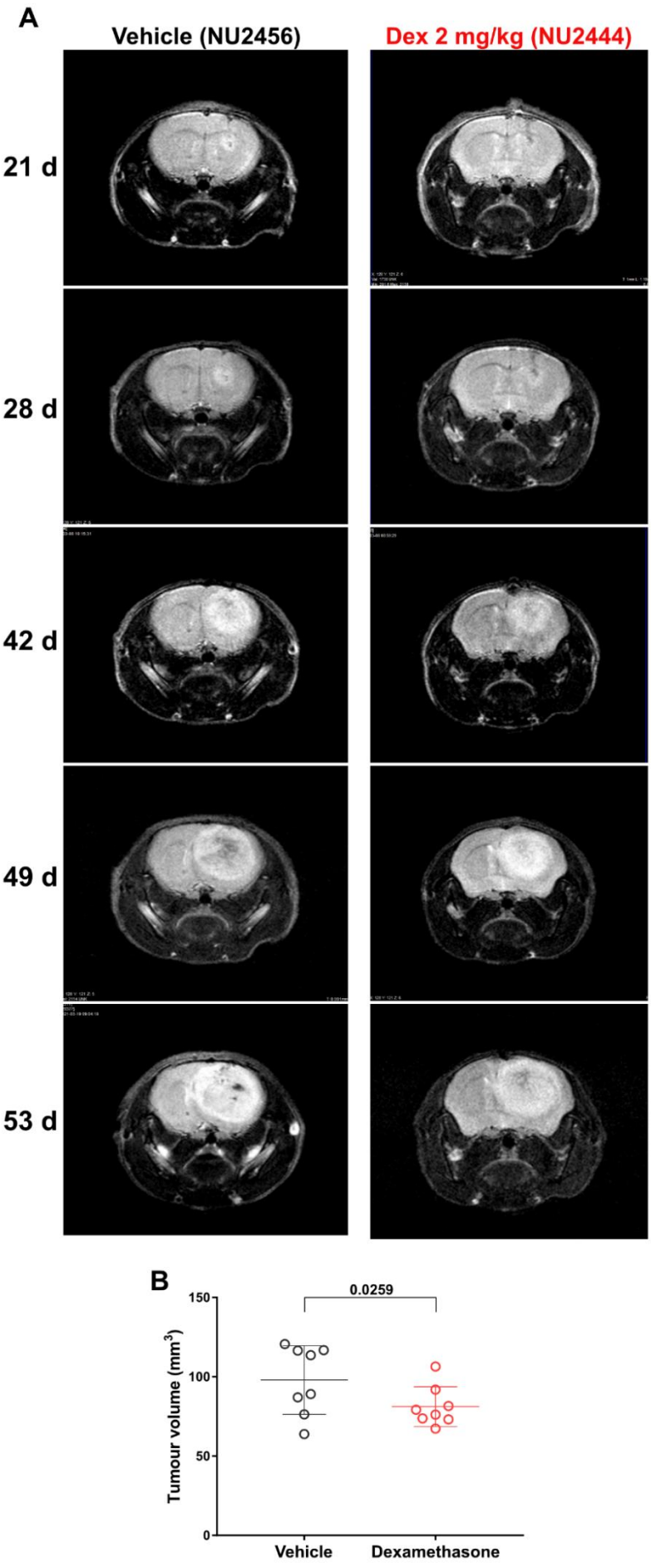

Figure 7-3 Dexamethasone affects the growth of T16 orthotopic tumour model

A) A cohort of nude mice was injected with patient-derived T16 glioblastoma cells. Tumour formation was assessed by MRI and tumour-bearing mice were randomized into two experimental arms: vehicle-treated or treated with relevant doses of dexamethasone (2 mg/kg) five days/week. Tumour volume was followed by T2 MRI until clinical signs appeared. Representative T2 MRI images showing T16 tumours in the brain of the mice after the indicated number of days from surgery. B) Quantification of tumour volume from MRI images of vehicle- and dexamethasone-treated T16 tumours-bearing mice (n=8 vehicle-treated mice, n=8 dexamethasone-treated mice). *P* values result from unpaired two-tailed t-tests.

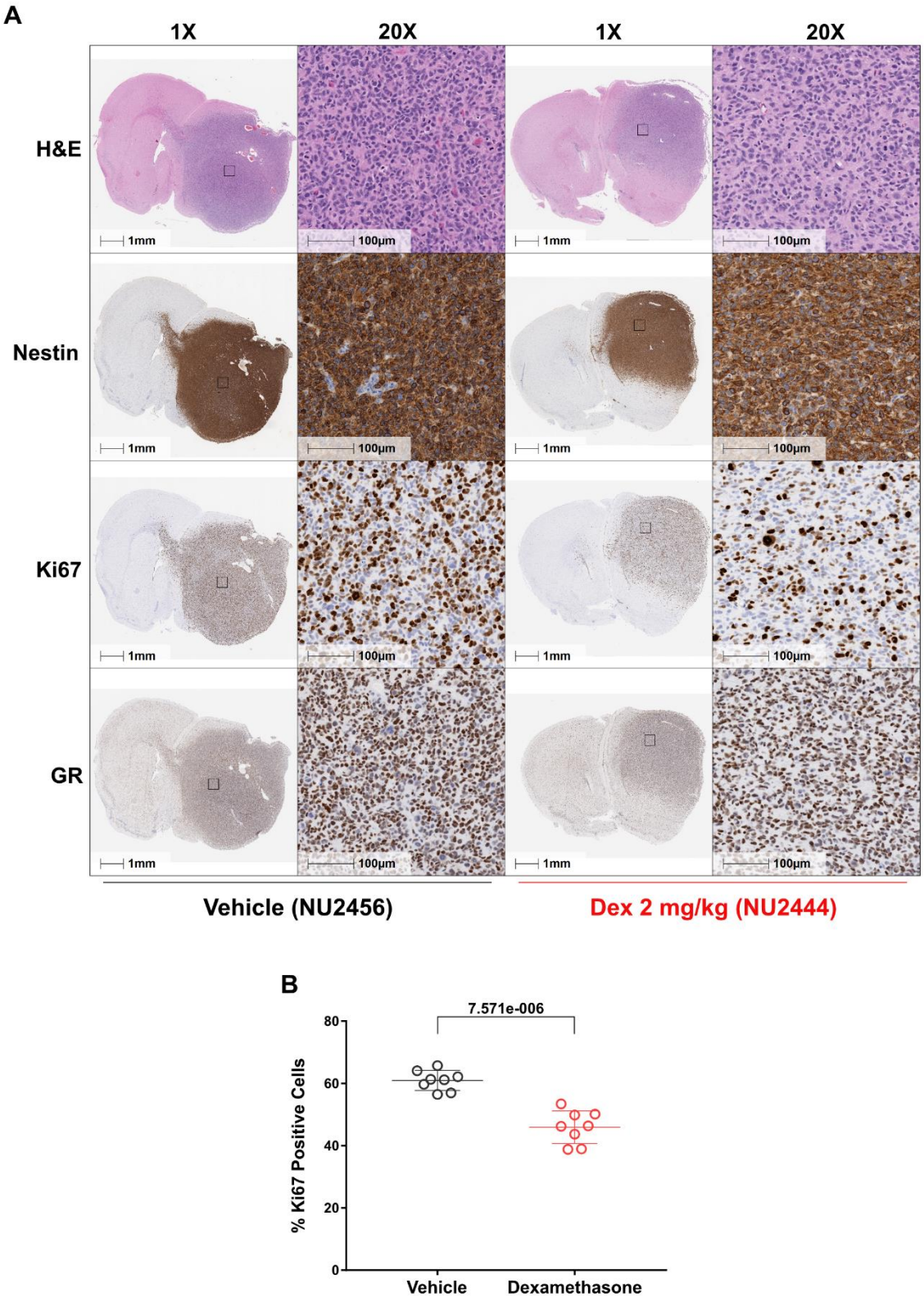

Figure 7-4 Dexamethasone causes a reduction in the proliferation of T16 GBM tumours

Once the T16 tumours-bearing mice reached experimental endpoint, the mice were euthanized and samples of their tissues collected for immunohistochemistry analyses. Tumour sections were stained with H&E staining, and antibodies against Nestin, Ki67 and GR. Brain sections are shown at two different magnifications (1X, 20X). B) Ki67 staining in the nuclei has been quantified through HALO software. The tumour area has been selected and the number of Ki67-positive nuclei/total number of nuclei in the selected area has been quantified. *P* value results from paired two-tailed t-test.

7.3.2 *N*1-methylnicotinamide is accumulating in GBM tumours upon dexamethasone treatment

Samples of tumour tissue and normal contralateral brain, liver and serum were immediately snap-frozen in order to preserve the metabolites content. Upon tissue homogenization in extraction solution, we analysed them through LC-MS for a targeted approach. Firstly, we evaluated the levels of dexamethasone in the tissues and as expected, we were able to detect it only in tissues from dexamethasone-treated mice (Figure 7-5). Importantly dexamethasone was detected in the tumour tissue, confirming that the drug reaches the target of interest. Next we looked at the level of *N*1-methylnicotinamide that was remarkably higher in the tumour tissue than in any other tissue analysed (Figure 7-5). In particular, we observed a substantial difference between the tumour tissue and the contralateral normal brain in line with the differential expression of NNMT. Furthermore, dexamethasone treatment selectively increased the levels of *N*1-methylnicotinamide in T16 tumours but not in contralateral brain. Consistently with the results obtained *in vitro* dexamethasone also caused a decrease in tumour SAM levels. These results strongly suggest that NNMT is a dexamethasone target also *in vivo,* and the increased production of *N*1-methylnicotinamide wears down the availability of methyl groups. Differently from what observed *in vitro*, nicotinamide and NAD+ levels were not affected by dexamethasone treatment in any of the tissues analysed (Figure 7-5).

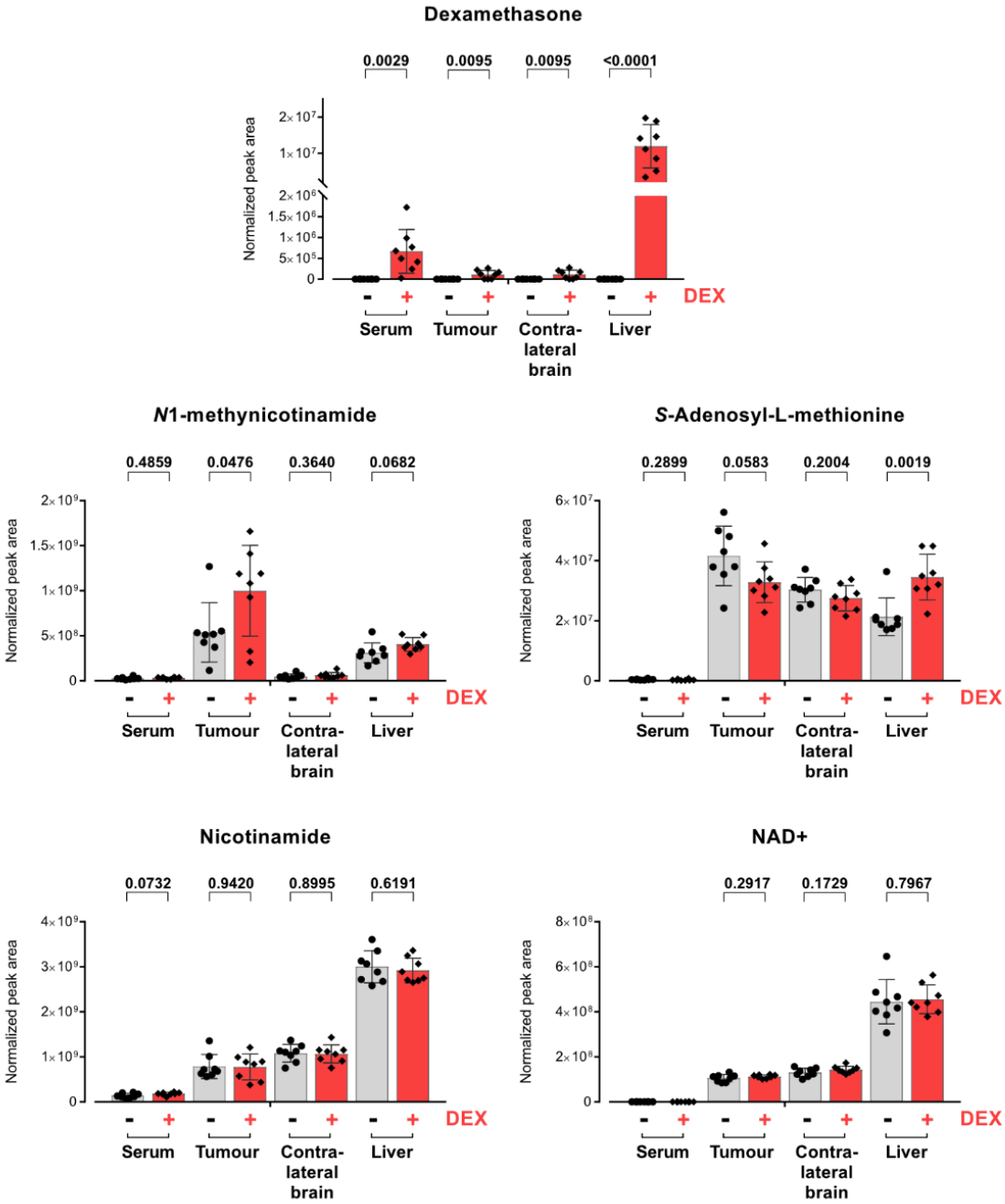

Figure 7-5 Metabolomics analysis of the tissues collected from T16 tumours bearing-mice upon vehicle or dexamethasone treatment

Samples of T16 tumour tissue, contralateral brain, liver and serum were collected and extracted in extraction buffer. Dexamethasone, *N*1-methylnicotinamide, *S*-adenosylmethionine, Nicotinamide, NAD+ levels are shown. The bar plots represent the peak areas of the metabolites normalized for the µL of serum and the mg of tissue samples extracted. *P* values result from unpaired two-tailed t-tests (n=8 vehicle-treated mice, n=8 dexamethasone-treated mice).

7.3.3 NNMT is overexpressed in tumour tissue compared to contralateral brain

The increased *N*1-methylnicotinamide levels in the tumours of the dexamethasone-treated mice anticipated that dexamethasone administration was inducing NNMT overactivity also in an *in vivo* context. In order to test if NNMT over-activity was due to an increased expression of the protein, we performed a Western blotting analysis comparing the contralateral and tumour tissue of the vehicle- and dexamethasone-treated mice. Figure 7-6 shows that tumour tissue exhibited higher levels of NNMT protein when compared to contralateral brain tissue from the same mouse. Moreover, dexamethasone administration caused a further overexpression of NNMT specifically in the tumour tissue of the dexamethasone-treated mice.

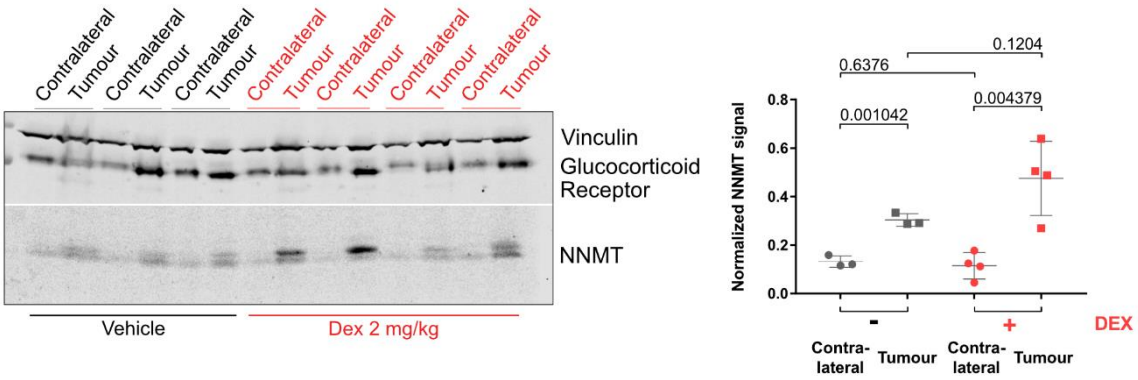

Figure 7-6 Dexamethasone causes NNMT overexpression in GBM tumour tissue

Upon sacrifice of the vehicle- and dexamethasone-treated T16 tumours-bearing mice, samples of tumour and contralateral normal brain were collected and lysated in RIPA buffer to extract the protein content. For each mouse, contralateral brain tissue and tumour tissue were processed. The same amount of protein was loaded for each sample, and vinculin was used as a loading control. The graph on the right shows the quantification of the Western blot. NNMT content was normalized on Vinculin content and *P* values result from unpaired two-tailed t-test.

7.3.4 Dexamethasone regulates amino acids metabolism in the brain

The targeted metabolomics approach allowed us to evaluate the changes of several nutrients in the tissues of vehicle- and dexamethasone-treated mice. Particularly, we focused on dexamethasone-induced alterations in the brain and observed that dexamethasone was causing a decrease of several amino acids in contralateral and tumour tissues (Figure 7-7). For instance, methionine levels were decreased upon dexamethasone administration, a result especially intriguing given the essentiality of this amino acid for cancer cells proliferation [218]. Similarly, dexamethasone was causing a reduction of tryptophan and tyrosine levels both in the contralateral and in the tumour tissue. Dexamethasone increased methionine levels in the liver but the serum levels were not affected. Moreover, tryptophan and tyrosine were not changing in liver and serum upon dexamethasone treatment. This suggests that the changes in the amino acids levels in the brain were not mediated by systemic dexamethasone-mediated alterations.

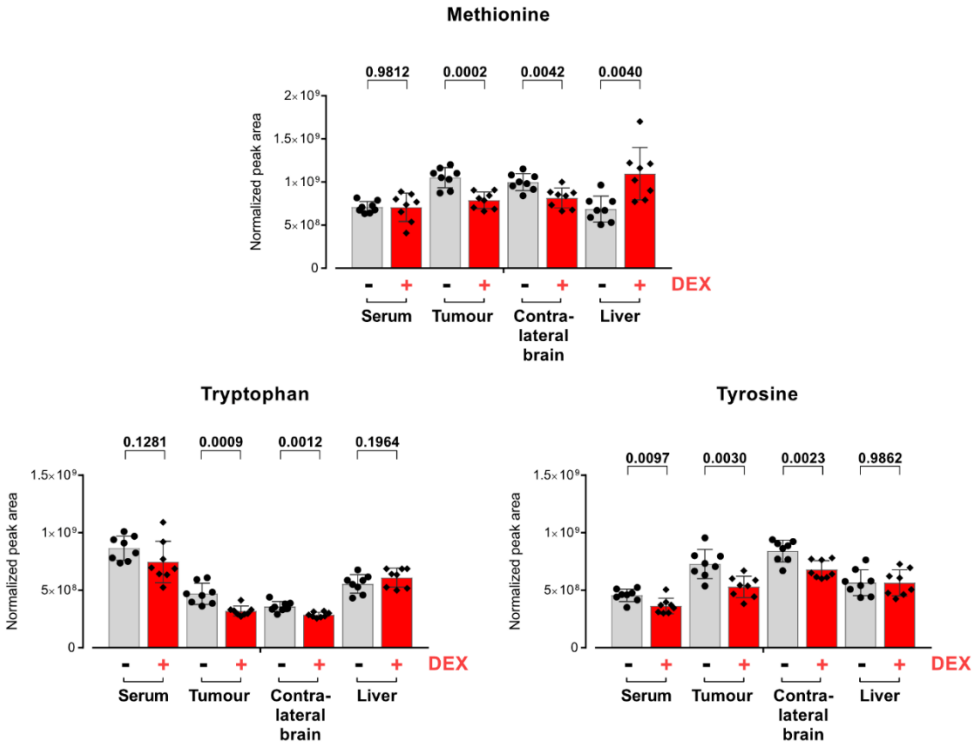

Figure 7-7 Methionine, tryptophan and tyrosine levels are decreased in the tumour and contralateral brain tissues of dexamethasone-treated mice

Samples of T16 tumour tissue, contralateral brain, liver and serum were collected and extracted in extraction solution. Methionine, tryptophan and tyrosine levels are shown. The bar plots represent the peak areas of the metabolites normalized for the µL of serum and the mg of tissue samples extracted. *P* values result from unpaired two-tailed t-tests (n=8 vehicle-treated mice, n=8 dexamethasone-treated mice).

7.4 Nicotinamide supplementation increases NNMT activity *in vivo*

Dexamethasone administration successfully increased NNMT activity in the tumour tissue, nevertheless nicotinamide levels did not change in any of the tissues analysed. Therefore, we decided to test the hypothesis that supplementing exogenous nicotinamide would increase NNMT activity. To this aim, we surgically implanted T16 tumour cells in a cohort of NSG mice and followed tumour growth by T2 MRI. When the mice started showing clinical signs of tumour development, we treated them with 500 mg/kg nicotinamide and sacrificed the mice two hours later to collect serum, tumour, contralateral brain and liver tissues for metabolomics analyses. We measured the circulating and tissue metabolites levels through a targeted approach. Upon nicotinamide supplementation, nicotinamide levels were elevated in all the tissues analysed (Figure 7-8). Moreover, we observed an increase in *N*1-methylnicotinamide levels in the brain – both in tumour and contralateral normal tissue – as well as in the liver, suggesting that nicotinamide supplementation did indeed boost NNMT activity (Figure 7-8). Remarkably, nicotinamide administration caused a decrease in the methionine levels in tumour and contralateral brain tissues, leaving SAM levels unchanged (Figure 7-8).

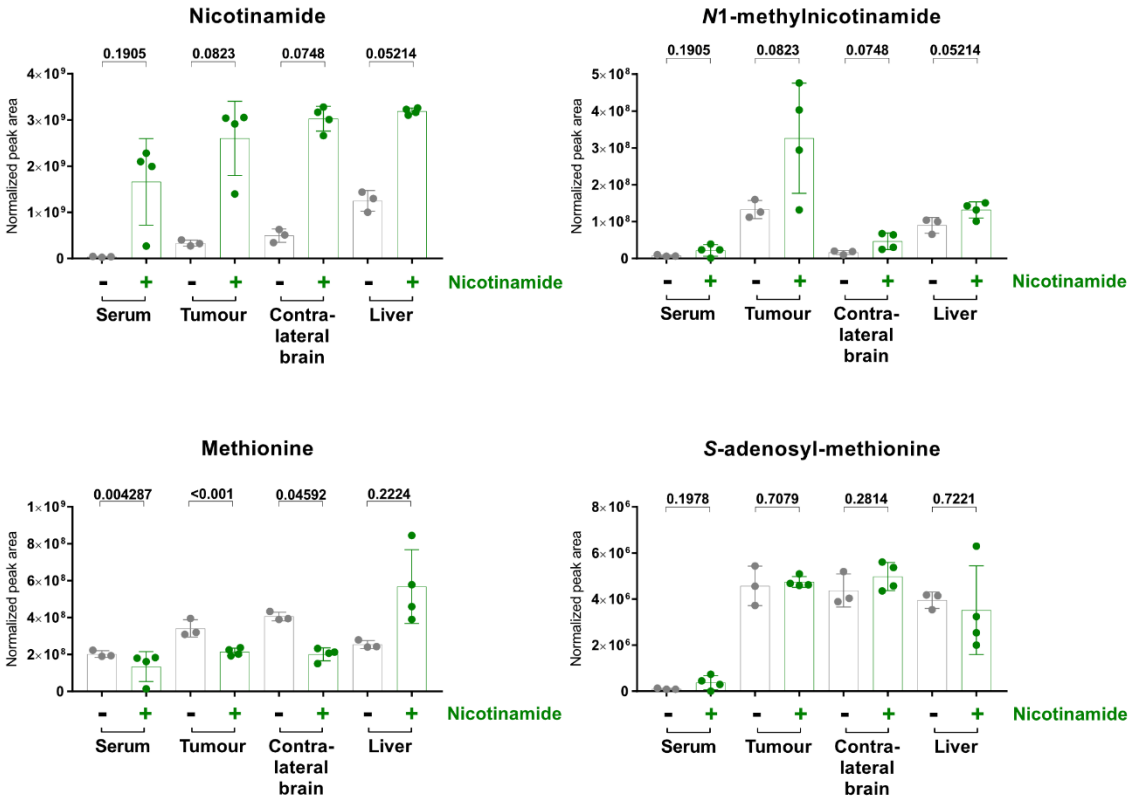

Figure 7-8 Nicotinamide supplementation increases NNMT activity *in vivo*

A cohort of NSG mice was intracranially injected with patient-derived T16 glioblastoma cells. Tumour formation was assessed by MRI and, when clinical signs of tumour development started appearing, 4 mice received a bolus of nicotinamide 500 mg/kg and were sacrificed two hours later. Samples of serum, tumour, contralateral brain and liver tissues were collected and extracted in extracted solution. Nicotinamide, *N*1-methylnicotinamide, methionine and *S*-adenosylmethionine levels are shown. The bar plots represent the peak area of the metabolites normalized for the µL of serum and mg of tissue extracted. P values result from unpaired two-tailed t-tests (n=3 control nude mice, n=4 NSG mice injected with nicotinamide 500 mg/kg two hours before being sacrificed).

7.5 Chapter discussion and results limitations

In this chapter, we showed the experiments performed in xenograft models of GBM to test if we could recapitulate the effects we characterized in the GBM cells upon dexamethasone administration. To this aim, firstly we investigated the pharmacokinetics of dexamethasone in *NOD scid* (NSG) mice. In all the tissues analysed, both female and male mice exhibited a peak in dexamethasone concentration after 1 hour from treatment. Dexamethasone concentrations were lower in female than in male mice, a result that might be due to a different metabolism of dexamethasone. Nonetheless, this sex-based difference was not further investigated since only female mice were xenografted with GBM cells. Based on these pharmacokinetic results we decided to harvest tumour-bearing mice 4 hours after the last dexamethasone administration. In order to better define the optimal experimental time-point to study dexamethasone effects, glucocorticoid receptor targets could be measured in tissues extracted from dexamethasone-treated mice and harvested at different time points.

When working on cancer cells-based models, there is always the possibility that *in vitro*-described events might not be recapitulated in animal models. Therefore, we considered crucial characterizing the effects of dexamethasone administration in GBM xenograft models. Among the four GBM cell lines employed in this project, we selected T16 cells because they have been previously characterized *in vivo* [26] and because they were consistently the most responsive to the effects of dexamethasone. However, the significant antitumor effect of dexamethasone observed in T16 tumour-bearing mice was in sharp contrast with the result obtained in cell culture, where dexamethasone favoured the proliferation of T16 adherent monolayers. However, as shown in Chapter 3 of this thesis, dexamethasone caused an anti-proliferative effect on T16 cells-derived spheroids, suggesting that this model might recapitulate better than monolayers the *in vivo* GBM biology.

The altered metabolism of cancer cells compared to neighbouring normal cells has been exploited by imaging technologies for diagnostic purposes [59]. In this regard, positron emission tomography (PET) imaging relies on the accumulation of ^{18}F-FDG, a positron-emitting tracer analogue of glucose, within the highly glycolytic cancer cells. Unfortunately, the brain functions heavily depend on

constant replenishment of glucose from the circulation, invalidating the use of ^{18}F-FDG for brain tumours. Differently from nicotinamide, the substrate of NNMT, its product *N*1-methylnicotinamide is positively charged, meaning that it is likely to be trapped intracellularly. Therefore, we speculated that the newly discovered dexamethasone-induced overexpression and consequent activation of NNMT could be exploited to convert a neutral tracer into a charged one to use for imaging purposes. Confirming this dexamethasone-mediated metabolic effect in a xenograft GBM model was crucial to prove the validity of NNMT as a dexamethasone target in a clinically relevant context. However, the hypothesis of using NNMT-catalysed reaction for non-invasive diagnosis requires further testing in GBM animal models. Gene Expression Profiling Interactive Analysis (GEPIA2) was used to visualize the levels of NNMT expression in human GBM tissue *versus* normal brain samples. Figure 7-9 (Panel A, left) shows that NNMT is upregulated in GBM tissue when compared to normal brain tissue and high NNMT expression correlates with worse disease free survival (Figure 7-9, Panel A, right). Moreover, tissues collected after surgery of a cohort of GBM patients and extracted for metabolomics analyses highlighted that *N*1-methylnicotinamide and the product of its metabolism *N*1-methyl-2-pyridone-5-carboxamide are enriched in tumour compared to the surrounding oedema tissue, importantly recapitulating the findings from models to patients (Figure 7-9, Panel B).

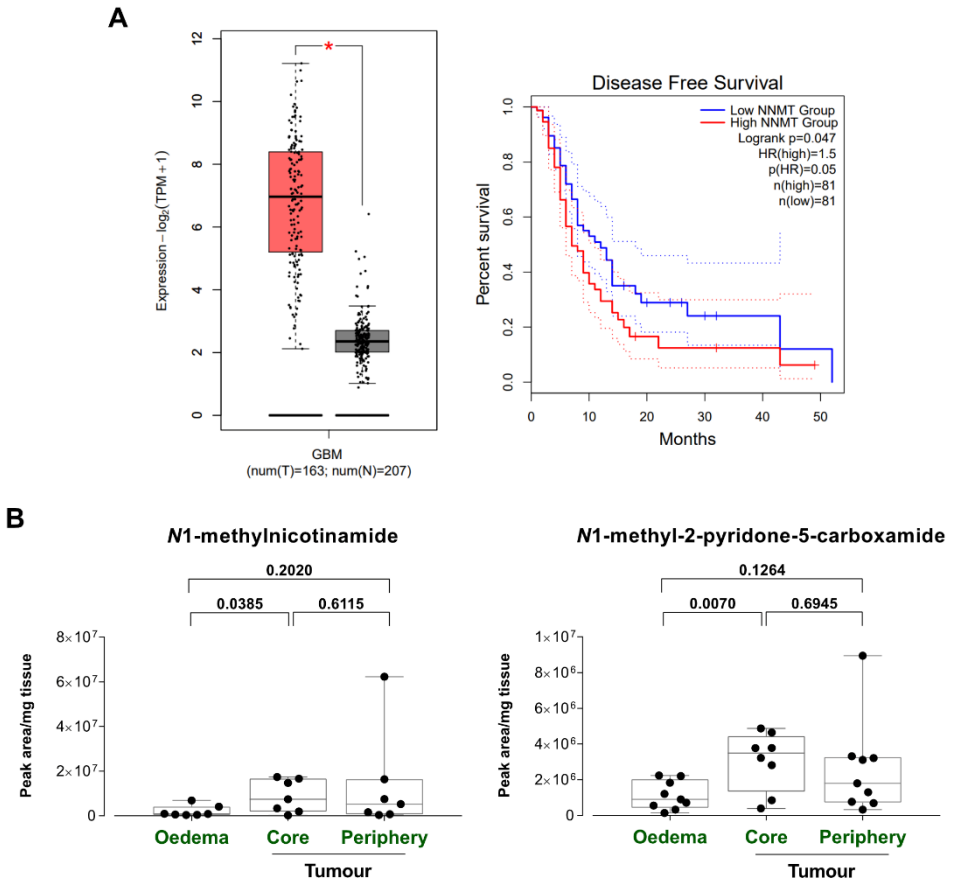

Figure 7-9 NNMT expression is enriched in human tumour tissue *versus* normal brain

A) Left: GEPIA2 (http://gepia2.cancer-pku.cn/#index) was used to compare NNMT expression levels in normal brain samples from GTEx database (grey) to TCGA-GBM tumour tissue samples (red). Right: Disease-free Survival Kaplan Meyer plot (blue: low NNMT expression, red: high NNMT expression). B) Human GBM biopsies were extracted in extraction buffer and analysed by LC-MS. The samples were collected from three different regions: oedema, tumour core and tumour periphery. *P* values result from unpaired two-tailed t-tests.

In T16 tumours-bearing mice, SAM levels were decreased by dexamethasone treatment in the tumour tissue. Using the LC-MS based protocol previously used to evaluate differences in the global methylation levels, we were not able to detect any difference in the DNA methylation between tumour samples from vehicle- and dexamethasone-treated mice (Figure 7-10, Panel A). We then isolated histones from tumour samples and tested the levels of selected histone markers, without finding consistent changes in response to dexamethasone treatment (Figure 7-10, Panel B). Despite their preliminary nature, these results suggest that dexamethasone-mediated NNMT overactivity does not grossly alter GBM cells epigenome. Interestingly, upon glucocorticoids treatment, tumour-bearing mice showed a decrease of methionine levels in the brain, both in contralateral and in tumour tissue, and an increase in the liver. The fact that no changes in methionine concentration are observed in the serum demonstrates that dexamethasone induces tissue-specific alterations in methionine metabolism. The RNA sequencing analysis in GBM cells showed that dexamethasone did not affect the RNA levels of the gene encoding for the methionine synthase (MTR), but significantly increased the levels of *MAT2A*, encoding for the enzyme responsible of SAM biosynthesis from methionine (as showed in Chapter 6, Figure 6-11). These transcriptional effects of dexamethasone might explain the decreased levels of methionine observed in T16 tumours and deserve further investigation.

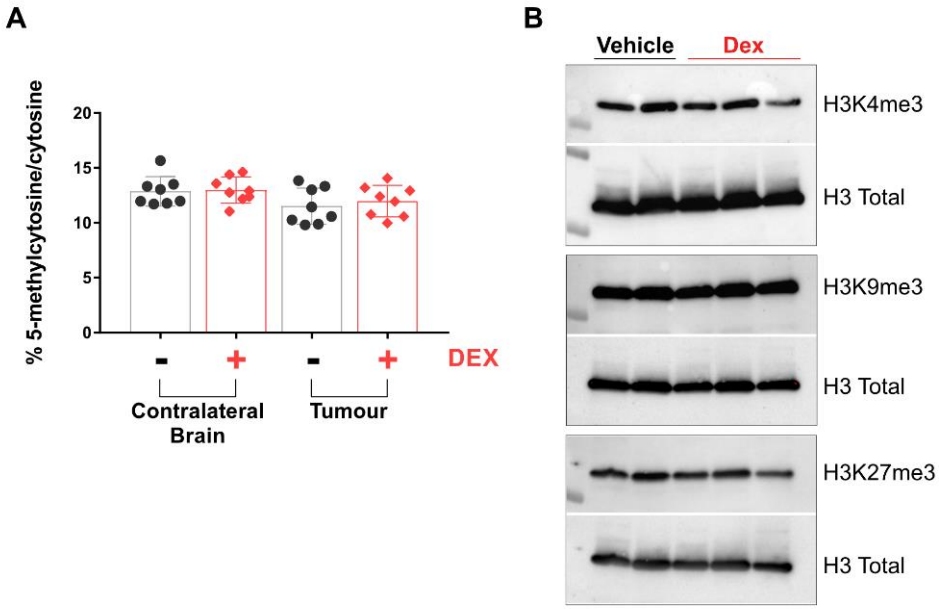

Figure 7-10 Investigating DNA and histones methylation levels in tumour tissues collected from T16 tumours-bearing mice

A) Whole DNA was extracted from contralateral brain and tumour tissues collected from T16 tumours-bearing mice (n=8 vehicle-treated mice, n=8 dexamethasone-treated mice). Following the protocol in [149], the DNA was subjected to acid hydrolysis and then extracted in extraction solution. The samples were analysed by LC-MS. The peak areas of total cytosine and 5-methylcytosine was and the ratio is illustrated in the figure. B) Histones were isolated from tumour tissues collected from T16 tumours-bearing mice (n=2 vehicle-treated mice, n=3 dexamethasone-treated mice) and quantified. The same amount of protein was loaded and H3 total levels were used as a loading control. Levels of H3K4me3, H3K9me3 and H3K27me3 are shown.

Nicotinamide supplementation in murine cancer models has been exploited in the past to sensitize tumours to radiation therapy [246, 247]. We referred to these studies to identify a safe nicotinamide dose (500 mg/kg) and investigate if nicotinamide supplementation could increase NNMT activity in the brain. Two hours after a single injection of nicotinamide 500 mg/kg, nicotinamide levels were elevated in all the tissues analysed and we observed an increase in the production of *N*1-methylnicotinamide in the tumour. Despite SAM levels were not altered by nicotinamide supplementation, methionine levels were decreased in the brain and tumours suggesting that a continuous nicotinamide supplementation of tumour-bearing mice might reduce methionine availability to levels suboptimal for tumour cells proliferation.

Finally, glucocorticoids are so widely used in the clinics mainly because of their anti-inflammatory and immunosuppressive capacity. Employing GBM patients-derived cells lines requires working with immuno-compromised animal models in order to avoid the rejection of the surgically transplanted cells. Unfortunately, this also prevents studying the interaction between cancer and immune cells. Kilgour et al. showed that *N*1-methylnicotinamide produced by CAFs in ovarian cancer has immune-modulatory activity [237], an aspect of dexamethasone effects that we cannot investigate in immunocompromised mice. Although, several groups have been using genetic GBM models to perform the implantation of GBM stem cells in immunocompetent hosts and thus characterize the immune evasion process [248]. In the future, we might take advantage of similar genetic models to define if glucocorticoids-induced *N*1-methylnicotinamide accumulation is affecting the GBM tumour microenvironment.

7.6 Summary

In this chapter, we described how dexamethasone administration affects T16 GBM cells proliferation and metabolism when they are intracranially implanted in the brain of immunocompromised mice. Firstly, we performed an experiment to evaluate the best time point for sampling the mice tissues upon dexamethasone treatment. Then, we performed intracranial surgery in a cohort of nude mice, and once the tumour formation was assessed by T2 MRI we started treating them with dexamethasone. Through this experiment, we found that glucocorticoids are reducing T16 cells proliferation *in vivo*, while inducing NNMT overexpression and *N*1-methylnicotinamide accumulation specifically in the tumour tissue. SAM levels were also decreasing upon dexamethasone administration in the tumour tissue. These changes in the metabolism of methyl groups did not translate into appreciable changes in global DNA and histones methylation. Importantly, we confirmed that NNMT is overexpressed and overactive in tumour tissue when compared to the normal contralateral brain. We then showed that nicotinamide supplementation is able to enhance NNMT catalytic activity, causing an increase of *N*1-methylnicotinamide in the tumour tissue. By interrogating publicly available databases, we found that NNMT expression is elevated in human GBM tumours compared to normal brain. Moreover, the metabolomics extraction of human-derived biopsy samples showing high levels of *N*1-methylnicotiamide in the tumour tissue compared to the surrounding tissue confirmed the relevance of NNMT activity in the clinical settings.

Chapter 8. Conclusions and Future Perspectives

Glioblastoma molecular profiling defined four different genetic GBM subtypes, i.e. mesenchymal, proneural, neural and classical [14]. Apart from partially informing on the tumour's aggressiveness, this classification is not used to stratify glioblastoma patients for treatment. Moreover, independently from the molecular features of the tumours, glioblastoma patients are routinely treated with dexamethasone to reduce the peritumoral oedema and the intracranial pressure [101]. Since the introduction of synthetic corticosteroids in the clinical management of gliomas in 1961, many research studies have investigated how they affect glioblastoma cells *in vitro* and *in vivo*. Despite several research groups have shown that corticotherapy might negatively impact glioblastoma patients' prognosis and survival, an alternative as effective and uncostly as glucocorticoids has not being adopted to treat tumour-associated oedema. Regardless of their extensive use in the clinics, many details of the cascade of events caused by synthetic glucocorticoids administration and their molecular targets are still unknown. Their name points at a role in glucose metabolism regulation but most of the information we have about their metabolic role comes from pathological settings. In fact, people affected by Cushing's syndrome, due to prolonged exposure to glucocorticoids, or its "opposite" Addison's disease, caused by an insufficient production of physiological glucocorticoids, exhibit metabolic syndrome pathologies such as glycaemic dysfunctions and fat deposition. Despite the many side effects of corticotherapy, the lack of a better alternative makes them necessary to ameliorate the clinical symptoms caused by an advanced brain tumour. Therefore, we decided to investigate how dexamethasone, the most commonly used glucocorticoid, affects glioblastoma cells in both *in vitro* and *in vivo* settings in order to find metabolic vulnerabilities to exploit for therapeutic purposes. We used naïve patient-derived GBM cell lines, cultured in serum-free media preserving glioma stem cells features, to study the effects of dexamethasone on their proliferation and metabolism. We found that dexamethasone exerts cell line-dependent effects in cells cultured as adherent monolayers and three-dimensional spheroids. Through the sequencing of the whole transcriptome, we found a dexamethasone signature common to all GBM lines. Among these 79 genes we found the anti-apoptotic protein BclxL and *ELOVL2,* encoding for the Elongation of very long chain fatty acids protein 2.

Therefore, we combined dexamethasone treatment with Bcl2 inhibitors or fatty acids restriction to impair glioblastoma cells growth, but these approaches did not produce appreciable effects on proliferation when combined with dexamethasone. Through an unbiased metabolomics approach, we identified *N*1-methylnicotinamide, a nicotinamide metabolite whose concentration increased upon dexamethasone treatment in all glioblastoma cells cultured as monolayers and spheroids. To elucidate the mechanism of this accumulation, we looked at the expression levels of the enzyme responsible of its synthesis, nicotinamide *N*-methyl transferase (NNMT). NNMT was found among the 79 genes of the dexamethasone upregulated signature. Through Western blotting, we confirmed that also NNMT protein levels were increased in a panel of 10 naïve GBM cell lines upon dexamethasone treatment. The validation of NNMT as a target of dexamethasone in glioblastoma tumours came from the surgical implantation of T16 glioblastoma cells in the brain of immunocompromised mice. In line with publicly available datasets such as TCGA, showing that NNMT expression is higher in glioblastoma tumours than in normal brain, we found that NNMT was overexpressed in the tumour tissue compared to the contralateral normal brain. Importantly, the administration of dexamethasone in T16-tumours bearing mice increased even further NNMT expression and activity specifically in the tumour tissue, as indicated by *N*1-methylnicotinamide levels. In order to identify the therapeutic leverage that dexamethasone-induced NNMT overactivity might have in the clinical settings, we restricted the access of glioblastoma cells to nicotinamide. We showed that glioblastoma cells were able to sustain their proliferation in a nicotinamide-restricted environment. Although, through LC-MS we found that upon nicotinamide deprivation the levels of nicotinamide were barely detectable and likely below the K_m of NNMT. In physiological conditions the increased NNMT activity promoted by dexamethasone caused a decrease in the intracellular levels of *S*-adenosyl-methionine. Nonetheless, the decreased availability of this central methyl donor did not significantly alter the epigenome of glioblastoma cells, as indicated by the global DNA methylation or histones methylation status. Then, we challenged glioblastoma cells with methionine restriction that decreased cell growth in all glioblastoma lines. We proposed that combining methionine depletion with nicotinamide supplementation would thrust NNMT activity and deplete SAM to levels incompatible with optimal cellular

proliferation. However, this approach did not cause a defect in cell growth exceeding that obtained by methionine restriction alone.

We then tested the effects of dexamethasone treatment *in vivo*. Dexamethasone administration caused significant reductions of T16 tumour growth and proliferation marker Ki67. These results require further investigation in other PDX models, but suggest that diet-based approaches, such as methionine restriction or nicotinamide supplementation could synergize with the dexamethasone inhibitory effect on glioblastoma tumours growth. Particularly, methionine has been proven to be essential for the proliferation of several cancer cells (including glioblastoma), which do not efficiently methylate homocysteine to produce methionine. With our analytical method it was not possible to reliably measure changes in homocysteine levels, but a functional experiment demonstrated that homocysteine in the medium did not rescue the antiproliferative effects of methionine deprivation. Methionine dependency has been exploited for the development of erythrocyte-encapsulated methionine gamma-lyase (MGL), a methionine-cleaving enzyme ubiquitous in all organisms, except mammals [249]. MGL has been found to be effective at blocking glioblastoma growth both *in vitro* and *in vivo*, but the dependency of the enzyme from pyridoxal-5'-phosphate challenges its efficacy in animal models. Consistently with exogenous methionine essentiality, radiolabelled methionine represents the most frequently used radiotracer for the imaging of brain tumours [250]. The observation that inflammatory cells uptake more methionine than the tumour cells has highlighted potential pitfalls in the interpretation of methionine-based imaging [251]. Given that *N*1-methylnicotinamide is a positively charged molecule, it is likely to be trapped within cell compartments. This, in addition to the results presented in this thesis, provides a good rationale to evaluate nicotinamide as a tracing agent to image GBM tumour, an approach for which we are designing a feasibility study with ^{14}C-nicotinamide. In fact, the observation that *N*1-methylnicotinamide is enriched in tumour tissues coming from glioblastoma patients support the idea of using NNMT activity for diagnostic purposes. It remains to be established if dexamethasone-induced NNMT overactivity has to do with NNMT ability to metabolize xenobiotics or the other functions that have been more recently unveiled. In fact, NNMT has attracted a lot of interest since the discovery of its high expression in adipose tissue [252], and the finding that its knock-down

protects from high-fat diet-induced obesity in mice [236]. This effect has been linked to NNMT ability to alter the polyamines pathway through the utilization of SAM molecules. In our models upon dexamethasone treatment we were not able to detect changes in the levels of *N*-acetylputrescine or in the genes for polyamines biosynthesis, but tailored analytical methods might allow us to directly measure polyamine biosynthesis in dexamethasone-treated tumours. Moreover, the importance of nicotinamide for NAD+ biosynthesis and the upregulation of *NAMPT* – responsible for NAD+ biosynthesis – we observed after dexamethasone administration *in vitro* advance the intriguing hypothesis that dexamethasone might have an impact on the stemness capacity of glioblastoma cells. In fact, the vast body of literature suggesting NAMPT as essential for the (de)differentiation process of glioma stem cells has been reviewed in [253]. Moreover, NNMT and *N*1-methylnicotinamide have been identified as metabolic factors important for the naïve-to-primed transition of embryonic stem cells [215], suggesting that similarly to NAMPT, also NNMT might be able to regulate the cellular stemness capacity. Cells transitioning from a quiescent to a proliferative status exhibit a progressive extracellular accumulation of *N*1-methylnicotinamide [254]. The switching between a proliferative and quiescent status becomes particularly relevant in the context of persister cells, i.e. slow-cycling and drug-tolerant cancer cells that might enable glioblastoma cells to resist therapeutic stresses and therefore reoccur [255]. Oren et al. showed that, upon treatment with an EGFR inhibitor, *N*1-methylnicotinamide and several polyamines were among the most abundant metabolites in cycling and non-cycling persister lung cancer cells when compared to the untreated cells [256]. This raises the possibility that the dexamethasone-mediated inhibition of tumour growth observed in T16 tumours might concur to make glioblastoma cells more 'persister-like' and therefore resistant to therapy. Liau et al. proposed that the transition between proliferative and slow-cycling state of glioblastoma cells is enabled by reversible epigenetic changes driven by the lysine histone demethylase KDM6 [255]. In both *in vitro* and *in vivo* settings, we have investigated the whole genome methylation levels and selected histones methylation markers, but we have not been able to link NNMT overactivity with epigenetic changes. Moreover, we are interested in elucidating more in details how dexamethasone regulates *NNMT* expression. Tomida et al. pointed at NNMT as a novel Stat3-regulated gene in colon cancer cells [257]. This suggests that dexamethasone might increase NNMT expression through the known GR/STAT3

tethering mode-of-action [258]. Furthermore, the recently discovered role of *N*1-methylnicotinamide in the immune microenvironment of ovarian cancer [237] advances the hypothesis that NNMT upregulation might have an impact on the GBM tumour microenvironment. In order to test this hypothesis, we would need immunocompetent mice models of GBM and also glioblastoma cells silenced for NNMT. Despite NNMT chemical inhibition did not have any consistent effect on glioblastoma cells proliferation, the genetic knockdown of NNMT might have different effects on glioblastoma metabolism. We were not successful in generating stable NNMT-silenced cells through the CRISPR-Cas9 technique, but we are aiming to try a different silencing approach that might allow us to study NNMT role in GBM biology. Drugs already approved in the clinics for the treatment of certain diseases can be effective in treating different pathologies. This 'drug repurposing' concept has been exploited also in glioblastoma therapy [259] and a further development of this project could be the screening for drugs that synergize with dexamethasone in targeting glioblastoma cells proliferation and viability. The activity of NNMT is increased in tumour tissues derived from glioblastoma patients, compared to adjacent oedematous brain tissue. Collectively, these results suggest that NNMT activity could be exploited for imaging of invasive tumours. Moreover, these tumour-specific dexamethasone-induced metabolic alterations may lead to rationally designed therapeutic options for glioblastomas with heterogeneous mutational status.

List of References

1. Furnari, F.B., et al., *Malignant astrocytic glioma: genetics, biology, and paths to treatment.* Genes & Development, 2007. **21**(21): p. 2683-710.
2. Wen, P.Y. and S. Kesari, *Malignant gliomas in adults.* New England Journal of Medicine, 2008. **359**(5): p. 492-507.
3. Smittenaar, C.R., et al., *Cancer incidence and mortality projections in the UK until 2035.* British Journal of Cancer, 2016. **115**(9): p. 1147-1155.
4. Cushing, P.B.a.H., *A classification of the tumours of the glioma group on a histogenetic basis, with a correlated study of prognosis.* JB Lipponcott, Philadelphia, 1926.
5. Bianco, J., et al., *On glioblastoma and the search for a cure: where do we stand?* Cellular and Molecular Life Sciences, 2017. **74**(13): p. 2451-2466.
6. Recht, L., et al., *Neural stem cells and neuro-oncology: quo vadis?* Journal of Cellular Biochemistry 2003. **88**(1): p. 11-9.
7. Galli, R., et al., *Isolation and characterization of tumorigenic, stem-like neural precursors from human glioblastoma.* Cancer Research, 2004. **64**(19): p. 7011-21.
8. Singh, S.K., et al., *Identification of human brain tumour initiating cells.* Nature, 2004. **432**(7015): p. 396-401.
9. Lombard, A., et al., *The Subventricular Zone, a Hideout for Adult and Pediatric High-Grade Glioma Stem Cells.* Frontiers in Oncology, 2020. **10**: p. 614930.
10. Lee, J.H., et al., *Human glioblastoma arises from subventricular zone cells with low-level driver mutations.* Nature, 2018. **560**(7717): p. 243-247.
11. Liu, C., et al., *Mosaic analysis with double markers reveals tumor cell of origin in glioma.* Cell, 2011. **146**(2): p. 209-21.
12. Vleeschouwer, S.D., *Glioblastoma*. 2017.
13. Cancer Genome Atlas Research, N., *Comprehensive genomic characterization defines human glioblastoma genes and core pathways.* Nature, 2008. **455**(7216): p. 1061-8.
14. Verhaak, R.G., et al., *Integrated genomic analysis identifies clinically relevant subtypes of glioblastoma characterized by abnormalities in PDGFRA, IDH1, EGFR, and NF1.* Cancer Cell, 2010. **17**(1): p. 98-110.
15. Wang, Z.L., et al., *Integrated analysis of genome-wide DNA methylation, gene expression and protein expression profiles in molecular subtypes of WHO II-IV gliomas.* Journal of Experimental & Clinical Cancer Research, 2015. **34**: p. 127.
16. Shiraishi, A., K. Sakumi, and M. Sekiguchi, *Increased susceptibility to chemotherapeutic alkylating agents of mice deficient in DNA repair methyltransferase.* Carcinogenesis, 2000. **21**(10): p. 1879-83.
17. Silber, J.R., et al., *Comparison of O6-methylguanine-DNA methyltransferase activity in brain tumors and adjacent normal brain.* Cancer Research, 1993. **53**(14): p. 3416-20.
18. Hegi, M.E., et al., *MGMT gene silencing and benefit from temozolomide in glioblastoma.* New England Journal of Medicine, 2005. **352**(10): p. 997-1003.
19. Yan, H., et al., *IDH1 and IDH2 mutations in gliomas.* The New Eengland Journal of Medicine, 2009. **360**(8): p. 765-73.

20. Turcan, S., et al., *IDH1 mutation is sufficient to establish the glioma hypermethylator phenotype.* Nature, 2012. **483**(7390): p. 479-83.
21. Noushmehr, H., et al., *Identification of a CpG island methylator phenotype that defines a distinct subgroup of glioma.* Cancer Cell, 2010. **17**(5): p. 510-22.
22. Shinojima, N., et al., *Prognostic value of epidermal growth factor receptor in patients with glioblastoma multiforme.* Cancer Research, 2003. **63**(20): p. 6962-70.
23. Amy B. Heimberger, R.H., Dima Suki, David Yang, Jeff Weinberg, Mark Gilbert, Raymond Sawaya, and Kenneth Aldape, *Prognostic Effect of Epidermal Growth Factor Receptor and EGFRvIII in Glioblastoma Multiforme Patients.* Clinical Cancer Research, 2005. **11**: p. 1462–1466.
24. Li, A., et al., *Genomic changes and gene expression profiles reveal that established glioma cell lines are poorly representative of primary human gliomas.* Molecular Cancer Research, 2008. **6**(1): p. 21-30.
25. Bakir, A., et al., *Establishment and characterization of a human glioblastoma multiforme cell line.* Cancer Genetics and Cytogenetics, 1998. **103**(1): p. 46-51.
26. Bougnaud, S., et al., *Molecular crosstalk between tumour and brain parenchyma instructs histopathological features in glioblastoma.* Oncotarget, 2016. **7**(22): p. 31955-71.
27. McKay, R., *Stem cells in the central nervous system.* Science, 1997. **276**(5309): p. 66-71.
28. Lee, J., et al., *Tumor stem cells derived from glioblastomas cultured in bFGF and EGF more closely mirror the phenotype and genotype of primary tumors than do serum-cultured cell lines.* Cancer Cell, 2006. **9**(5): p. 391-403.
29. Dulbecco, R. and G. Freeman, *Plaque production by the polyoma virus.* Virology, 1959. **8**(3): p. 396-7.
30. Eagle, H., *Amino acid metabolism in mammalian cell cultures.* Science, 1959. **130**(3373): p. 432-7.
31. McKee, T.J. and S.V. Komarova, *Is it time to reinvent basic cell culture medium?* American Journal of Physiology-Cell Physiology, 2017. **312**(5): p. C624-C626.
32. Davidson, S.M., et al., *Environment Impacts the Metabolic Dependencies of Ras-Driven Non-Small Cell Lung Cancer.* Cell Metabolism, 2016. **23**(3): p. 517-28.
33. Muir, A. and M.G. Vander Heiden, *The nutrient environment affects therapy.* Science, 2018. **360**(6392): p. 962-963.
34. Cantor, J.R., et al., *Physiologic Medium Rewires Cellular Metabolism and Reveals Uric Acid as an Endogenous Inhibitor of UMP Synthase.* Cell, 2017. **169**(2): p. 258-272 e17.
35. Vande Voorde, J., et al., *Improving the metabolic fidelity of cancer models with a physiological cell culture medium.* Science Advances, 2019. **5**(1): p. eaau7314.
36. De Witt Hamer, P.C., et al., *The genomic profile of human malignant glioma is altered early in primary cell culture and preserved in spheroids.* Oncogene, 2008. **27**(14): p. 2091-6.
37. Ernst, A., et al., *Genomic and expression profiling of glioblastoma stem cell-like spheroid cultures identifies novel tumor-relevant genes associated with survival.* Clinical Cancer Research, 2009. **15**(21): p. 6541-50.

38. Golebiewska, A., et al., *Patient-derived organoids and orthotopic xenografts of primary and recurrent gliomas represent relevant patient avatars for precision oncology.* Acta Neuropathologica, 2020. **140**(6): p. 919-949.
39. Russell, W. and R. Burch, *The principles of humane experimental technique*, ed. L. Methuen. 1959. xiv + 238 pp.
40. Burch, R.L., *The progress of humane experimental technique since 1959: a personal view.* Altern Lab Anim, 1995. **23**(6): p. 776-83.
41. Kienle, G. and H. Kiene, *From Reductionism to Holism: Systems-oriented Approaches in Cancer Research.* Glob Adv Health Med, 2012. **1**(5): p. 68-77.
42. Mehrian-Shai, R., et al., *The Gut-Brain Axis, Paving the Way to Brain Cancer.* Trends Cancer, 2019. **5**(4): p. 200-207.
43. Venkatesh, H.S., et al., *Electrical and synaptic integration of glioma into neural circuits.* Nature, 2019. **573**(7775): p. 539-545.
44. Venkataramani, V., et al., *Glutamatergic synaptic input to glioma cells drives brain tumour progression.* Nature, 2019. **573**(7775): p. 532-538.
45. Arvanitis, C.D., G.B. Ferraro, and R.K. Jain, *The blood-brain barrier and blood-tumour barrier in brain tumours and metastases.* Nat Rev Cancer, 2020. **20**(1): p. 26-41.
46. Huszthy, P.C., et al., *In vivo models of primary brain tumors: pitfalls and perspectives.* Neuro Oncology, 2012. **14**(8): p. 979-93.
47. Hanahan, D. and R.A. Weinberg, *Hallmarks of cancer: the next generation.* Cell, 2011. **144**(5): p. 646-74.
48. Ward, P.S. and C.B. Thompson, *Metabolic reprogramming: a cancer hallmark even warburg did not anticipate.* Cancer Cell, 2012. **21**(3): p. 297-308.
49. Louis, D.N., et al., *The 2016 World Health Organization Classification of Tumors of the Central Nervous System: a summary.* Acta Neuropathologica, 2016. **131**(6): p. 803-20.
50. Louis, D.N., et al., *The 2021 WHO Classification of Tumors of the Central Nervous System: a summary.* Neuro Oncology, 2021. **23**(8): p. 1231-1251.
51. Deshmukh, R., M.F. Allega, and S. Tardito, *A map of the altered glioma metabolism.* Trends in Molecular Medicine, 2021. **27**(11): p. 1045-1059.
52. Brandes, A.A., et al., *Disease progression or pseudoprogression after concomitant radiochemotherapy treatment: pitfalls in neurooncology.* Neuro Oncology, 2008. **10**(3): p. 361-7.
53. Sanghera, P., et al., *Pseudoprogression following chemoradiotherapy for glioblastoma multiforme.* LE JOURNAL CANADIEN DES SCIENCES NEUROLOGIQUES, 2010. **37**(1): p. 36-42.
54. Chawla, S., et al., *Metabolic and physiologic magnetic resonance imaging in distinguishing true progression from pseudoprogression in patients with glioblastoma.* NMR in Biomedicine, 2022: p. e4719.
55. Som, P., et al., *A fluorinated glucose analog, 2-fluoro-2-deoxy-D-glucose (F-18): nontoxic tracer for rapid tumor detection.* The Journal of Nuclear Medicine, 1980. **21**(7): p. 670-5.
56. Wiriyasermkul, P., et al., *Transport of 3-fluoro-L-alpha-methyl-tyrosine by tumor-upregulated L-type amino acid transporter 1: a cause of the tumor uptake in PET.* The Journal of Nuclear Medicine, 2012. **53**(8): p. 1253-61.
57. Shields, A.F., et al., *Imaging proliferation in vivo with [F-18]FLT and positron emission tomography.* Nature Medicine, 1998. **4**(11): p. 1334-6.

58. Wei Chen, M., PhD1; Timothy Cloughesy, MD2; Nirav Kamdar, BS1; Nagichettiar Satyamurthy, PhD1; Marvin Bergsneider, MD3; Linda Liau, MD, PhD3; Paul Mischel, MD4; Johannes Czernin, MD1; Michael E. Phelps, PhD1; and Daniel H.S. Silverman, MD, PhD1, *Imaging Proliferation in Brain Tumors with 18F-FLT PET: Comparison with 18F-FDG*. The Journal of Nuclear Medicine, 2005. **46**(6): p. 945-952.
59. Kim, M.M., et al., *Non-invasive metabolic imaging of brain tumours in the era of precision medicine*. Nature Reviews Clinical Oncology, 2016. **13**(12): p. 725-739.
60. Choi, C., et al., *2-hydroxyglutarate detection by magnetic resonance spectroscopy in IDH-mutated patients with gliomas*. Nature Medicine, 2012. **18**(4): p. 624-9.
61. Rigotti, D.J., M. Inglese, and O. Gonen, *Whole-brain N-acetylaspartate as a surrogate marker of neuronal damage in diffuse neurologic disorders*. AJNR Am J Neuroradiol, 2007. **28**(10): p. 1843-9.
62. Bulik, M., et al., *Potential of MR spectroscopy for assessment of glioma grading*. Clinical Neurology and Neurosurgery, 2013. **115**(2): p. 146-53.
63. Zhao, S.G., et al., *Increased expression of ABCB6 enhances protoporphyrin IX accumulation and photodynamic effect in human glioma*. Annals of Surgical Oncology, 2013. **20**(13): p. 4379-88.
64. Stummer, W., et al., *Fluorescence-guided surgery with 5-aminolevulinic acid for resection of malignant glioma: a randomised controlled multicentre phase III trial*. The Lancet Oncology, 2006. **7**(5): p. 392-401.
65. Tajan, M. and K.H. Vousden, *Dietary Approaches to Cancer Therapy*. Cancer Cell, 2020. **37**(6): p. 767-785.
66. Maurer, G.D., et al., *Differential utilization of ketone bodies by neurons and glioma cell lines: a rationale for ketogenic diet as experimental glioma therapy*. BMC Cancer, 2011. **11**: p. 315.
67. Wheless, J.W., *History of the ketogenic diet*. Epilepsia, 2008. **49 Suppl 8**: p. 3-5.
68. Simone, B.A., et al., *Selectively starving cancer cells through dietary manipulation: methods and clinical implications*. Future Oncol, 2013. **9**(7): p. 959-76.
69. Abdelwahab, M.G., et al., *The ketogenic diet is an effective adjuvant to radiation therapy for the treatment of malignant glioma*. PLoS One, 2012. **7**(5): p. e36197.
70. Stafford, P., et al., *The ketogenic diet reverses gene expression patterns and reduces reactive oxygen species levels when used as an adjuvant therapy for glioma*. Nutrition & Metabolism, 2010. **7**: p. 74.
71. Derr, R.L., et al., *Association between hyperglycemia and survival in patients with newly diagnosed glioblastoma*. Journal of Clinical Oncology, 2009. **27**(7): p. 1082-6.
72. Schreck, K.C., et al., *Feasibility and Biological Activity of a Ketogenic/Intermittent-Fasting Diet in Patients With Glioma*. Neurology, 2021. **97**(9): p. e953-e963.
73. Rieger, J., et al., *ERGO: a pilot study of ketogenic diet in recurrent glioblastoma*. International Journal of Oncology, 2014. **44**(6): p. 1843-52.
74. Voss, M., et al., *ERGO2: A Prospective, Randomized Trial of Calorie-Restricted Ketogenic Diet and Fasting in Addition to Reirradiation for Malignant Glioma*. International Journal of Radiation Oncology, 2020. **108**(4): p. 987-995.

75. Golla, H., et al., *Glioblastoma multiforme from diagnosis to death: a prospective, hospital-based, cohort, pilot feasibility study of patient reported symptoms and needs.* Support Care Cancer, 2014. **22**(12): p. 3341-52.
76. Simpson, J.R., et al., *Influence of location and extent of surgical resection on survival of patients with glioblastoma multiforme: results of three consecutive Radiation Therapy Oncology Group (RTOG) clinical trials.* International Journal of Radiation Oncology Biology Physics, 1993. **26**(2): p. 239-44.
77. Muller, D.M.J., et al., *Timing of glioblastoma surgery and patient outcomes: a multicenter cohort study.* Neuro-Oncology Advances, 2021. **3**(1): p. vdab053.
78. Li, R., et al., *Radiotherapy for glioblastoma: clinical issues and nanotechnology strategies.* Biomaterial Sciences, 2022. **10**(4): p. 892-908.
79. Walker, M.D., T.A. Strike, and G.E. Sheline, *An analysis of dose-effect relationship in the radiotherapy of malignant gliomas.* International Journal of Radiation Oncology Biology Physics, 1979. **5**(10): p. 1725-31.
80. Stupp, R., et al., *Radiotherapy plus concomitant and adjuvant temozolomide for glioblastoma.* New England Journal of Medicine, 2005. **352**(10): p. 987-96.
81. Yuile, P., et al., *Survival of glioblastoma patients related to presenting symptoms, brain site and treatment variables.* Journal of Clinical Neuroscience, 2006. **13**(7): p. 747-51.
82. Matsuyama, T., et al., *A prospective comparison of adaptive and fixed boost plans in radiotherapy for glioblastoma.* Radiation Oncology, 2022. **17**(1): p. 40.
83. Tang, P.L.Y., et al., *The potential of advanced MR techniques for precision radiotherapy of glioblastoma.* MAGMA, 2022. **35**(1): p. 127-143.
84. Carruthers, R.D., et al., *Replication Stress Drives Constitutive Activation of the DNA Damage Response and Radioresistance in Glioblastoma Stem-like Cells.* Cancer Research, 2018. **78**(17): p. 5060-5071.
85. Ali, M.Y., et al., *Radioresistance in Glioblastoma and the Development of Radiosensitizers.* Cancers (Basel), 2020. **12**(9).
86. Yung, W.K., et al., *A phase II study of temozolomide vs. procarbazine in patients with glioblastoma multiforme at first relapse.* Br J Cancer, 2000. **83**(5): p. 588-93.
87. Takakura, K., et al., *Effects of ACNU and radiotherapy on malignant glioma.* Journal of Neurosurgery, 1986. **64**(1): p. 53-7.
88. Happold, C., et al., *ACNU-based chemotherapy for recurrent glioma in the temozolomide era.* Journal of Neuro-Oncology, 2009. **92**(1): p. 45-8.
89. Plate, K.H., et al., *Vascular endothelial growth factor is a potential tumour angiogenesis factor in human gliomas in vivo.* Nature, 1992. **359**(6398): p. 845-8.
90. Gil-Gil, M.J., et al., *Bevacizumab for the treatment of glioblastoma.* Clinical Medicine Insights: Oncology, 2013. **7**: p. 123-35.
91. Keunen, O., et al., *Anti-VEGF treatment reduces blood supply and increases tumor cell invasion in glioblastoma.* Proceedings of the National Academy of Sciences, 2011. **108**(9): p. 3749-54.
92. de Groot, J.F., et al., *Tumor invasion after treatment of glioblastoma with bevacizumab: radiographic and pathologic correlation in humans and mice.* Neuro-Oncology, 2010. **12**(3): p. 233-42.

93. Furuta, T., et al., *Molecular analysis of a recurrent glioblastoma treated with bevacizumab.* Brain Tumor Pathology, 2014. **31**(1): p. 32-9.
94. Lucio-Eterovic, A.K., Y. Piao, and J.F. de Groot, *Mediators of glioblastoma resistance and invasion during antivascular endothelial growth factor therapy.* Clinical Cancer Research, 2009. **15**(14): p. 4589-99.
95. Chinot, O.L., et al., *Bevacizumab plus radiotherapy-temozolomide for newly diagnosed glioblastoma.* New England Journal of Medicine, 2014. **370**(8): p. 709-22.
96. Wick, W., et al., *Lomustine and Bevacizumab in Progressive Glioblastoma.* New England Journal of Medicine, 2017. **377**(20): p. 1954-1963.
97. Wenger, K.J., et al., *Bevacizumab as a last-line treatment for glioblastoma following failure of radiotherapy, temozolomide and lomustine.* Oncology Letters, 2017. **14**(1): p. 1141-1146.
98. Piette, C., et al., *Treating gliomas with glucocorticoids: from bedside to bench.* Acta Neuropathologica, 2006. **112**(6): p. 651-64.
99. Klatzo, I., *Presidental address. Neuropathological aspects of brain edema.* Journal of Neuropathology & Experimental Neurology, 1967. **26**(1): p. 1-14.
100. Hossmann, K.A., *The pathophysiology of experimental brain edema.* Neurosurgical Review, 1989. **12**(4): p. 263-80.
101. Galicich, J.H., L.A. French, and J.C. Melby, *Use of dexamethasone in treatment of cerebral edema associated with brain tumors.* The Lancet, 1961. **81**: p. 46-53.
102. Maurice-Dror, C., R. Perets, and G. Bar-Sela, *Glucocorticoids as an adjunct to oncologic treatment in solid malignancies - Not an innocent bystander.* Critical Reviews in Oncology/Hematology, 2018. **126**: p. 37-44.
103. Ryken, T.C., et al., *The role of steroids in the management of brain metastases: a systematic review and evidence-based clinical practice guideline.* Journal of Neuro-Oncology, 2010. **96**(1): p. 103-14.
104. Sarin, R. and V. Murthy, *Medical decompressive therapy for primary and metastatic intracranial tumours.* Lancet Neurology, 2003. **2**(6): p. 357-65.
105. Biddie, S.C., B.L. Conway-Campbell, and S.L. Lightman, *Dynamic regulation of glucocorticoid signalling in health and disease.* Rheumatology (Oxford), 2012. **51**(3): p. 403-12.
106. Oakley, R.H. and J.A. Cidlowski, *Cellular processing of the glucocorticoid receptor gene and protein: new mechanisms for generating tissue-specific actions of glucocorticoids.* Journal of Biological Chemistry, 2011. **286**(5): p. 3177-84.
107. Kadmiel, M. and J.A. Cidlowski, *Glucocorticoid receptor signaling in health and disease.* Trends in Pharmacological Sciences, 2013. **34**(9): p. 518-30.
108. Song, I.H. and F. Buttgereit, *Non-genomic glucocorticoid effects to provide the basis for new drug developments.* Molecular and Cellular Endocrinology, 2006. **246**(1-2): p. 142-6.
109. Tasker, J.G., S. Di, and R. Malcher-Lopes, *Minireview: rapid glucocorticoid signaling via membrane-associated receptors.* Endocrinology, 2006. **147**(12): p. 5549-56.
110. Panettieri, R.A., et al., *Non-genomic Effects of Glucocorticoids: An Updated View.* Trends Pharmacological Sciences, 2019. **40**(1): p. 38-49.

111. Jackson, R.K., J.A. Irving, and G.J. Veal, *Personalization of dexamethasone therapy in childhood acute lymphoblastic leukaemia.* British Journal of Haematology, 2016. **173**(1): p. 13-24.
112. Guner, M., et al., *Effects of dexamethasone and betamethasone on in vitro cultures from human astrocytoma.* British Journal of Cancer, 1977. **35**(4): p. 439-47.
113. Gagne, D., M. Pons, and D. Philibert, *RU 38486: a potent antiglucocorticoid in vitro and in vivo.* Journal of Steroid Biochemistry, 1985. **23**(3): p. 247-51.
114. Heiss, J.D., et al., *Mechanism of dexamethasone suppression of brain tumor-associated vascular permeability in rats.* The Journal of Clinical Investigation, 1996. **98**(6): p. 1400–1408.
115. Harke, N., et al., *Glucocorticoids regulate the human occludin gene through a single imperfect palindromic glucocorticoid response element.* Molecular & Cellular Endocrinology, 2008. **295**(1-2): p. 39-47.
116. Kostopoulou, O.N., et al., *Glucocorticoids promote a glioma stem cell-like phenotype and resistance to chemotherapy in human glioblastoma primary cells: Biological and prognostic significance.* International Journal of Cancer, 2018. **142**(6): p. 1266-1276.
117. Armelin, M.C.S. and H.A. Armelin, *Glucocorticoid hormone modulation of both cell surface and cytoskeleton related to growth control of rat glioma cells.* The Journal of Cell Biology, 1983. **97**: p. 459-465.
118. Weller, M., et al., *Chemotherapy of human malignant glioma: prevention of efficacy by dexamethasone?* Neurology, 1997. **48**(6): p. 1704-9.
119. Das, A., et al., *Dexamethasone protected human glioblastoma U87MG cells from temozolomide induced apoptosis by maintaining Bax:Bcl-2 ratio and preventing proteolytic activities.* Molecular Cancer, 2004. **3**(1): p. 36.
120. Grasso, R.J., et al., *Combined growth-inhibitory responses and ultrastructural alterations produced by 1,3-bis(2-chloroethyl)-1-nitrosourea and dexamethasone in rat glioma cell cultures.* Cancer Research, 1977. **37**(2): p. 585-94.
121. Wang, H., et al., *Pretreatment with dexamethasone increases antitumor activity of carboplatin and gemcitabine in mice bearing human cancer xenografts: in vivo activity, pharmacokinetics, and clinical implications for cancer chemotherapy.* Clinical Cancer Research, 2004. **10**(5): p. 1633-44.
122. Hempen, C., E. Weiss, and C.F. Hess, *Dexamethasone treatment in patients with brain metastases and primary brain tumors: do the benefits outweigh the side-effects?* Support Care Cancer, 2002. **10**(4): p. 322-8.
123. Shields, L.B., et al., *Dexamethasone administration during definitive radiation and temozolomide renders a poor prognosis in a retrospective analysis of newly diagnosed glioblastoma patients.* Radiat Oncol, 2015. **10**: p. 222.
124. Hattingen, E., et al., *Quantitative T2 mapping of recurrent glioblastoma under bevacizumab improves monitoring for non-enhancing tumor progression and predicts overall survival.* Neuro-Oncology, 2013. **15**(10): p. 1395-404.
125. Pitter, K.L., et al., *Corticosteroids compromise survival in glioblastoma.* Brain, 2016. **139**(Pt 5): p. 1458-71.

126. Luedi, M.M., et al., *A Dexamethasone-regulated Gene Signature Is Prognostic for Poor Survival in Glioblastoma Patients.* Journal of Neurosurgical Anesthesiology, 2017. **29**(1): p. 46-58.
127. Wong, E.T., et al., *Dexamethasone exerts profound immunologic interference on treatment efficacy for recurrent glioblastoma.* Br J Cancer, 2015. **113**(2): p. 232-41.
128. Batchelor, T.T., et al., *AZD2171, a pan-VEGF receptor tyrosine kinase inhibitor, normalizes tumor vasculature and alleviates edema in glioblastoma patients.* Cancer Cell, 2007. **11**(1): p. 83-95.
129. Tjuvajev, J., et al., *Corticotropin-releasing factor decreases vasogenic brain edema.* Cancer Research, 1996. **56**(6): p. 1352-60.
130. Villalona-Calero, M.A., et al., *A phase I trial of human corticotropin-releasing factor (hCRF) in patients with peritumoral brain edema.* Annals of Oncology, 1998. **9**(1): p. 71-7.
131. Gerstner, E.R., et al., *VEGF inhibitors in the treatment of cerebral edema in patients with brain cancer.* Nature Reviews in Clinical Oncology, 2009. **6**(4): p. 229-36.
132. Exton, J.H., *Regulation of gluconeogenesis by glucocorticoids.* Monogr Endocrinol, 1979. **12**: p. 535-46.
133. Kuo, T., C.A. Harris, and J.C. Wang, *Metabolic functions of glucocorticoid receptor in skeletal muscle*. Molecular and Cellular Endocrinology, 2013. **380**(1-2): p. 79-88.
134. Pilkis, S.J., M.R. el-Maghrabi, and T.H. Claus, *Hormonal regulation of hepatic gluconeogenesis and glycolysis.* Annual Reviews in Biochemistry, 1988. **57**: p. 755-83.
135. Charmandari, E., C. Tsigos, and G. Chrousos, *Endocrinology of the stress response*. Annual Reviews in Physiology, 2005. **67**: p. 259-84.
136. Mergenthaler, P., et al., *Sugar for the brain: the role of glucose in physiological and pathological brain function.* Trends in Neuroscience, 2013. **36**(10): p. 587-97.
137. Sethi, R., et al., *Evaluation of hyperglycaemic response to intra-operative dexamethasone administration in patients undergoing elective intracranial surgery: A randomised, prospective study.* Asian Journal of Neurosurgery, 2016. **11**(2): p. 98-102.
138. Olefsky, J.M., *Effect of dexamethasone on insulin binding, glucose transport, and glucose oxidation of isolated rat adipocytes.* The Journal of Clinical Investigation, 1975. **56**(6): p. 1499-1508.
139. Shen, H., et al., *Sensitization of Glioblastoma Cells to Irradiation by Modulating the Glucose Metabolism.* Molecular Cancer Therapeutics, 2015. **14**(8): p. 1794-804.
140. Einstein, M., et al., *Selective glucocorticoid receptor nonsteroidal ligands completely antagonize the dexamethasone mediated induction of enzymes involved in gluconeogenesis and glutamine metabolism.* Journal of Steroid Biochemistry &Molecular Biology, 2004. **92**(5): p. 345-56.
141. Moscona, A.A. and R. Piddington, *Enzyme induction by corticosteroids in embryonic cells: steroid structure and inductive effect.* Science, 1967. **158**(3800): p. 496-7.
142. Arcuri, C., et al., *Glutamine synthetase gene expression in a glioblastoma cell-line of clonal origin: regulation by dexamethasone and dibutyryl cyclic AMP.* Neurochemical Research, 1995. **20**(10): p. 1133-9.

143. Wu, T., et al., *Chronic glucocorticoid treatment induced circadian clock disorder leads to lipid metabolism and gut microbiota alterations in rats.* Life Sciences, 2018. **192**: p. 173-182.
144. Bordag, N., et al., *Glucocorticoid (dexamethasone)-induced metabolome changes in healthy males suggest prediction of response and side effects.* Scientific Reports, 2015. **5**: p. 15954.
145. von Mässenhausen, A., et al., *Dexamethasone sensitizes to ferroptosis by glucocorticoid receptor–induced dipeptidase-1 expression and glutathione depletion.* Sciences Advances, 2022. **8**.
146. Smith, P.K., et al., *Measurement of protein using bicinchoninic acid.* Analytical Biochemistry, 1985. **150**(1): p. 76-85.
147. Lowry, O.H., et al., *Protein measurement with the Folin phenol reagent.* J Biol Chem, 1951. **193**(1): p. 265-75.
148. Tardito, S., et al., *Glutamine synthetase activity fuels nucleotide biosynthesis and supports growth of glutamine-restricted glioblastoma.* Nature Cell Biology, 2015. **17**(12): p. 1556-68.
149. Newman, A.C., et al., *Use of (13)C3(15)N1-Serine or (13)C5(15)N1-Methionine for Studying Methylation Dynamics in Cancer Cell Metabolism and Epigenetics.* Methods in Molecular Biology, 2019. **1928**: p. 55-67.
150. Oudin, A., et al., *Protocol for derivation of organoids and patient-derived orthotopic xenografts from glioma patient tumors.* STAR Protocols, 2021. **2**(2): p. 100534.
151. Brady, M.E., et al., *The pharmacokinetics of single high doses of dexamethasone in cancer patients.* Eur J Clin Pharmacol, 1987. **32**(6): p. 593-6.
152. Chalk, J.B., et al., *Phenytoin impairs the bioavailability of dexamethasone in neurological and neurosurgical patients.* J Neurol Neurosurg Psychiatry, 1984. **47**(10): p. 1087-90.
153. Nestler, U., M. Winking, and D.K. Boker, *The tissue level of dexamethasone in human brain tumors is about 1000 times lower than the cytotoxic concentration in cell culture.* Neurol Res, 2002. **24**(5): p. 479-82.
154. Takahashi, T., et al., *Pharmacokinetics of aprepitant and dexamethasone after administration of chemotherapeutic agents and effects of plasma substance P concentration on chemotherapy-induced nausea and vomiting in Japanese cancer patients.* Cancer Chemother Pharmacol, 2011. **68**(3): p. 653-9.
155. Imamura, Y., et al., *Comparison of 2D- and 3D-culture models as drug-testing platforms in breast cancer.* Oncology Reports, 2015. **33**(4): p. 1837-43.
156. Pinto, B., et al., *Three-Dimensional Spheroids as In Vitro Preclinical Models for Cancer Research.* Pharmaceutics, 2020. **12**(12).
157. Klein, E., et al., *Glioblastoma Organoids: Pre-Clinical Applications and Challenges in the Context of Immunotherapy.* Front Oncol, 2020. **10**: p. 604121.
158. Ramamoorthy, S. and J.A. Cidlowski, *Ligand-induced repression of the glucocorticoid receptor gene is mediated by an NCoR1 repression complex formed by long-range chromatin interactions with intragenic glucocorticoid response elements.* Molecular and Cellular Biology, 2013. **33**(9): p. 1711-22.

159. Mackie, A.E., et al., *Glucocorticoids and the cell surface of human glioma cells: relationship to cytostasis.* British Journal of Cancer, 1988. **9**: p. 101-7.
160. Saklatvala, J., *Glucocorticoids: do we know how they work?* Arthritis Research, 2002. **4**: p. 146-150.
161. Cui, A., et al., *Dexamethasone-induced Kruppel-like factor 9 expression promotes hepatic gluconeogenesis and hyperglycemia.* Journal of Clinical Investigation, 2019. **129**(6): p. 2266-2278.
162. Pereira, M.J., et al., *FKBP5 expression in human adipose tissue increases following dexamethasone exposure and is associated with insulin resistance.* Metabolism, 2014. **63**(9): p. 1198-208.
163. Warren, C.F.A., M.W. Wong-Brown, and N.A. Bowden, *BCL-2 family isoforms in apoptosis and cancer.* Cell Death and Disease, 2019. **10**(3): p. 177.
164. Inaba, H. and C.H. Pui, *Glucocorticoid use in acute lymphoblastic leukaemia.* Lancet Oncology, 2010. **11**(11): p. 1096-106.
165. Matulis, S.M., et al., *Dexamethasone treatment promotes Bcl-2 dependence in multiple myeloma resulting in sensitivity to venetoclax.* Leukemia, 2016. **30**(5): p. 1086-93.
166. Gimple, R.C., et al., *Glioma Stem Cell-Specific Superenhancer Promotes Polyunsaturated Fatty-Acid Synthesis to Support EGFR Signaling.* Cancer Discovery, 2019. **9**(9): p. 1248-1267.
167. Tano, K., et al., *Isolation and structural characterization of a cDNA clone encoding the human DNA repair protein for O6-alkylguanine.* Proceedings of the National Academy of Sciences of the United States of America, 1990. **87**(2): p. 686-90.
168. Kahn, M., *Can we safely target the WNT pathway?* Nature Reviews in Drug Discovery, 2014. **13**(7): p. 513-32.
169. Clevers, H. and R. Nusse, *Wnt/beta-catenin signaling and disease.* Cell, 2012. **149**(6): p. 1192-205.
170. Liu, J., et al., *Targeting Wnt-driven cancer through the inhibition of Porcupine by LGK974.* Proceedings of the National Academy of Sciences of the United States of America, 2013. **110**(50): p. 20224-9.
171. Jakobsson, A., R. Westerberg, and A. Jacobsson, *Fatty acid elongases in mammals: their regulation and roles in metabolism.* Progress in Lipid Research, 2006. **45**(3): p. 237-49.
172. Sur, P., et al., *Dexamethasone decreases temozolomide-induced apoptosis in human gliobastoma T98G cells.* Glia, 2005. **50**(2): p. 160-7.
173. Yuan, Y., et al., *Dexamethasone induces cross-linked actin networks in trabecular meshwork cells through noncanonical wnt signaling.* Investigative Ophthalmology & Visual Science, 2013. **54**(10): p. 6502-9.
174. Guan, Y., et al., *Glucocorticoids control beta-catenin protein expression and localization through distinct pathways that can be uncoupled by disruption of signaling events required for tight junction formation in rat mammary epithelial tumor cells.* Molecular Endocrinology, 2004. **18**(1): p. 214-27.
175. Wickstrom, M., et al., *Wnt/beta-catenin pathway regulates MGMT gene expression in cancer and inhibition of Wnt signalling prevents chemoresistance.* Nature Communications, 2015. **6**: p. 8904.
176. Baid, S.K. and L.K. Nieman, *Therapeutic doses of glucocorticoids: implications for oral medicine.* Oral Diseases, 2006. **12**(5): p. 436-42.

177. Vegiopoulos, A. and S. Herzig, *Glucocorticoids, metabolism and metabolic diseases.* Molecular and Cellular Endocrinology, 2007. **275**(1-2): p. 43-61.
178. Salceda, S. and J. Caro, *Hypoxia-inducible factor 1alpha (HIF-1alpha) protein is rapidly degraded by the ubiquitin-proteasome system under normoxic conditions. Its stabilization by hypoxia depends on redox-induced changes.* Journal of Biological Chemistry, 1997. **272**(36): p. 22642-7.
179. Oyinlade, O., et al., *Targeting UDP-alpha-D-glucose 6-dehydrogenase inhibits glioblastoma growth and migration.* Oncogene, 2018. **37**(20): p. 2615-2629.
180. van Gorsel, M., I. Elia, and S.M. Fendt, *(13)C Tracer Analysis and Metabolomics in 3D Cultured Cancer Cells.* Methods in Molecular Biology, 2019. **1862**: p. 53-66.
181. Hanahan, D. and R.A. Weinberg, *The hallmarks of cancer.* Cell, 2000. **100**(1): p. 57-70.
182. Higgins, S.C. and G.J. Pilkington, *The in vitro effects of tricyclic drugs and dexamethasone on cellular respiration of malignant glioma.* Anticancer Research, 2010. **30**(2): p. 391-7.
183. Warburg, O., *On the origin of cancer cells.* Science, 1956. **123**(3191): p. 309-14.
184. Vander Heiden, M.G., L.C. Cantley, and C.B. Thompson, *Understanding the Warburg effect: the metabolic requirements of cell proliferation.* Science, 2009. **324**(5930): p. 1029-33.
185. Lee, D.C., et al., *A lactate-induced response to hypoxia.* Cell, 2015. **161**(3): p. 595-609.
186. Colen, C.B., et al., *Metabolic targeting of lactate efflux by malignant glioma inhibits invasiveness and induces necrosis: an in vivo study.* Neoplasia, 2011. **13**(7): p. 620-32.
187. Machler, P., et al., *In Vivo Evidence for a Lactate Gradient from Astrocytes to Neurons.* Cell Metab, 2016. **23**(1): p. 94-102.
188. Kodama, T., et al., *Role of the glucocorticoid receptor for regulation of hypoxia-dependent gene expression.* The Journal Of Biological Chemistry, 2003. **278**(35): p. 33384-91.
189. Li, Y., Y. Wei, and L. Gu, *Effect of hypoxia on proliferation and glucocorticoid resistance of T-cell acute lymphoblastic leukaemia.* Hematology, 2021. **26**(1): p. 775-784.
190. Yudkoff, M., et al., *Brain glutamate metabolism: neuronal-astroglial relationships.* Developmental Neuroscience, 1993. **15**(3-5): p. 343-50.
191. Parkin, G.M., et al., *Glutamate transporters, EAAT1 and EAAT2, are potentially important in the pathophysiology and treatment of schizophrenia and affective disorders.* World Journal of Psychiatry, 2018. **8**(2): p. 51-63.
192. Popoli, M., et al., *The stressed synapse: the impact of stress and glucocorticoids on glutamate transmission.* Nature Review Neuroscience, 2011. **13**(1): p. 22-37.
193. Yao, Z., et al., *Modeling circadian rhythms of glucocorticoid receptor and glutamine synthetase expression in rat skeletal muscle.* Pharmaceutical Research, 2006. **23**(4): p. 670-9.
194. Parsons, D.W., et al., *An integrated genomic analysis of human glioblastoma multiforme.* Science, 2008. **321**(5897): p. 1807-12.
195. Hongyang Zhang, Zhi-Hao Chen, and a.T.M. Savarese, *Codeletion of the Genes for p16INK4, Methylthioadenosine Phosphorylase, Interferon-alfa1,*

Interferon-beta1, and other 9p21 Markers in Human Malignant Cell Lines. Cancer Genetics and Cytogenetics, 1996. **86**: p. 22-28.
196. Della Ragione, F., et al., *Purification and characterization of 5'-deoxy-5'-methylthioadenosine phosphorylase from human placenta.* The Journal Of Biological Chemistry, 1986. **261**(26): p. 12324-9.
197. Hansen, L.J., et al., *MTAP Loss Promotes Stemness in Glioblastoma and Confers Unique Susceptibility to Purine Starvation.* Cancer Research, 2019. **79**(13): p. 3383-3394.
198. Marjon, K., et al., *MTAP Deletions in Cancer Create Vulnerability to Targeting of the MAT2A/PRMT5/RIOK1 Axis.* Cell Reports, 2016. **15**(3): p. 574-587.
199. Barekatain, Y., et al., *Homozygous MTAP deletion in primary human glioblastoma is not associated with elevation of methylthioadenosine.* Nature Communications, 2021. **12**(1): p. 4228.
200. Clarkin, C.E., et al., *Regulation of UDP-glucose dehydrogenase is sufficient to modulate hyaluronan production and release, control sulfated GAG synthesis, and promote chondrogenesis.* Journal of Cellular Physiology, 2011. **226**(3): p. 749-61.
201. Aksoy, S., C.L. Szumlanski, and R.M. Weinshilboum, *Human liver nicotinamide N-methyltransferase. cDNA cloning, expression, and biochemical characterization.* J Biol Chem, 1994. **269**(20): p. 14835-40.
202. Cantoni, G.L., *Methylation of Nicotinamide with a Soluble Enzyme System from Rat Liver.* Journal of Biological Chemistry, 1951. **189**(1): p. 203-216.
203. Lal, A., et al., *A public database for gene expression in human cancers.* Cancer Research, 1999. **59**(21): p. 5403-7.
204. Markert, J.M., et al., *Differential gene expression profiling in human brain tumors.* Physiological Genomics, 2001. **5**(1): p. 21-33.
205. Felsted, R.L. and S. Chaykin, *N1-methylnicotinamide oxidation in a number of mammals.* The Journal Of Biological Chemistry, 1967. **242**(6): p. 1274-9.
206. Bo-Hyun Lim, B.-I.C., Yu Na Kim, Jae Won Kim, Soon-Tae Park and Chang-Won Lee, *Overexpression of nicotinamide N-methyltransferase in gastric cancer tissues and its potential post-translational modification.* EXPERIMENTAL and MOLECULAR MEDICINE, 2006. **38**(5): p. 455-465.
207. Sartini, D., et al., *Nicotinamide N-methyltransferase upregulation inversely correlates with lymph node metastasis in oral squamous cell carcinoma.* Molecular Medicine, 2007. **13**(7-8): p. 415-21.
208. Roessler, M., et al., *Identification of nicotinamide N-methyltransferase as a novel serum tumor marker for colorectal cancer.* Clinical Cancer Research, 2005. **11**(18): p. 6550-7.
209. Ulanovskaya, O.A., A.M. Zuhl, and B.F. Cravatt, *NNMT promotes epigenetic remodeling in cancer by creating a metabolic methylation sink.* Nat Chem Biol, 2013. **9**(5): p. 300-6.
210. Jung, J., et al., *Nicotinamide metabolism regulates glioblastoma stem cell maintenance.* JCI Insight, 2017. **2**(10).
211. Eckert, M.A., et al., *Proteomics reveals NNMT as a master metabolic regulator of cancer-associated fibroblasts.* Nature, 2019. **569**(7758): p. 723-728.
212. Obradovic, M.M.S., et al., *Glucocorticoids promote breast cancer metastasis.* Nature, 2019. **567**(7749): p. 540-544.
213. Finkelstein, J.D., *Methionine metabolism in mammals.* The Journal of Nutritional Biochemistry, 1990. **1**: p. 228-237.

214. Stresemann, C. and F. Lyko, *Modes of action of the DNA methyltransferase inhibitors azacytidine and decitabine*. International Journal of Cancer, 2008. **123**(1): p. 8-13.
215. Sperber, H., et al., *The metabolome regulates the epigenetic landscape during naive-to-primed human embryonic stem cell transition*. Nature Cell Biology, 2015. **17**(12): p. 1523-35.
216. Engstrom, P.G., et al., *Digital transcriptome profiling of normal and glioblastoma-derived neural stem cells identifies genes associated with patient survival*. Genome Medicine, 2012. **4**(10): p. 76.
217. Parkhitko, A.A., et al., *Methionine metabolism and methyltransferases in the regulation of aging and lifespan extension across species*. Aging Cell, 2019. **18**(6): p. e13034.
218. Hoffman, R.M. and R.W. Erbe, *High in vivo rates of methionine biosynthesis in transformed human and malignant rat cells auxotrophic for methionine*. Proceedings of the National Academy of Sciences, 1976. **73**(5): p. 1523-7.
219. Stern, P.H., C.D. Wallace, and R.M. Hoffman, *Altered methionine metabolism occurs in all members of a set of diverse human tumor cell lines*. Journal of Cell Physiology, 1984. **119**(1): p. 29-34.
220. Rajman, L., K. Chwalek, and D.A. Sinclair, *Therapeutic Potential of NAD-Boosting Molecules: The In Vivo Evidence*. Cell Metabolism, 2018. **27**(3): p. 529-547.
221. Stratford, M.R. and M.F. Dennis, *High-performance liquid chromatographic determination of nicotinamide and its metabolites in human and murine plasma and urine*. Journal of Chromatography, 1992. **582**(1-2): p. 145-51.
222. Neelakantan, H., et al., *Structure-Activity Relationship for Small Molecule Inhibitors of Nicotinamide N-Methyltransferase*. Journal of Medicinal Chemistry, 2017. **60**(12): p. 5015-5028.
223. Alston, T.A. and R.H. Abeles, *Substrate specificity of nicotinamide methyltransferase isolated from porcine liver*. Archives of Biochemistry and Biophysics, 1988. **260**(2): p. 601-8.
224. Pissios, P., *Nicotinamide N-Methyltransferase: More Than a Vitamin B3 Clearance Enzyme*. Trends in Endocrinology & Metabolism, 2017. **28**(5): p. 340-353.
225. Irwin, I., J.W. Langston, and L.E. DeLanney, *4-Phenylpyridine (4PP) and MPTP: the relationship between striatal MPP+ concentrations and neurotoxicity*. Life Sciences, 1987. **40**(8): p. 731-40.
226. Williams, A.C. and D.B. Ramsden, *Autotoxicity, methylation and a road to the prevention of Parkinson's disease*. Journal of Clinical Neuroscience, 2005. **12**(1): p. 6-11.
227. Murata, M.M., et al., *NAD+ consumption by PARP1 in response to DNA damage triggers metabolic shift critical for damaged cell survival*. Molecular Biology of the Cell, 2019. **30**(20): p. 2584-2597.
228. Buenrostro, J.D., et al., *ATAC-seq: A Method for Assaying Chromatin Accessibility Genome-Wide*. Current Protocols in Molecular Biology, 2015. **109**: p. 21 29 1-21 29 9.
229. Locasale, J.W., et al., *Metabolomics of human cerebrospinal fluid identifies signatures of malignant glioma*. Molecular & Cellular Proteomics, 2012. **11**(6): p. M111 014688.

230. Shiraki, N., et al., *Methionine metabolism regulates maintenance and differentiation of human pluripotent stem cells.* Cell Metabolism, 2014. **19**(5): p. 780-94.
231. Gao, X., et al., *Dietary methionine influences therapy in mouse cancer models and alters human metabolism.* Nature, 2019. **572**(7769): p. 397-401.
232. Yuxiang Wang, et al., *Targeting therapeutic vulnerabilities with PARP inhibition and radiation in IDH-mutant gliomas and cholangiocarcinomas.* Science Advances, 2020. **6**.
233. Gujar, A.D., et al., *An NAD+-dependent transcriptional program governs self-renewal and radiation resistance in glioblastoma.* Proceedings of the National Academy of Sciences, 2016. **113**(51): p. E8247-E8256.
234. Lucena-Cacace, A., et al., *NAMPT overexpression induces cancer stemness and defines a novel tumor signature for glioma prognosis.* Oncotarget, 2017. **8**(59): p. 99514-99530.
235. Burgos, E.S. and V.L. Schramm, *Weak Coupling of ATP Hydrolysis to the Chemical Equilibrium of Human Nicotinamide Phosphoribosyltransferase.* Biochemistry, 2008. **47**: p. 11086–11096.
236. Kraus, D., et al., *Nicotinamide N-methyltransferase knockdown protects against diet-induced obesity.* Nature, 2014. **508**(7495): p. 258-62.
237. Kilgour, M.K., et al., *1-Methylnicotinamide is an immune regulatory metabolite in human ovarian cancer.* Sci Adv, 2021. **7**(4).
238. Chlopicki, S., et al., *1-Methylnicotinamide (MNA), a primary metabolite of nicotinamide, exerts anti-thrombotic activity mediated by a cyclooxygenase-2/prostacyclin pathway.* British Journal of Pharmacology, 2007. **152**(2): p. 230-9.
239. Blazejczyk, A., et al., *1-methylnicotinamide and its structural analog 1,4-dimethylpyridine for the prevention of cancer metastasis.* Journal of Experimental & Clinical Cancer Research, 2016. **35**(1): p. 110.
240. Parsons, R.B., et al., *Expression of nicotinamide N-methyltransferase (E.C. 2.1.1.1) in the Parkinsonian brain.* Journal of Neuropathology and Experimental Neurology, 2002. **61**(2): p. 111-24.
241. Aldaz, P., et al., *Identification of a Dexamethasone Mediated Radioprotection Mechanism Reveals New Therapeutic Vulnerabilities in Glioblastoma.* Cancers (Basel), 2021. **13**(2).
242. Adeberg, S., et al., *The influence of hyperglycemia during radiotherapy on survival in patients with primary glioblastoma.* Acta Oncologica, 2016. **55**(2): p. 201-7.
243. Rohdewald, P., et al., *Pharmacokinetics of dexamethasone and its phosphate ester.* Biopharmaceutics & Drug Disposition, 1987. **8**(3): p. 205-12.
244. Hasselgren, P.O., et al., *Corticosteroids and muscle wasting: role of transcription factors, nuclear cofactors, and hyperacetylation.* Current Opinion in Clinical Nutrition and Metabolic Care, 2010. **13**(4): p. 423-8.
245. Gerdes, J., et al., *Production of a mouse monoclonal antibody reactive with a human nuclear antigen associated with cell proliferation.* Int J Cancer, 1983. **31**(1): p. 13-20.
246. Horsman, M.R., D.J. Chaplin, and J.M. Brown, *Tumor radiosensitization by nicotinamide: a result of improved perfusion and oxygenation.* Radiation Research, 1989. **118**(1): p. 139-50.

247. Stratford, M.R. and M.F. Dennis, *Pharmacokinetics and biochemistry studies on nicotinamide in the mouse.* Cancer Chemotherapy & Pharmacology, 1994. **34**(5): p. 399-404.
248. Gangoso, E., et al., *Glioblastomas acquire myeloid-affiliated transcriptional programs via epigenetic immunoediting to elicit immune evasion.* Cell, 2021. **184**(9): p. 2454-2470 e26.
249. Gay, F., et al., *Methionine tumor starvation by erythrocyte-encapsulated methionine gamma-lyase activity controlled with per os vitamin B6.* Cancer Medicine, 2017. **6**(6): p. 1437-1452.
250. Glaudemans, A.W., et al., *Value of 11C-methionine PET in imaging brain tumours and metastases.* European Journal of Nuclear Medicine and Molecular Imaging, 2013. **40**(4): p. 615-35.
251. Stober, B., et al., *Differentiation of tumour and inflammation: characterisation of [methyl-3H]methionine (MET) and O-(2-[18F]fluoroethyl)-L-tyrosine (FET) uptake in human tumour and inflammatory cells.* European Journal of Nuclear Medicine and Molecular Imaging, 2006. **33**(8): p. 932-9.
252. Riederer, M., et al., *Adipose tissue as a source of nicotinamide N-methyltransferase and homocysteine.* Atherosclerosis, 2009. **204**(2): p. 412-7.
253. Lucena-Cacace, A., et al., *NAMPT as a Dedifferentiation-Inducer Gene: NAD(+) as Core Axis for Glioma Cancer Stem-Like Cells Maintenance.* Frontiers in Oncology, 2019. **9**: p. 292.
254. Lee, H.J., et al., *Proteomic and Metabolomic Characterization of a Mammalian Cellular Transition from Quiescence to Proliferation.* Cell Reports, 2017. **20**(3): p. 721-736.
255. Liau, B.B., et al., *Adaptive Chromatin Remodeling Drives Glioblastoma Stem Cell Plasticity and Drug Tolerance.* Cell Stem Cell, 2017. **20**(2): p. 233-246 e7.
256. Oren, Y., et al., *Cycling cancer persister cells arise from lineages with distinct programs.* Nature, 2021. **596**(7873): p. 576-582.
257. Tomida, M., et al., *Stat3 up-regulates expression of nicotinamide N-methyltransferase in human cancer cells.* Journal of Cancer Research and Clinical Oncology, 2008. **134**(5): p. 551-9.
258. Langlais, D., et al., *The Stat3/GR interaction code: predictive value of direct/indirect DNA recruitment for transcription outcome.* Molecular Cell, 2012. **47**(1): p. 38-49.
259. Alomari, S., et al., *Drug Repurposing for Glioblastoma and Current Advances in Drug Delivery-A Comprehensive Review of the Literature.* Biomolecules, 2021. **11**(12).